

Functional Characterization of the SAS-4-Related Protein CPAP in Centrosome Biology of Human Cells

THÈSE N° 4491 (2009)

PRÉSENTÉE LE 25 SEPTEMBRE 2009

À LA FACULTÉ DES SCIENCES DE LA VIE

Institut Suisse de Recherche Expérimentale sur le Cancer

PROGRAMME DOCTORAL EN BIOLOGIE MOLÉCULAIRE DU CANCER ET DE L'INFECTION

ÉCOLE POLYTECHNIQUE FÉDÉRALE DE LAUSANNE

POUR L'OBTENTION DU GRADE DE DOCTEUR ÈS SCIENCES

PAR

Gregor Kohlmaier

Mag.rer.nat., Université de Vienne, Autriche

acceptée sur proposition du jury:

Prof. J. Lingner, président du jury
Prof. P. Gönczy, directeur de thèse
Prof. P. Beard, rapporteur
Prof. A. Constantinou, rapporteur
Prof. M. Mogensen, rapporteur



Lausanne, Suisse
2009

Summary

The centrosome is an organelle that resides at the center of most animal cells and comprises two microtubule-based centriole cylinders surrounded by pericentriolar material (PCM). The centrosome plays a fundamental role for nucleating and organizing a radial array of cytoplasmic microtubules during interphase and promoting the assembly of the mitotic spindle during mitosis. In proliferating cells, the centrosome duplicates once per cell cycle, a process that involves notably the formation of one procentriole at the base of each centriole. The procentriole then grows until it reaches the same size of its associated centriole. The formation of supernumerary centrosomes causes severe problems, since this can lead to multipolar spindle formation, chromosome missegregation and genomic instability, which are hallmarks of cancer cells. The mechanisms regulating centrosome duplication are still incompletely understood.

We have studied the role of the centrosomal P4.1-associated protein (CPAP) in human cells. We found that this protein is required for efficient growth of cytoplasmic microtubules from centrosomes as well as for centrosome duplication. There, CPAP is required at an early step during procentriole assembly, after the incorporation of HsSAS-6 but before that of Centrin. Importantly, we found also that the overexpression of CPAP leads to abnormal elongation of procentrioles and centrioles, indicating that the levels of CPAP determine centriole length. Excess CPAP levels furthermore lead to the formation of multiple procentrioles along overly elongated centrioles, multipolar spindle formation and cell division errors. Therefore, proper regulation of proteins such as CPAP that set centriole length contributes to ensure genome integrity.

Overall, we gained important insights into the functions of CPAP at the centrosome and identified a novel control mechanism of centriole length. This will be relevant for a better understanding of how centrosomes function in the progression of cancer and other diseases.

Key words: centrosome, centriole, cell division, cancer

Zusammenfassung

Das Zentrosom ist ein Organell im Zentrum der meisten tierischen Zellen und besteht aus zwei zylinderförmigen Zentriolen, die aus Mikrotubuli zusammengesetzt und von perizentriolärer Matrix (PCM) umgeben sind. Das Zentrosom spielt während der Interphase eine fundamentale Rolle bei der Bildung und strahlenförmigen Organisation von zytoplasmatischen Mikrotubuli. Während der Mitose fördert es die Ausbildung der mitotischen Spindel. Die Duplikation des Zentrosoms erfolgt in sich teilenden Zellen nur einmal pro Zellzyklus. Dabei bildet sich an der Basis eines jeden Zentriols jeweils ein Prozentriol aus. Dieses wächst, bis es dieselbe Größe wie das Zentriol erreicht. Die Bildung von überzähligen Zentrosomen verursacht schwerwiegende Probleme, da dies zu mehrpoligen Spindeln, falscher Aufteilung von Chromosomen und genomischer Instabilität führen kann. Diese Merkmale sind kennzeichnend für Krebszellen. Die Mechanismen der Zentrosomenduplikation sind jedoch noch nicht genau bekannt.

Die vorliegende Untersuchung befaßt sich mit der Rolle des zentrosomalen P4.1-assoziierten Proteins (CPAP) in menschlichen Zellen. Dabei wurde klar, daß dieses Protein nicht nur für effizientes Wachstum von Mikrotubuli ausgehend von Zentrosomen verantwortlich ist, sondern auch die Zentrosomenduplikation reguliert. Hierbei wird CPAP bei einem frühen Schritt während der Bildung von Prozentriolen benötigt, und zwar nach dem Einbau von HsSAS-6 aber vor dem von Centrin. Die Überexprimierung von CPAP führt interessanterweise zu einer abnormen Verlängerung von Zentriolen und Prozentriolen. Dies deutet darauf hin, daß die Menge von CPAP die Zentriolenlänge bestimmt. Übermäßige Mengen an CPAP führen des weiteren zur Bildung von mehreren Prozentriolen entlang von verlängerten Zentriolen, zur Bildung von mehrpoligen Spindeln und zu Fehlern bei der Zellteilung. Daher trägt die exakte Regulierung von Proteinen wie CPAP, welche die Zentriolenlänge bestimmen, zur Integrität des Genoms bei.

Zusammenfassend wurden wichtige Einsichten in die Funktionen von CPAP am Zentrosom gewonnen sowie ein neuer Kontrollmechanismus der Zentriolenlänge entdeckt. Dies wird auch für ein besseres Verständnis dafür sorgen, welche Rolle Zentrosomen bei der Entstehung von Krebs und anderen Krankheiten spielen.

Stichworte: Zentrosom, Zentriol, Zellteilung, Krebs

Contents

1	Introduction.....	1
1.1	Evolution of the Centrosome.....	1
1.2	Centrosome Structure.....	3
1.3	Centrosome Function.....	6
1.4	Centrosome Duplication.....	10
1.5	Regulation of Centriole Number.....	17
1.6	Centrosomes in Cancer and Other Diseases.....	21
1.7	Centrosomal Protein 4.1-Associated Protein (CPAP).....	23
1.8	Aims of this study.....	25
2	Results.....	26
2.1	Analysis of CPAP Protein Structure and Evolutionary Relationship.....	26
2.2	Characterization of CPAP Localization and Dynamics.....	28
2.2.1	CPAP is present in the cytoplasm and at the centrioles.....	28
2.2.2	CPAP protein levels are regulated throughout the cell cycle.....	30
2.2.3	A centriole targeting domain of CPAP lies in the C-terminus.....	32
2.2.4	GFP-CPAP shuttles between the cytoplasm and centrioles.....	34
2.3	The Role of CPAP in Centrosome Duplication.....	36
2.3.1	CPAP is required for centrosome overduplication during prolonged S phase.....	36
2.3.2	CPAP is required for centriole duplication in proliferating cells.....	37
2.3.3	CPAP functions after centriolar recruitment of HsSAS-6.....	41
2.4	The Role of CPAP in Microtubule Regrowth from Centrosomes.....	44
2.5	Effects of Excess CPAP Levels on Centrosome Structure and Function.....	46
2.5.1	CPAP threads protrude from centrosomes and expand over time.....	46
2.5.2	CPAP threads contain core centriolar proteins.....	48
2.5.3	CPAP threads resemble abnormally elongated centrioles.....	49
2.5.4	CPAP threads can elongate from procentrioles and centrioles.....	53
2.5.5	CPAP threads elongate in G2 or shortly thereafter.....	54
2.5.6	CPAP threads associate with PCM and nucleate cytoplasmic microtubules.....	57
2.5.7	CPAP threads template for more than one procentriole per cell cycle.....	57
2.5.8	CPAP overexpression promotes multipolar spindle formation.....	59
2.5.9	CPAP and CP110 regulate centriole length.....	61
2.5.10	CPAP aggregates are assemblies of α -Tubulin, γ -Tubulin and Pericentrin.....	64
2.6	Initial Structure-Function Analysis.....	67

3	Discussion	69
3.1.1	The role of CPAP in procentriole assembly.....	70
3.1.2	A common mechanism for SAS-4, DSas-4 and CPAP?	73
3.1.3	Normal vs. abnormal centriole elongation	75
3.1.4	Regulation of procentriole number	79
4	Materials and Methods	84
4.1	Molecular Biology and Antibody Generation	84
4.2	Cell Culture and Cell Lines.....	86
4.3	Cell Cycle Synchronization and FACS Analysis	87
4.4	RNAi and Transient Plasmid Transfection	87
4.5	Fluorescence Recovery After Photobleaching.....	88
4.6	Multi-Mode Time-Lapse Microscopy	89
4.7	Immunoblotting and Immunofluorescence Microscopy	89
4.8	Electron Microscopy (EM)	91
5	References	93
6	Acknowledgements	103
7	Curriculum Vitae	105

1 Introduction

1.1 Evolution of the Centrosome

The centrosome is the principal microtubule-organizing center (MTOC) of animal cells and is composed of centrioles surrounded by pericentriolar material (PCM). The centrosome is found in eukaryotic species and is notably absent from bacteria and archaea (Figure 1). It is not understood how exactly the centrosome emerged, but it is currently believed that it appeared autogenously together with a microtubule cytoskeleton in early eukaryotic species (discussed in Cavalier-Smith, 2002). Centrioles are microtubule containing structures that can behave as basal bodies to form the axoneme of flagella and cilia (reviewed in Chapman et al., 2000). The presence of flagella and cilia in very ancient eukaryotic species such as *Paramecium* and *Tetrahymena* suggests that the evolutionary appearance of the centriole/basal body structure was intimately linked with its ability to form the axoneme. This link was retained in many eukaryotic species up to humans, where most cells of the body still exhibit a primary cilium that stems from the centriole/basal body (discussed in Dawe et al., 2007). However, in the process of specialization and adaptation, the centriole/basal body underwent changes leading to a great variability in structure and function (discussed in sections 1.2 and 1.3). Sometimes morphological changes are so great that one would be led to conclude that the structures are of different origin. This is the case for the spindle pole body (SPB) in yeast or the nucleus-associated body (NAB) in slime molds. Many of the SPB and NAB components are conserved in centrosomes (reviewed in Adams and Kilmartin, 2000; Dauderer et al., 1999), leading to the notion that these two organelles were derived from centrosomes (Azimzadeh and Bornens, 2004). Certain eukaryotic species, including red algae and most seed plants, do not contain any recognizable centriolar structure, indicating that they have lost the centrosome during evolution. Overall, it seems plausible that the centrosome is a monophyletic organelle that was invented only once, at the root of the eukaryotic lineage.

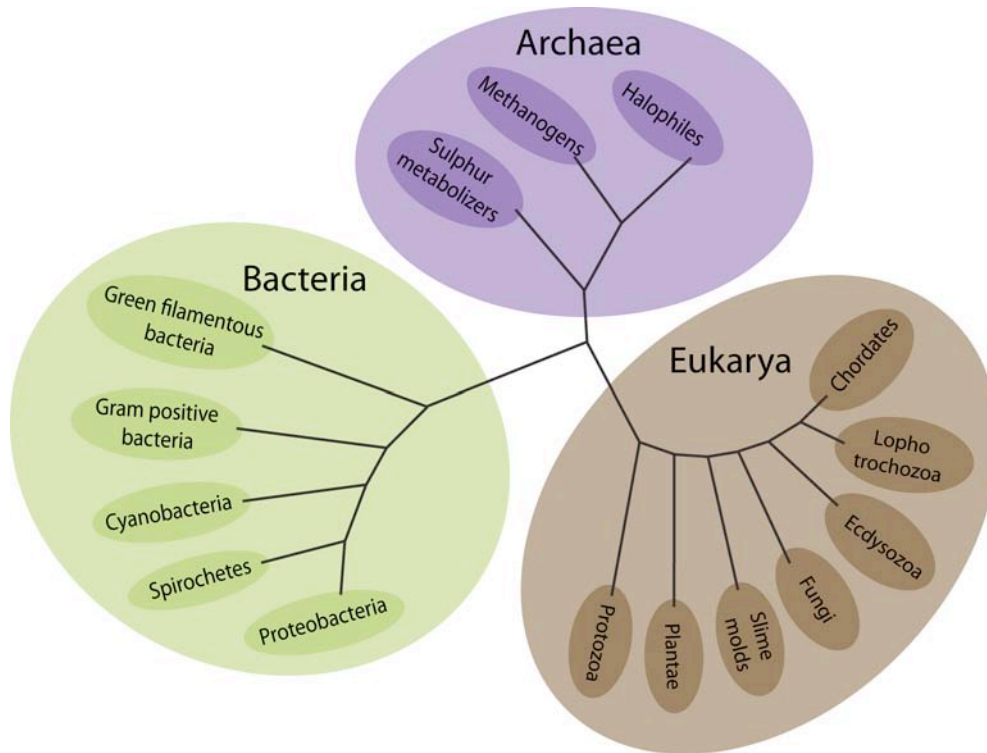


Figure 1: Conservation of the centriolar structure in the tree of life

Simplified phylogenetic tree of life based on Woese's three domain classification (Woese et al., 1990). Within these domains, selected groups of organisms based on recent advances in molecular systematics (Pennisi, 2003) are shown. Model system organisms which contain centrosomes or centrosome-like structures include **protozoa** (the diplomonad *Giardia lamblia*, the euglenozoa *Trypanosoma brucei*, the heterolobosea *Naegleria gruberi*, the apicomplexan *Plasmodium falciparum* and the ciliates *Paramecium tetraurelia* and *Tetrahymena pyriformis*), **plantae** (the green alga *Chlamydomonas reinhardtii* and the fern *Marsilea vestita*), **slime molds** (the mycetozoa *Dictyostelium discoideum* and *Physarum polycephalum*), **fungi** (the ascomycota *Aspergillus nidulans*, *Saccharomyces cervisiae* and *Saccharomyces pombe*), **ecdyszoa** (the arthropod *Drosophila melanogaster* and the nematode *Caenorhabditis elegans*), **lophotrochozoa** (the mollusc *Spisula solidissima*) and **chordates** (the tunicate *Ciona intestinalis*, the zebrafish *Danio rerio* and the vertebrates *Mus musculus*, *Xenopus laevis* and *Homo sapiens*). The term metazoa (animals) collectively refers to chordates, lophotrochozoa and ecdyszoa. Centrosome-like structures are seemingly absent from certain eukaryotic species, among them the red algae (rhodophytes) and some seed plants (angiosperms like *Arabidopsis thaliana* and *Oryza sativa* and conifers like *Ginkgo biloba*) (nomenclature after Azimzadeh and Bornens, 2004).

1.2 Centrosome Structure

The centrosome was seen by early developmental biologists under the light microscope as a “single granule of extraordinary minuteness which stains intensely with iron-hematoxylin” (described by Wilson, 1900, page 309). Advances in electron microscopy (EM) allowed getting more insight into the morphological features of the centrosome. From such analyses, it became clear that a mature centrosome contains two structurally well-defined centrioles surrounded by an amorphous PCM.

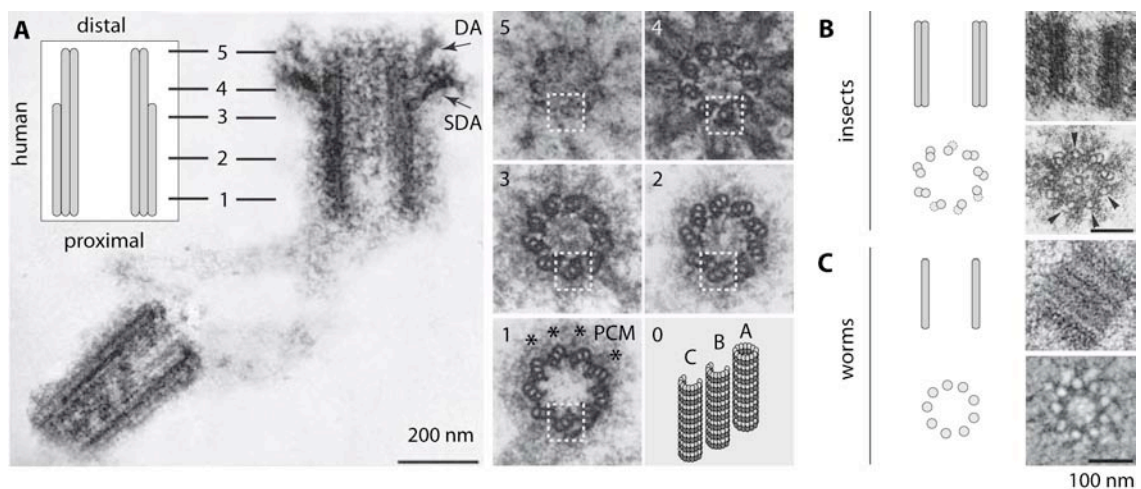


Figure 2: Structural architecture of centrioles

(A) Longitudinal section through a human centrosome revealing two centrioles connected by a linker structure. The PCM surrounds both centrioles as a thin layer. The prominent subdistal appendages (SDA) at the distal end of the mature centriole are followed by less pronounced distal appendages (DA). Note that the mature centriole is filled with electron-dense material except at its proximal end. This place corresponds to where the cartwheel structure is thought to be present in growing procentrioles (reviewed by Strnad and Gönczy, 2008). The inset shows a schematic representation of the mature centriole. Numbers 1-5 correspond to subsequent cross sections through the centriole cylinder, as shown in panels 1-5 on the right. The PCM is indicated with asterisks in panel 1. Note that projections around the centriole cylinder in panel 4 correspond to SDA and in panel 5 to DA. The dashed squares highlight one centriole blade. It is composed of three microtubules termed A-, B- and C-tubule (panel 0) throughout 2/3 of the centriole cylinder and only of the A- and B-tubules throughout its last third. Pictures were adapted from (Hagan and Palazzo, 2006).

(B-C) Longitudinal and cross sections of a *D. melanogaster* centriole during nuclear cycle 14 (B) (Callaini et al., 1997) and a centriole of the early *C. elegans* embryo (C) (Hagan and Palazzo, 2006; Pelletier et al., 2006). Schematic representations are shown on the left. Note that microtubule doublets can be incomplete (arrowheads in B). A circular structure with the diameter of a microtubule is usually seen in the lumen of *Drosophila* centrioles (B). *C. elegans* centrioles do not contain comparable luminal structures but a rim-like central tube that seems to connect centriolar microtubules (C).

Centrioles are the major structural components of centrosomes and universally exhibit a ninefold radial symmetry. A mature centriole in human cells is a ~200 x 500 nm cylinder (Figure 2A) whose walls are formed of nine microtubule blades. These blades consist of microtubule triplets from the “proximal” end until approximately two-thirds of the cylinder (Figure 2A, panel 1-3) and of microtubule doublets thereafter until the “distal” end (Figure 2A, panel 4-5) (Paintrand et al., 1992). The microtubules of such a blade generally have a unique configuration, in that only the innermost A-tubule exhibits the full complement of 13 tubulin protofilaments, whereas the middle B-tubule and the outermost C-tubule share some protofilaments with the neighboring tubules (Figure 2A, panel 0) (Tilney et al., 1973). The C-tubule is approximately one-third shorter than the A- and B-tubules at the distal centriole region. The microtubules forming the centriolar walls resist microtubule depolymerizing conditions (Kuriyama, 1982), indicating that they are especially stable. Accordingly, they also exhibit posttranslational modifications like acetylation and polyglutamylation, which are associated with stabilized forms of microtubules (Bobinnec et al., 1998a; Bobinnec et al., 1998b). Outside of their walls in the distal region, mature centrioles exhibit a tight ring of nine electron-dense subdistal appendages (SDA) (Figure 2A, panel 4) (Paintrand et al., 1992), which appear as γ -shaped projections connecting two adjacent centriole blades in electron tomographic reconstitutions (Ibrahim et al., 2008). The lumen of mature centrioles seems empty at its proximal end but displays an organized internal structure thereafter until its distal end (Figure 2A, panel 2-5) (Ibrahim et al., 2008; Paintrand et al., 1992), supporting the view that the human centriole is not an “empty” cylinder but has a complex internal structure.

Centrioles/basal bodies of different eukaryotic species can exhibit variations notably in length, diameter, number of microtubules per blade, appendages and internal organization. In *C. elegans*, centrioles are ~100 x 150 nm cylinders that are composed of microtubule singlets and do not bear prominent appendages (Figure 2B) (O'Toole et al., 2003; Pelletier et al., 2006; Wolf et al., 1978). In *D. melanogaster*, centrioles exhibit singlet, doublet or triplet microtubules of ~200 nm length depending on the tissue and developmental stage (Figure 2C) (Callaini et al.,

1999). Centrioles/basal bodies in *Drosophila* spermatocytes can reach a length of ~2.6 μm , which is readily visible under the light microscope (reviewed in González et al., 1998). It is notable that centrioles start elongating in primary spermatocytes that still undergo two meiotic divisions, indicating that progression through M-phase can occur with unusually long centrioles.

The PCM is seen by EM as an accumulation of electron-dense material around centrioles (Figure 2A, asterisks in panel 1). The amount of PCM associated with centrioles varies during the cell cycle in mammalian cells. Electron-dense material is seen as a thin sheath of 50-100 nm around the centriole cylinder during interphase and can expand to a diameter of ~1 μm during mitosis (Paintrand et al., 1992; Robbins et al., 1968; Vorobjev and YuS, 1982). The tight association between centrioles and the PCM is preserved during centrosome isolation (Paintrand et al., 1992). Addition of EDTA during centrosome isolation leads to a collapse of PCM around centrioles (Paintrand et al., 1992), indicating that a normal PCM sheath requires Ca^{2+} ions. In centrosomes isolated under very harsh conditions from *Spisula*, centrioles and part of the PCM disassemble, whereas a sponge-like network ('centromatrix') remains intact (Schnackenberg et al., 1998). This filamentous network was interpreted as the basic structural scaffold underlying the PCM. Furthermore, a reticular lattice containing γ -tubulin and pericentrin was described in the PCM of mammalian centrosomes (Dictenberg et al., 1998), suggesting that proteins inside the PCM are also organized in a somewhat structured manner.

1.3 Centrosome Function

The centrosome contributes to several important cellular functions but is not essential for all of them (reviewed by Marshall, 2007). First, the centrosome exhibits the remarkable ability to nucleate and organize a radial array of cytoplasmic microtubules during interphase and promote the formation of the mitotic spindle, which is important for cell division. Proteins like γ -tubulin and pericentrin that concentrate in the PCM contribute to this function (Young et al., 2000). Interestingly, the cytoplasmic microtubule network is not always organized by centrosomes, for instance in polarized epithelial cells, where the microtubule cytoskeleton is organized instead in apico-basal arrays anchored at noncentrosomal sites (Bellett et al., 2009). Conversely, γ -tubulin can focus at spindle poles in the absence of centrioles (Brown et al., 2004; Debec et al., 1995). It is still unclear what is the exact function of the PCM at spindle poles in acentriolar systems. Spindles can also be organized independently of centrosomes, for example during the meiotic divisions of mouse, fly or worm oocytes (Albertson and Thomson, 1993; Matthies et al., 1996; Szollosi et al., 1972). Furthermore, mitotic spindles still form after removal of one or both centrosomes by laser ablation or microsurgery in vertebrate cells (Hinchcliffe et al., 2001; Khodjakov et al., 2000). This is consistent with the ability of microtubules to self-organize into spindles in *Xenopus* egg extracts (Heald et al., 1996), which depends on a gradient of RanGTP around chromatin and molecular motors that focus the spindle poles (reviewed by Karsenti and Vernos, 2001; Ohba et al., 1999). Thus, centrosomes are not essential for the organization of interphase microtubules and the formation of a spindle, although they are dominant in spindle formation if present. Being the primary microtubule-organizing center of animal cells, the centrosome also regulates nuclear positioning, cell polarization, and cell locomotion, and its contribution to these processes is the subject of intense research (reviewed in Higginbotham and Gleeson, 2007; Morris, 2003).

In addition to regulating microtubule-related processes, the centrosome also regulates aspects of cell cycle progression. This becomes evident in cells in which centrosomes are

experimentally removed by laser ablation or microsurgery. Although such cells can build normal mitotic spindles, they often exhibit problems in late stages of cytokinesis and eventually fail to divide (Hinchcliffe et al., 2001; Khodjakov and Rieder, 2001). Partially penetrant cytokinesis defects are seen in a *Drosophila* cell line lacking centrosomes (Piel et al., 2001) as well as larval neuroblasts of DSas-4 mutants that also lack centrosomes (Basto et al., 2006). Careful examination of centrioles by live imaging and fixed cell analysis in vertebrate cells revealed a conspicuous movement of centrioles to the midbody at the time of cytokinesis (Piel et al., 2001). Most interestingly, their movement back in the cell center always correlates with successful abscission, the moment when two cells eventually divide, suggesting that the presence of centrioles near the midbody plays a critical role during cytokinesis. Conflicting reports exist about the requirement of centrioles for progression through the G1 phase. Initial experiments with transformed cell lines indicated that ~88% of cells in which centrosomes were removed with a microneedle arrest in the following G1 phase for up to 60 hours (Hinchcliffe et al., 2001). Khodjakov and coworkers observed related results after laser ablation of one centrosome of a mitotic spindle. While the resulting daughter cells with a single centrosome always progress into S phase, the daughters without a centrosome stay in G1 for more than 70 hours in all cases (Khodjakov and Rieder, 2001). It was also reported that knockdown of any of a dozen centrosomal proteins in retinal pigment epithelial (RPE-1) cells results in a severe G1 arrest that depends on p53 signaling (Mikule et al., 2007). In contrast to these results, however, RPE-1 cells in which centrosomes were removed by either micromanipulation or laser ablation progress through the following G1 and into S phase in ~80% of cases (Uetake et al., 2007). The origin of these apparent discrepancies remains to be determined, but it was suggested that impairment of centrosome structure or function alone does not arrest cells in G1 (Uetake et al., 2007). Only the combination of an additional stress, for instance high intensity laser light during imaging, would lead to a G1 arrest (discussed in Uetake et al., 2007). Removal of centrosomes does not impair progression through S/G2 (Hinchcliffe et al., 2001) and entry into mitosis (Hinchcliffe et al., 2001; Khodjakov and Rieder, 2001). However, centrosomes contribute to nuclear envelope

breakdown in vertebrate cells (Beaudouin et al., 2002) and promote the timing of mitotic entry in *C. elegans* (Hachet et al., 2007). Furthermore, active cyclin B/Cdk1 first appears on centrosomes at the beginning of mitosis (Jackman et al., 2003), and evidence exists that the anaphase-promoting complex (APC) becomes active towards cyclin B initially near centrosomes (Clute and Pines, 1999). Thus, centrosomes seem to serve also as central sites for the coordination of cell cycle transitions (discussed in Doxsey et al., 2005).

A function of centrosomes that is mainly executed by centrioles is the formation of cilia and flagella. Almost every resting cell of the human body harbors a primary cilium, which is an extension of the centriole/basal body that bears appendages. Some specialized epithelial tissues like the airways, the oviduct or the ventricular system in the brain contain many hundreds of cilia in each cell. While there are considerable differences during ciliogenesis in these systems, early stages of ciliogenesis are believed to rely on similar mechanisms (reviewed in Dawe et al., 2007). First, the centriole/basal body is transported to the plasma membrane where it docks via its appendages/transition fibers. Then, the distal region of centriolar microtubules elongates to form the axoneme (Sorokin, 1962; Sorokin, 1968). Cilia and flagella without underlying centrioles/basal bodies have not been observed thus far, suggesting that the centriole/basal body structure is essential for axoneme formation. How axoneme formation from a centriole/basal body is regulated at the molecular level remains enigmatic. Ciliogenesis is inhibited upon interfering with centriole migration to the cell surface by cytochalasin D in quail epithelial cells (Boisvieux-Ulrich et al., 1990), indicating that centrioles need to be in the vicinity of the plasma membrane to form axonemes. Primary cilia formation is also impaired in *Odf2* deficient mouse F9 cells that lack subdistal and distal appendages and exhibit defective docking of centrioles to the plasma membrane (Ishikawa et al., 2005). Centrioles that do not migrate to the membrane still acquire appendages (Boisvieux-Ulrich et al., 1990), suggesting that appendages do not function directly in axoneme formation but rather by enabling centriole docking to the plasma membrane, which in turn allows axoneme formation. Interestingly, core centriolar proteins that are not needed for appendages also regulate the formation of axonemes. This is the case for the centriolar end

capping proteins Cep97 and CP110, whose overexpression in quiescent 3T3 cells results in strongly reduced primary cilia assembly (Spektor et al., 2007). Moreover, the frequency of primary cilia formation in proliferating RPE-1 and 3T3 cells increases by more than twofold upon inactivation of Cep97 or CP110 (Spektor et al., 2007). Using CP110-specific antibodies, the same authors observed a striking disappearance of endogenous CP110 from the centriole/basal body forming the cilium, whereas the neighboring centriole retained the signal. CP110 interacts with CEP290, the depletion of which reduces primary cilia formation in RPE-1 cells (Tsang et al., 2008). Based on these and other data, the authors suggest a model in which CP110 is present at the distal end of the centriole and plays a protective role to prevent inappropriate axoneme formation. Only upon CP110 removal from the centriole end, positive regulators would be allowed to promote axoneme growth from the centriole. In a screen for defective primary cilia formation in RPE-1 cells, many other centrosomal genes were found (Graser et al., 2007). Depletion of pericentrin and Cep164 totally abolishes primary cilia formation, whereas incomplete cilia assemble upon depletion of other centrosomal proteins (Graser et al., 2007). Furthermore, SAS-6 is needed for axoneme formation in mouse tracheal epithelial cells (Vladar and Stearns, 2007). SAS-6 depletion also results in a strongly reduced number of centrioles in these cells, in line with data from human cells where HsSAS-6 depletion impairs centriole duplication (Strnad et al., 2007). These results raise the possibility that SAS-6 depletion might not directly impair axoneme formation but lead to formation of structurally defective centrioles incapable of forming axonemes. Overall, a number of centrosomal proteins regulates ciliogenesis, but their exact roles during this process remain to be determined in most cases.

What other functions do centrioles have? Injection of antibodies against polyglutamylated tubulin in HeLa cells leads to a transient loss of centrioles and PCM assayed by both IF and EM analysis, suggesting that centrioles have an essential function in organizing and maintaining PCM (Bobinnec et al., 1998a). Furthermore, the size of centrioles seems to determine the amount of associated PCM in *C. elegans* (Kirkham et al., 2003). Centrioles have another key function for the duplication of the entire centrosome, which is discussed in the following section.

1.4 Centrosome Duplication

Centrosomes in proliferating cells duplicate once per cell cycle. In human cells, this process can be divided in several steps that were originally described at the ultrastructural level (Kuriyama and Borisy, 1981; Robbins et al., 1968) and can be followed to some extent also under the light microscope using specific markers. One of the most widely used centriole marker that is also employed throughout this thesis is Centrin (Figure 3A), which is an EF-hand protein that is incorporated in the distal centriole lumen (Paoletti et al., 1996). There are four isoforms, with Centrin-2 and -3 being ubiquitously expressed and Centrin-1 and -4 being specific to ciliated epithelia (reviewed in Azimzadeh and Bornens, 2004). Centrin is conserved in a variety of eukaryotes including yeast, where it is called Cdc31p and localizes to a specific domain of the SPB called the half bridge (Spang et al., 1993). Other proteins that localize to specific centriolar regions and that are used throughout this study are summarized in Figure 3A-B.

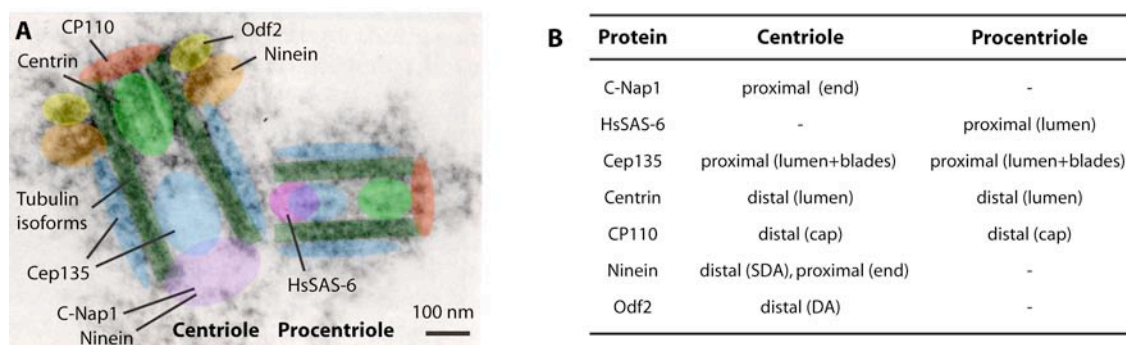


Figure 3: Approximate position of various proteins at human centrioles

(A) Longitudinal section through a human centriole with an associated procentriole, overlaid with the approximate position of various centriolar markers. The indicated localization is based on immuno-EM analysis of centrosomes in tissue culture cells for C-Nap1 (Fry et al., 1998; Mayor et al., 2000), HsSAS-6 (Strnad et al., 2007), Cep135 (Ohta et al., 2002), Centrin (Paoletti et al., 1996), Ninein (Mogensen et al., 2000) and Odf2 (Nakagawa et al., 2001), and on immuno-EM analysis of centrioles forming multiple procentrioles upon Plk4 overexpression in U2OS cells for HsSAS-6, Cep135, Centrin and CP110 (Kleylein-Sohn et al., 2007). Picture was adapted from (Paintrand et al., 1992).

(B) Summary of the localization of the indicated proteins with respect to the centriole or procentriole.

The centrosome in G1 contains two centrioles that are loosely attached through a flexible linker (Figure 4A, 1). One of the centrioles is older and contains appendages that can be detected by the coiled-coil proteins Ninein (Mogensen et al., 2000) or Odf2 (Nakagawa et al., 2001). The physical nature of the centriole linker structure is not known, but it contains the coiled-coil proteins C-Nap1 (Fry et al., 1998) and Rootletin (Bahe et al., 2005). At some point between the G1 and S phase, one procentriole forms at right angle near the proximal region of each parent centriole (Figure 4A, 2). This procentriole is seen by EM initially as an electron-dense fibrous structure without associated microtubules, around which singlet, doublet and triplet microtubules sequentially appear (Anderson and Brenner, 1971; Kalnins and Porter, 1969; Sorokin, 1968). The growing procentriole extends orthogonally to the centriole axis and eventually reaches the same size as the centriole. Due to the small distance between the centriole and its procentriole, which is at or below the resolution limit of light microscopy, very few markers exist that can monitor growing procentrioles by conventional IF analysis. Direct incorporation of α/β -tubulin in procentriolar microtubules cannot be easily visualized because of the high tubulin background signal elsewhere in cells. One reliable readout for the assembly of a procentriole is the appearance of a dimmer procentriolar Centrin signal in close proximity to the brighter centriolar Centrin signal during early S phase (Loncarek et al., 2008; Paoletti et al., 1996). It is not known whether Centrin is incorporated before or after the assembly of centriolar microtubules, but a procentriolar Centrin signal can be discriminated earlier than an associated α -tubulin signal in isolated centrosomes (Middendorp et al., 1997). Another procentriole marker is the coiled-coil protein HsSAS-6, which localizes to the proximal end of growing procentrioles as seen also by immunoelectron microscopy (immuno-EM) analysis (Strnad et al., 2007). In HeLa cells released from an S phase block, there is a transient population of cells with one clear HsSAS-6 focus near each centriole, but without an apparent procentriolar Centrin signal (Strnad et al., 2007), indicating that HsSAS-6 is incorporated in procentrioles before Centrin. Proper procentriole growth seems to depend on cell cycle progression through G2 since only short procentrioles are found in cells arrested in S phase (Loncarek et al., 2008; Rattner and Phillips, 1973). It should be noted that the

procentriole grows to only $4/5^{\text{th}}$ of its full length until the first mitosis (Chrétien et al., 1997), and it takes one more cell cycle for the procentriole – which is now a parent centriole - to reach its final length and also to acquire appendages (discussed in Azimzadeh and Bornens, 2007). Shortly before mitosis, the two centriole/procentriole pairs and associated PCM split and move apart (Figure 4A, 3). This correlates with a major relocalization of centrosomal proteins, with proteins including C-Nap1 (Fry et al., 1998) and Ninein (Chen et al., 2003) disappearing and others including NuMa (Merdes et al., 1996) and Plk1 (Golsteyn et al., 1995) appearing on centrosomes. During mitosis (Figure 4A, 4), the PCM expands in size, as observed also by the expansion of γ -tubulin (Khodjakov and Rieder, 1999) or pericentrin (Doxsey et al., 1994) around centrioles. Late in mitosis, each centriole/procentriole pair loses its orthogonal orientation in a process called disengagement, which is essential for the next round of centrosome duplication (reviewed by Tsou and Stearns, 2006a; Wong and Stearns, 2003).

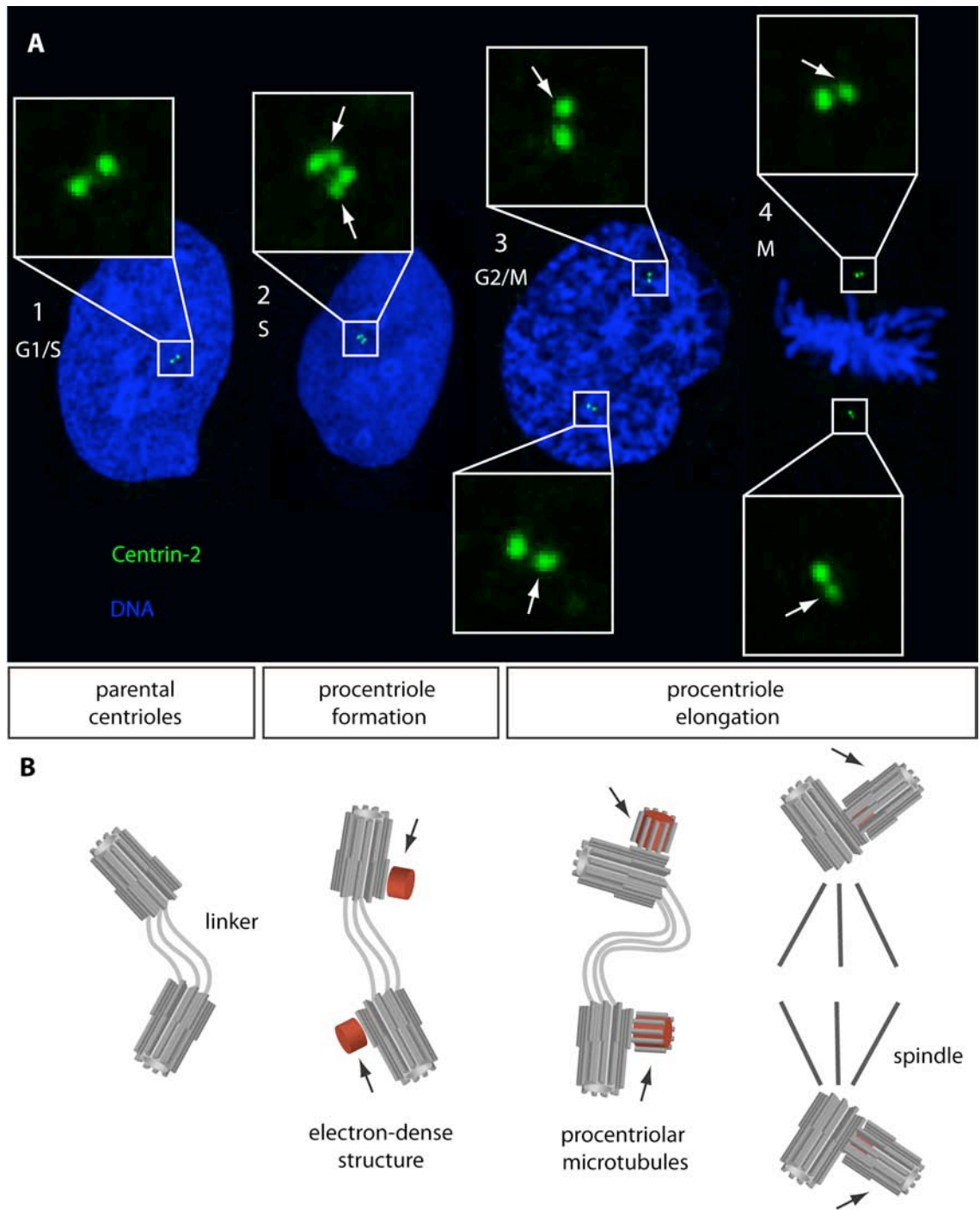


Figure 4: The centrosome duplication cycle in human cells

(A) Proliferating U2OS cells stained with antibodies against Centrin-2 (green). DNA is shown in blue. Centrin stains both centrioles and procentrioles and is commonly used as a rough readout for the status of centrioles in the cell cycle. Two unduplicated centrioles are typical of the G1 phase (1). During S phase, a procentriole appears next to each parent centriole (2). Shortly before mitosis, the two centrosomes split (3) and build up the mitotic spindle in metaphase (4).

(B) Schematic representation of the centrioles / procentrioles corresponding to the cells shown in (A). Arrows highlight procentrioles during subsequent steps of their assembly. It is not known whether the procentriolar Centrin signal (2) corresponds to a procentriole without or with microtubules. It is also believed that microtubules singlets, doublets and triplets are sequentially added. Procentriole elongation continues during S/G2 until mitosis when procentrioles reach nearly full-length.

Centrosome duplication is also extensively studied in the early *C. elegans* embryo. Although centrioles in *C. elegans* differ in some aspects from those in human cells (see section 1.2), it seems that the basic principles of the duplication cycle are conserved across evolution (discussed in Leidel and Gönczy, 2005). In this model system, the sperm contributes two centrioles that recruit maternal PCM components and duplicate, and the resulting centrosomes separate to set up the first mitotic spindle, which all happens within ~20 minutes. Time-resolved electron tomography (ET) allowed to visualize the ultrastructure of procentriole assembly intermediates in *C. elegans* (Pelletier et al., 2006). During S phase, a seemingly hollow tube with the inner diameter of a centriole (~70 nm) but without microtubules appears perpendicularly to centrioles. This central tube elongates to approximately $2/3^{\text{rd}}$ of the final length of the procentriole by prometaphase, when microtubules assemble around this central tube. The procentriole reaches full length at metaphase. Five proteins are known to be essential to build centrioles in *C. elegans* – ZYG-1 (O'Connell et al., 2001), SPD-2 (Kemp et al., 2004; Pelletier et al., 2004), SAS-4 (Kirkham et al., 2003; Leidel and Gönczy, 2003), SAS-5 (Dammermann et al., 2004; Delattre et al., 2004) and SAS-6 (Dammermann et al., 2004; Leidel et al., 2005). While ZYG-1 contains a kinase domain, the remaining four proteins exhibit coiled-coil domains, which are typical of structural proteins and are also frequently observed in centrosomal components of other species (Andersen et al., 2003; Keller et al., 2005). Besides this, other functional domains or motifs are not apparent. Molecular epistasis experiments established an almost linear hierarchy in the recruitment of these proteins to newly forming centrioles (Delattre et al., 2006; Pelletier et al., 2006). First, SPD-2 localizes to the parental centrioles and is required for the recruitment of ZYG-1. SPD-2 and ZYG-1 are required for the recruitment of SAS-5 and SAS-6, which associate with each other and in turn are required for the recruitment of SAS-4. While depletion of ZYG-1, SAS-5 and SAS-6 impairs formation of any detectable procentriolar structure by ET, a central tube without associated microtubules still forms if SAS-4 is depleted by RNA interference (RNAi) (Pelletier et al., 2006). Fluorescence recovery after photobleaching (FRAP) experiments with GFP-SAS-4 show that this protein is recruited only once per cell cycle and stably maintained

thereafter (Leidel and Gönczy, 2003). A more refined FRAP analysis during early stages of procentriole assembly indicates that GFP-SAS-4 apparently exchanges with the cytoplasm between S phase and prometaphase but not any more thereafter (Dammermann et al., 2008). Since prometaphase is the time when procentriolar microtubules are assembled in *C. elegans*, it was hypothesized that this event leads to stable SAS-4 incorporation in procentrioles. Overall, SAS-4 is believed to play a key role for the assembly of procentriolar microtubules in *C. elegans*, but how it does so at the molecular level is unclear.

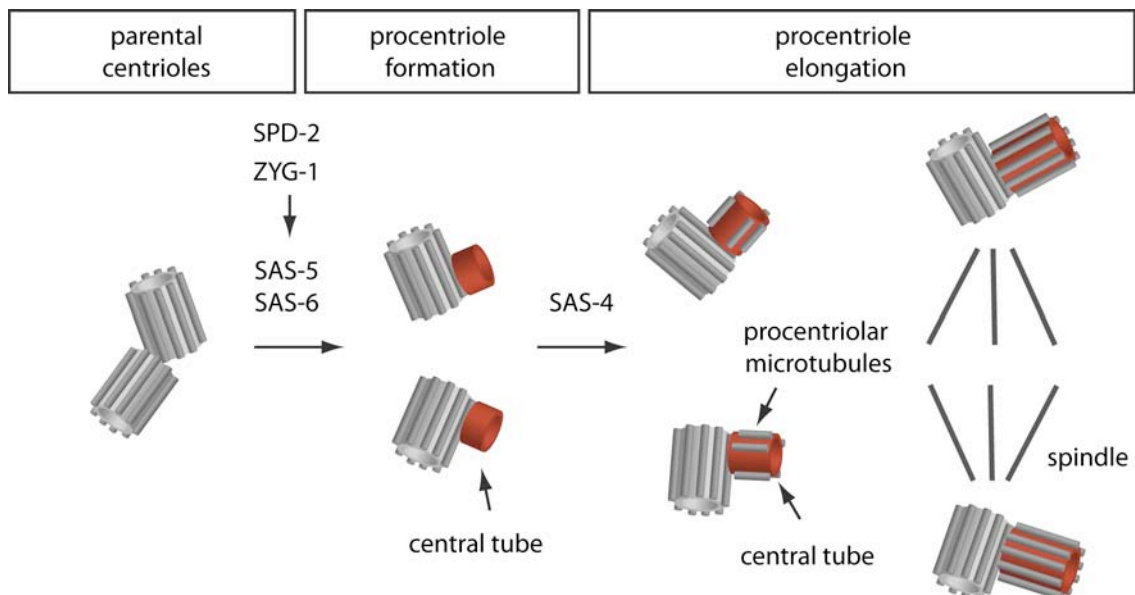


Figure 5: The centrosome cycle in early *C. elegans* embryos

Schematic representation of procentriole assembly intermediates as identified by electron tomography (Pelletier et al., 2006). The first detectable sign of growing procentrioles is a hollow, central tube (red) of ~60 nm length during S phase. It is not clear whether a comparable structure exists in other eukaryotic species. This tube grows to ~110 nm until prometaphase, when singlet microtubules appear around it. Note that procentriolar microtubules do not seem to grow synchronously from the base, but that they become visible as preformed units of a certain length around the central tube. Procentrioles grow to ~150 nm until metaphase. The process of procentriole initiation and elongation takes 12 minutes in the first cell cycle after fertilization. SPD-2, ZYG-1, SAS-5 and SAS-6 are required for central tube formation, whereas SAS-4 is required for assembly of procentriolar microtubules around it.

Distant relatives of four of these five proteins identified in *C. elegans* are also found in other metazoans, including *D. melanogaster* and *H. sapiens*. The overall sequence similarity is generally low and restricted to a block of ~200 aa in SPD-2 (SPD-2 domain) (Pelletier et al., 2004), ~50 aa in SAS-6 (PISA domain) (Leidel et al., 2005) and a loose region of ~70 aa with low sequence similarity in SAS-4 (Leidel and Gönczy, 2003). ZYG-1 was reported to share some sequence similarity with the polo-like kinase Plk4 (also known as SAK) (Bettencourt-Dias et al., 2005), but whether there is a direct evolutionary relationship remains uncertain (pers.comm. Pereira-Leal, ASCB meeting 2007). Despite the low similarity at the amino acid (aa) level, Plk4 is also essential for centriole duplication in *D. melanogaster* (Bettencourt-Dias et al., 2005) and *H. sapiens* (Habedanck et al., 2005). Similarly, the SAS-6-related proteins DSas-6 (Rodrigues-Martins et al., 2007a) and HsSAS-6 (Strnad et al., 2007) are essential for centriole duplication in flies and humans, respectively. Conflicting data about a possible function in centriole duplication were reported for the SPD-2-related proteins DSpd-2 (Dix and Raff, 2007; Giansanti et al., 2008) and Cep192 (Gomez-Ferreria et al., 2007; Zhu et al., 2008). Most relevant to this thesis, somewhat conflicting reports were published for the SAS-4-related proteins DSas-4 and CPAP in flies and humans, respectively. DSas-4 is clearly required for centriole duplication in flies (Basto et al., 2006), and accordingly, depletion of CPAP impairs Plk4-induced centriole amplification in human U2OS cells (Kleylein-Sohn et al., 2007). However, it was also reported that cycling HeLa cells accumulate multipolar spindles in the absence of CPAP (Cho et al., 2006), which is not easily reconciled with a putative function in promoting centriole duplication. Overall, it appears that relatives of at the least some of the proteins regulating centriole duplication in worms similarly do so in flies and humans, confirming the concept that the basic mechanisms of centriole formation are evolutionary conserved.

1.5 Regulation of Centriole Number

Centrioles promote the formation of exactly one procentriole during each cell cycle in proliferating cells. Since the components needed to produce procentrioles are likely to be present in excess, it is not obvious a priori that only one procentriole forms near an existing centriole. Important insight into the regulation of procentriole number comes from cell fusion experiments. Fusion between a G1 and a G2 cell allows duplication of the G1 centrosome but does not induce reduplication of the G2 centrosome (Wong and Stearns, 2003), suggesting that centrosomes contain an intrinsic block to reduplication. The molecular nature of this inhibitory effect is not known. It was proposed that the close association of the procentriole with its centriole (engagement) would somehow contribute to this block, as artificial separation of the procentriole from its centriole (disengagement) in cytostatic factor (CSF) released *Xenopus* extracts results in reformation of a procentriole from the centriole (Tsou and Stearns, 2006b). Laser ablation experiments allowed determining more directly whether physical attachment of the procentriole to its parental centriole inhibits additional procentriole formation. Ablation of the procentriole by a laser microbeam in S phase arrested HeLa cells results in the regrowth of a different procentriole in all cases, which can occur at any position around the proximal centriole region and can also be repeated (Loncarek et al., 2008). These striking results demonstrate that 1) the site of procentriole formation is not predetermined at the parental centriole; 2) the proximal centriole region provides an environment that favors procentriole formation over the distal centriole region; 3) procentriole formation can be repeatedly initiated at a single parental centriole; and 4) regulatory mechanisms that set procentriole number do not act globally but *in cis* for each parental centriole.

More than the normal number of two centrioles and two associating procentrioles can form under several circumstances. Early EM analyses revealed the presence of up to ten procentrioles around a single centriole/basal body in multiciliated cells of the human lung or the rhesus monkey oviduct (Anderson and Brenner, 1971; Sorokin, 1968). These procentrioles are typically arranged

in a radial array around the proximal base of the centriole, although sometimes a second array encircling the centriole midregion can be discerned. This pathway of procentriole formation accounts for ~5% of centrioles/basal bodies in those tissues. However, the vast majority of procentrioles in multiciliated cells assembles around electron-dense granules that do not resemble centrioles and that have been named deuterosomes (Sorokin, 1968).

Multiple centrioles also form in some cell lines like Chinese hamster ovary (CHO) and human osteosarcoma (U2OS) cells arrested for prolonged times in S phase (Balczon et al., 1995; Meraldi et al., 1999). Under those conditions, procentrioles surrounding the parent centriole in a flower-like configuration are seen in ~10% of CHO cells (Loncarek et al., 2008). Live imaging of GFP-Centrin-1 in CHO cells released from mitosis and arrested in the following S phase by hydroxyurea (HU) revealed that the increased centriole number in this case results predominantly from repeated cycles of centriole duplication and disengagement (Loncarek et al., 2008). Notably, procentrioles produced during prolonged S phase do not grow to their final length and also do not acquire appendages (Guarguaglini et al., 2005; Loncarek et al., 2008; Rattner and Phillips, 1973). Nevertheless, such procentrioles are sufficiently mature to promote formation of new procentrioles from their base. Centrosome overduplication during prolonged S phase is often used as a model to study mechanisms of centriole formation. However, inactivation of some proteins, like Cdk2 or CP110, that affect centriole overduplication during prolonged S phase arrest (Chen et al., 2002; Lacey et al., 1999; Matsumoto et al., 1999; Meraldi et al., 1999) do not seem to block centriole duplication in proliferating cells (Chen et al., 2002; Duensing et al., 2006). This raises the possibility that HU-induced procentriole formation is more sensitive to perturbations than regular procentriole formation, or that partially distinct mechanisms underlie both processes.

Interestingly, elevated levels of the centriolar proteins Plk4 (Kleylein-Sohn et al., 2007) and HsSAS-6 (Strnad et al., 2007) can result in the formation of multiple procentrioles around a single centriole in U2OS cells. These supernumerary procentrioles look morphologically normal and harbor the same markers as regular procentrioles (Kleylein-Sohn et al., 2007). Moreover,

depletion of proteins like HsSAS-6, Cep135 or γ -tubulin that regulate centriole duplication in proliferating cells (Haren et al., 2006; Ohta et al., 2002; Strnad et al., 2007) also impairs formation of multiple procentrioles upon Plk4 overexpression (Kleylein-Sohn et al., 2007). This indicates that the mechanisms of Plk4-induced centriole amplification resemble those of regular procentriole formation.

An increased PCM size likewise promotes multiple procentriole formation, as is seen upon overexpression of the PCM component pericentrin in S phase arrested CHO cells (Loncarek et al., 2008). These procentrioles are not arranged in a flower-like configuration as in the previously mentioned cases but more randomly distributed in the PCM cloud around centrioles. Normally, the PCM decorates predominantly the proximal centriole regions (discussed in Azimzadeh and Bornens, 2007), which might explain why procentrioles preferentially form in these regions during regular centriole duplication. The PCM also regulates centriole duplication in HeLa cells, as depletion of the PCM component AKAP450 results in displacement of the endogenous protein from the centrosome and in a reduction of GFP-Centrin-1 foci, which is typical of centrosome duplication defects (Keryer et al., 2003). Moreover, *C. elegans* embryos depleted of the PCM components SPD-5 or γ -tubulin exhibit defects in centriole assembly (Dammermann et al., 2004). Thus, the PCM seems to play important roles during centriole duplication as well as overduplication.

Large numbers of centrioles can arise *de novo* in epithelial cells of the rat nose septum (Stockinger and Cireli, 1965), indicating that this is one means of generating a large amount of centrioles/basal bodies in multiciliated cells. Strikingly, *de novo* centriole formation can be induced also in tissue culture cells like CHO, HeLa and RPE-1 cells by ablating resident centrioles with a laser microbeam (Khodjakov et al., 2002; La Terra et al., 2005; Uetake et al., 2007). *De novo* centrioles are not generated unless the last centriole in a cell is ablated (Khodjakov et al., 2002), suggesting that the presence of a single centriole is sufficient to suppress this process. In the case of HeLa cells in which all centrioles were ablated, dispersed

Centrin aggregates of undefined structure become visible in the cytoplasm during S phase and somehow transform into ultrastructurally recognizable centrioles by the time of mitosis (La Terra et al., 2005). However, the number of centrioles generated in this manner is less stringently controlled, leading to the assembly of multiple centrioles, the formation of extra cleavage furrows and defective cell division in half of the cases. It is currently unclear if the mechanisms to assemble such centrioles are similar to those in regular centriole formation, but at least HsSAS-6 and Plk4 are required also for *de novo* centriole formation in human cells (A. Khodjakov, pers.comm.). Another experimental system where *de novo* centriole formation can be induced is the *Drosophila* oocyte. Here, overexpression of either Plk4, DSas-6 or DSas-4 is sufficient to produce a large amount of new centriole-like structures (Peel et al., 2007). This result is surprising, since it implicates that also downstream regulators of centriole assembly, like DSas-4, can somehow initiate rapid *de novo* formation of centriole-like structures. It remains to be determined by EM whether those structures resemble normal centrioles. However, this response to overexpression of all three proteins seems to be restricted to the oocyte, since in somatic brain cells overexpression of DSas-4 is not sufficient to induce overduplication (Peel et al., 2007), as expected from findings in cultured human cells. This is compatible with the idea that centriole assembly is a multistep process that depends on the sequential activity of upstream, intermediate and downstream regulators.

1.6 Centrosomes in Cancer and Other Diseases

Human tumors frequently exhibit centrosomal abnormalities, including disrupted centriole structure, centrioles of unusual length, excess PCM around centrioles and supernumerary centrioles (Lingle and Salisbury, 1999). A variety of mechanisms can produce such centrosome abnormalities. Aberrations in centrosome structure can arise from defects in centrosome assembly or integrity, and increased centrosome numbers can result from bona fide centrosome overduplication, unscheduled centriole *de novo* formation, failed cytokinesis or cell fusion (reviewed in Nigg, 2002). It is currently unclear how much each of these centrosomal and noncentrosomal mechanisms contributes to the centrosome abnormalities seen in various tumors. Generally, it is also not known to what extent such centrosome abnormalities are the cause or consequence of tumorigenesis *in vivo* (reviewed in Nigg, 2006). An obvious potential consequence of supernumerary centrosomes is the assembly of multipolar spindles, which can result in unequal segregation of the genetic material and thus genetic instability/aneuploidy. However, multipolar mitoses alone cannot explain the high proportion of aneuploidy in human cancers, since mechanisms exist that cluster additional centrosomes and allow bipolar spindle formation in such cases (Quintyne et al., 2005). Nevertheless, cells with multiple centrosomes often undergo a transient multipolar phase before their clustering into two poles, which is a source of kinetochore-microtubule attachment errors and subsequently chromosome missegregation and aneuploidy (Ganem et al., 2009). Aneuploid cells are expected to die in most cases, but might in rare cases acquire oncogenic traits or lose tumor suppressor functions and thus gain tumorigenic potential (reviewed by Hanahan and Weinberg, 2000). Overall, centrosome overduplication can be envisaged to contribute causally to malignant transformation.

Analyses of tumor samples show a correlation between the aberrant centrosome numbers and tumor progression (Pihan et al., 1998; Pihan et al., 2003), and the frequency of centrosome amplification seems to correlate with tumor aggressiveness in breast cancer (D'Assoro et al., 2002). Plk4 heterozygous mutant mice exhibit centrosome amplification, multipolar spindle formation

and development of spontaneous tumors that are most prominent in the liver and lung (Ko et al., 2005). At first glance, this seems to contradict results from *Drosophila* and human tissue culture cells, where overexpression of Plk4 also results in centrosome amplification (Basto et al., 2008; Habedanck et al., 2005; Rodrigues-Martins et al., 2007b). However, the partial loss of Plk4 during development in mice correlates with a strong delay in cell cycle progression notably in S phase and subsequently in mitosis (Ko et al., 2005). This raises the possibility that impaired cell cycle progression contributes to abnormal centrosome amplification in this system. Regardless of the mechanism, the centriole duplication master regulator Plk4 also has an important role as a tumor suppressor during mouse development, and it is tempting to speculate that deregulation of centriole duplication is causally involved in tumorigenesis. *Drosophila* provides an assay for tumor formation, in which donor tissue of any origin is transplanted in the abdomen of wild type adult flies, allowing it to maintain its proliferative potential for longer times (discussed in Gonzalez, 2007). Mutant tissue for Plk4, DSas-6 and DSas-4 can lead to tumor growth in this assay (Basto et al., 2008; Castellanos et al., 2008), whereas mutant tissue for other genes regulating genome stability does not lead to tumor formation, indicating that genome instability alone cannot account for tumorigenicity in this system. Thus, centrosome alterations by various means seem to play a critical role for tumorigenesis.

Heritable human diseases are also associated with centrosome abnormalities. Most of these are linked with defects in ciliogenesis and include Kartagener's Syndrome/Primary Ciliary Diskinesia (PCD), Polycystic Kidney Disease (PKD), Bardet-Biedl Syndrome (BBS), Meckel-Gruber Syndrome (MKS) and Joubert Syndrome (JS) (reviewed in Lancaster and Gleeson, 2009). Autosomal Recessive Primary Microcephaly (MCPH, MIM 251200) is a disorder of fetal brain growth and has been linked with at least seven loci (reviewed in Woods et al., 2005). Genes for four of these loci were identified thus far and code for the centrosomal proteins Microcephalin (MCPH1), CDK5RAP2/Cep215 (MCPH3), ASPM (MCPH5) and CPAP (MCPH6). Mutations identified in these genes mostly result in premature truncations and probably result in loss of function. Intriguingly, a missense mutation in CPAP, identified in one affected family and

expected to change the amino acid glutamate (position 1235) to valine, probably does not lead to a premature truncation (Bond et al., 2005). It remains to be determined what is the consequence of this mutation for CPAP function that eventually leads to development of Primary Microcephaly. It is also unclear why defects in several centrosomal proteins lead to a common phenotype in human brain growth. The currently favored hypothesis posits that these centrosomal proteins by some means generate or maintain the normal number of neurons during development (discussed in Bond and Woods, 2006).

1.7 Centrosomal Protein 4.1-Associated Protein (CPAP)

Several proteins required for centriole assembly in *C. elegans* also regulate this process in human cells, but it was unclear at the beginning of our study whether this is also true for the SAS-4-related protein CPAP. CPAP was first identified in a yeast two-hybrid screen, where its C-terminal 442 amino acids were found to interact with the N-terminal domain of the 135 kD isoform of protein 4.1R (Hung et al., 2000). Protein 4.1R exists in many other isoforms with various intracellular localizations, and immunoreactive epitopes are found around centrioles and in the PCM (Krauss et al., 1997). The 135 kD isoform of protein 4.1R also exhibits binding sites for the nuclear mitotic apparatus (NuMA) protein (Mattagajasingh et al., 1999), and its depletion by RNA interference (RNAi) in HeLa cells results in defective NuMA localization and defective spindle assembly and cytokinesis (Huang et al., 2005; Krauss et al., 2008), indicating that protein 4.1R is required for organizing or maintaining mitotic spindle poles.

CPAP localizes to centrosomes and the cytoplasm in human tissue culture cells (Hung et al., 2000; Peng et al., 2002). In addition, a weak nuclear signal is discernible in MCF-7 cells, which can be enhanced by TNF- α stimulation (Koyanagi et al., 2005). Some reports indicate that CPAP has a nuclear function as transcriptional activator of the NF- κ B (Koyanagi et al., 2005) and Stat5 (Peng et al., 2002) pathways. A wealth of other reports shows that CPAP primarily acts outside the nucleus as a regulator of microtubule dynamics, but the exact role of CPAP in this process is not yet clear. First, addition of CPAP antibodies to isolated human centrosomes inhibits

formation of microtubule asters *in vitro*, indicating that CPAP plays a positive role during microtubule nucleation (Hung et al., 2000). However, a fragment of CPAP corresponding to aa 311 – 422 of the full length protein can inhibit formation of microtubule asters around isolated centrosomes *in vitro*, suggesting that this domain might play a similar role also within CPAP (Hung et al., 2004). The PN2-3 fragment was furthermore shown to depolymerize taxol-stabilized microtubules *in vitro* (Hung et al., 2004), and its overexpression in U2OS cells results in the breakdown of the cytoplasmic microtubule network (Hsu et al., 2008), indicating that this domain is sufficient to destabilize preformed microtubules. Overexpression of the full-length protein does not have a dramatic effect on cytoplasmic microtubule stability (Hsu et al., 2008), but strongly inhibits microtubule reassembly after cold-treatment in mitotic cells (Hung et al., 2004). *In vitro* tubulin binding assays and gel filtration analyses indicate that the PN2-3 fragment stoichiometrically binds α/β -tubulin dimers (Cormier et al., 2009; Hung et al., 2004). The ability to bind α/β -tubulin dimers is abolished when the amino acids 377 and 378 are mutated (Hsu et al., 2008), suggesting that these residues are functionally important. Interestingly, these amino acids reside in the region that shares highest sequence similarity with *C.elegans* SAS-4 (Hsu et al., 2008; Leidel and Gönczy, 2003), furthermore indicating that this region plays an important functional role.

Multiple and in part contradicting results were reported upon depletion of CPAP in tissue culture cells. First, treatment of U2OS cells with CPAP siRNAs resulted in the formation of monopolar spindles (initial analysis by Sebastian Leidel in our laboratory), raising the possibility that CPAP is somehow needed for centrosome duplication. Second, ~40% multipolar spindles with foci of γ -tubulin and NuMa at each pole were observed upon CPAP RNAi in HeLa cells (Cho et al., 2006), which can be the result of centrosome overduplication, impaired centrosome integrity or cytokinesis defects. Third, CPAP inactivation by siRNAs impaired Plk4-mediated centriole overduplication (Kleylein-Sohn et al., 2007), supporting the notion that CPAP regulates centrosome duplication.

1.8 Aims of this study

To clarify the contributions of CPAP to centrosome duplication and microtubule nucleation from the PCM, and to potentially uncover novel roles of CPAP at the centrosome in human cells, we focused our research on four main topics during this PhD study:

1. Characterizing the localization and dynamics of CPAP at human centrosomes
2. Determining the role of CPAP in centrosome duplication
3. Determining the role of CPAP in microtubule nucleation
4. Analyzing the effects of excess CPAP levels on the structure and function of centrosomes

2 Results

2.1 Analysis of CPAP Protein Structure and Evolutionary Relationship

CPAP has been reported to contain five coiled-coil regions and a T-complex protein 10-like domain (TCP domain from here on) (Hung et al., 2000). To reexamine the boundaries of these domains and perhaps identify new ones, we analyzed the sequence of CPAP with several classification tools¹²³ (Figure 6). This analysis revealed that the fourth and fifth coiled-coil (CC) domains are probably fused and therefore referred to as CC4 from here on. In addition, CPAP contains two predicted D-boxes (aa 162-169 and 1112-1120) and two regions (aa 500-502 and 570-572) that resemble the proposed KEN-box consensus sequence (Pfleger and Kirschner, 2000), suggesting that the protein might be cell cycle regulated. In addition, five nuclear localization signals (aa 671-677, 840-857, 988-994, 1054-1070, 1093-1110) are predicted, indicating that CPAP may also localize to the nucleus.

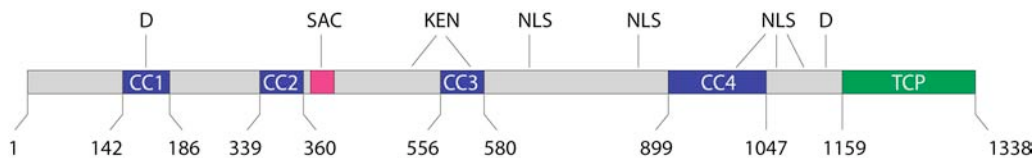


Figure 6: CPAP structure and putatively interesting regions

Schematic representation of the CPAP protein (grey) with regions of putative interest. The four coiled-coil (CC) domains are represented in blue, the TCP domain in green and the SAC-box (described in Figure 7) in pink. Positions of the amino acids (aa) bordering each CC, the TCP domain and the full-length protein are shown.

Distant amino acid sequence similarity between *H. sapiens* CPAP, *D. melanogaster* DSas-4 and *C. elegans* SAS-4 was observed in the protein N-termini (Leidel and Gönczy, 2003). To refine the evolutionary relationship between these proteins, we compared the CPAP protein sequence with putative homologs from recently sequenced species. We found the highest conservation among putative CPAP homologs from arthropods to primates in their C-termini,

¹ http://smart.embl-heidelberg.de/smart/set_mode.cgi?NORMAL=1 (query for Q9HC77)

² <http://bioinfo.weizmann.ac.il/~danag/d-box/main.html>

³ <https://npd.hgu.mrc.ac.uk/> (query for CENPJ)

with 31% sequence identity in the last coiled coil and 44% sequence identity in the TCP domain between *H. sapiens* CPAP and *D. melanogaster* DSas-4. Thus, CPAP and DSas-4 are clearly evolutionary related. The highest homology with the SAS-4 protein in nematodes was found in a stretch of 16 amino acids, which we dubbed the SAC-box (similar in SAS-4 and CPAP, aa 370 - 385) (Figure 7). A ~70 amino acid region surrounding the SAC-box also contained some conserved residues (Leidel and Gönczy, 2003). Due to this very restricted sequence relatedness it was uncertain whether CPAP and SAS-4 would be functionally related at the onset of our study.

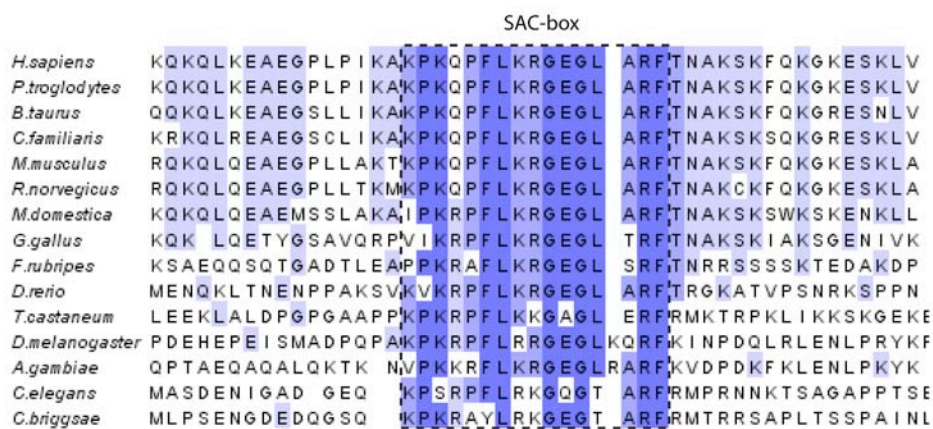


Figure 7: The conserved SAC-box

Multiple sequence alignment of a short region around the SAC-box (dashed box) in putative CPAP homologues from different species. Alignment and coloring were made in ClustalW and Jalview (light blue=over 50% conservation, dark blue=over 75% conservation). The SAC-box of *H. sapiens* displays 76% sequence identity with the one in *D. melanogaster* and 62% with the one in *C. elegans*.

2.2 Characterization of CPAP Localization and Dynamics

2.2.1 CPAP is present in the cytoplasm and at the centrioles

CPAP was described as a protein that is enriched at centrosomes, similarly to γ -tubulin (Hung et al., 2000). To reinvestigate the distribution of CPAP, we raised antibodies against the protein C-terminus (aa 1070 – 1338, CPAP^{C-term}) and the PN2-3 fragment (aa 311 – 422, CPAP^{PN2-3}) (see 4.1, p.84). As expected, both antibodies labelled two major dots in interphase cells that were also recognized by γ -tubulin antibodies (Figure 8A, C). The CPAP^{C-term} antibodies also labelled the cytoplasm to a lesser extent (Figure 8A'). These signals were specific, since they were greatly reduced or gone in CPAP siRNA treated cells (Figure 8B, B' and D). The CPAP^{C-term} antibodies were also tested by Western Blot analysis of whole cell extracts and detected one specific band above ~180 kD, which is ~30 kD higher than predicted (Figure 14I).

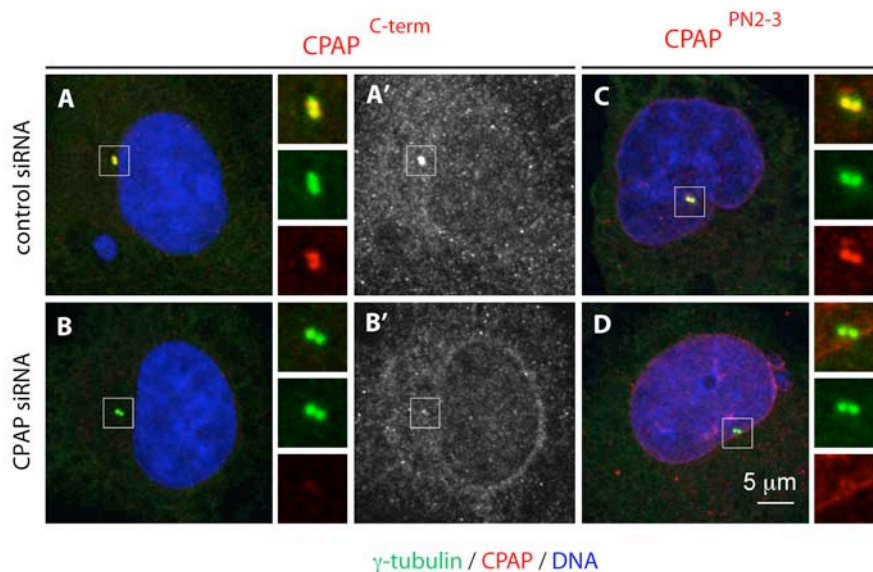


Figure 8: Antibodies against CPAP are specific

(A-D) U2OS cells transfected with the indicated siRNAs for 48 hours and stained with antibodies against γ -tubulin (green) and CPAP (red). Signals for both CPAP^{C-term} (A-B) and CPAP^{PN2-3} (C-D) antibodies are shown. DNA is viewed in blue in this and following figure panels (except in Figure 9), and insets show higher magnification views of denoted regions of interest. (A') and (B') show the electronically enhanced CPAP signals of the cells in (A) and (B), respectively, to highlight the specific CPAP signals in the cytoplasm. Note that the CPAP^{PN2-3} antibodies also stain the edges of the nucleus, which is most likely unspecific. Note also that control siRNAs here and in following figure panels, if not otherwise indicated, target GFP as described (Strnad et al., 2007).

We characterized the localization of CPAP at the centrosomes using a triple-labeling protocol and high-resolution confocal microscopy. In this experimental setup, GFP-Centrin-1 stably expressed in U2OS cells (Piel et al., 2000) served as a marker for the distal part of the centriole and procentriole, whereas γ -tubulin antibodies marked the PCM. Both γ -tubulin and CPAP - as determined with CPAP^{C-term} antibodies - localized at the centrioles in interphase (Figure 9A). During mitosis, the CPAP signals concentrated at the centriole and procentriole of each spindle pole, whereas γ -tubulin signals concentrated in the PCM cloud around the centrioles (Khodjakov and Rieder, 1999) (Figure 9B). It should be noted that slight CPAP signals were also detected in the PCM. Analogous CPAP distributions were found with CPAP^{PN2-3} antibodies (Figure 9C-D) as well as in HeLa cells stably expressing GFP-Centrin-1 (Piel et al., 2000) (data not shown). We conclude that CPAP largely concentrates at centrioles and procentrioles during interphase and mitosis.

To map the position of the CPAP signal on the centriole cylinder, we used C-Nap1 and GFP-Centrin-1 antibodies to mark the proximal and distal centriole ends, respectively (Strnad et al., 2007). The center of the CPAP signal was consistently found on the centriole axis between the C-Nap1 and GFP-Centrin-1 foci. Measuring the distances between the center of each signal in favorably oriented centrioles revealed that the CPAP focus lies ~230 nm away from that of C-Nap1 (Figure 9E, F), corresponding approximately to the middle of the centriole cylinder (Figure 9G). Using immuno-EM analysis, another study reported that CPAP localizes to the proximal centriole lumen upon Plk4-induced centriole overduplication (Kleylein-Sohn et al., 2007), although additional association of CPAP with the outer centriole walls could not be excluded. Our own attempts to localize CPAP by immuno-EM did not meet with success, as the epitopes recognized by our antibodies were not preserved upon glutaraldehyde or paraformaldehyde fixation (collaboration with Ursula Euteneuer), precluding us to further determine where exactly at the centriole cylinder CPAP resides.

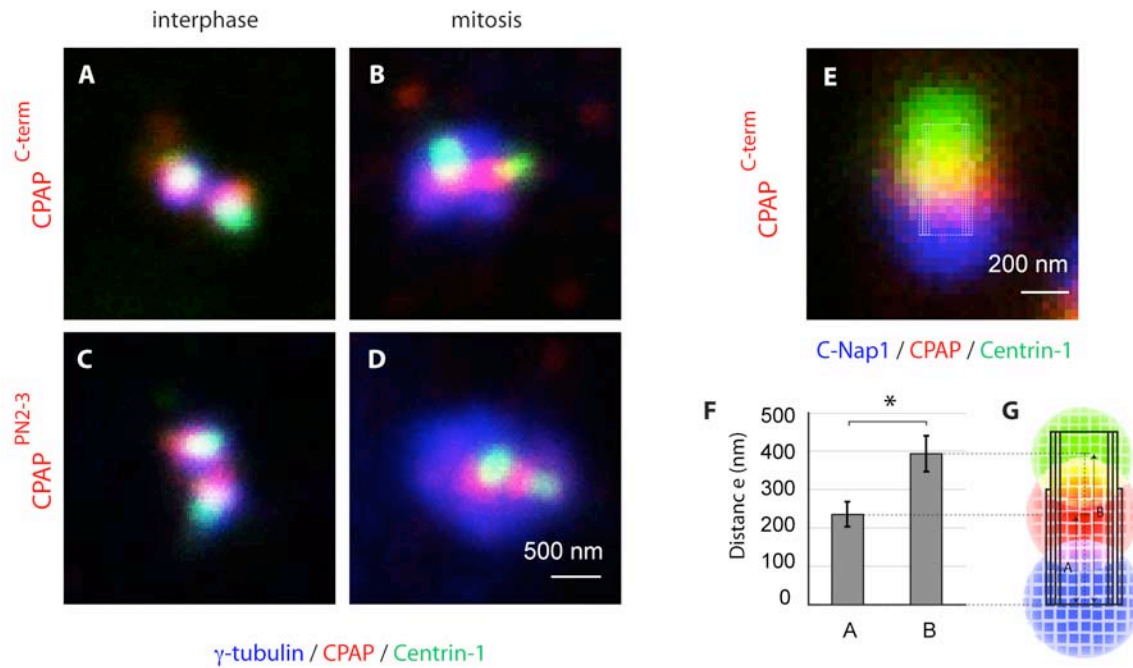


Figure 9: CPAP localizes to the centriole cylinder

(A-D) U2OS cells stably expressing GFP-Centrin-1 were stained with antibodies against γ -tubulin (blue), CPAP (red) and GFP (green). Both CPAP^{C-term} (A-B) and CPAP^{PN2-3} antibodies (C-D) were used to detect CPAP in interphase (A, C) and mitosis (B, D). For mitotic cells, only the centrosome of one spindle pole is shown (B, D). Note that the CPAP signals concentrate at centrioles and procentrioles in mitosis, but that some CPAP signals are also detected in the PCM (B, D).

(E-G) U2OS cells stably expressing GFP-Centrin-1 were stained with antibodies against C-Nap1 (blue), CPAP (red) and GFP (green). Only CPAP^{C-term} antibodies were tested in this assay. Distances between the center of C-Nap1 and CPAP were measured for 20 interphase centrioles with a minimal distance of 300 nm between the center of C-Nap1 and GFP signals (F). Error bars represent standard deviation of the measurements, and the star indicates that both values (A and B) are significantly different (two-tailed Student's t-test, $p < 0.05$). The center of each signal was mapped on a hypothetical centriole with $\sim 150 \times 450$ nm dimensions (E, G).

2.2.2 CPAP protein levels are regulated throughout the cell cycle

We determined the fluctuation in CPAP protein levels during the cell cycle. To this end, we synchronized HeLa cells by a double thymidine arrest and took samples at various times upon their release into S phase, mitosis and the following G1 phase. These samples were analyzed by flow cytometry and Western blot analysis. Interestingly, CPAP protein levels were not constant but gradually increased during S/G2 up to mitosis, after which they again decreased (Figure 10A-B). This is slightly different from HsSAS-6, which also displays a cycling behavior but increases earlier during S/G2 and decreases more abruptly during mitosis (Figure 10A-B) (Strnad et al., 2007). To corroborate these results, we analyzed CPAP protein levels by quantitative

immunofluorescence microscopy in unsynchronized U2OS cells labelled with antibodies against Centrin-2. The pattern of Centrin-2 foci usually allows us to distinguish cells in the G1 or early S phase (two clear Centrin foci) from cells in the late S or G2 phase (two strong and two weak Centrin foci) (Strnad et al., 2007). We found that CPAP signals steadily increased during G2 and mitosis, both at the centrioles (Figure 10C) and in the cytoplasm (Figure 10D, visualized in E-G). Centriolar signals were still detected during cytokinesis and in the early G1 phase when the midbody was present (data not shown), indicating that CPAP persists at the centrioles after mitosis. Together, these results establish that CPAP levels in the cytoplasm and at the centrioles are cell cycle regulated.

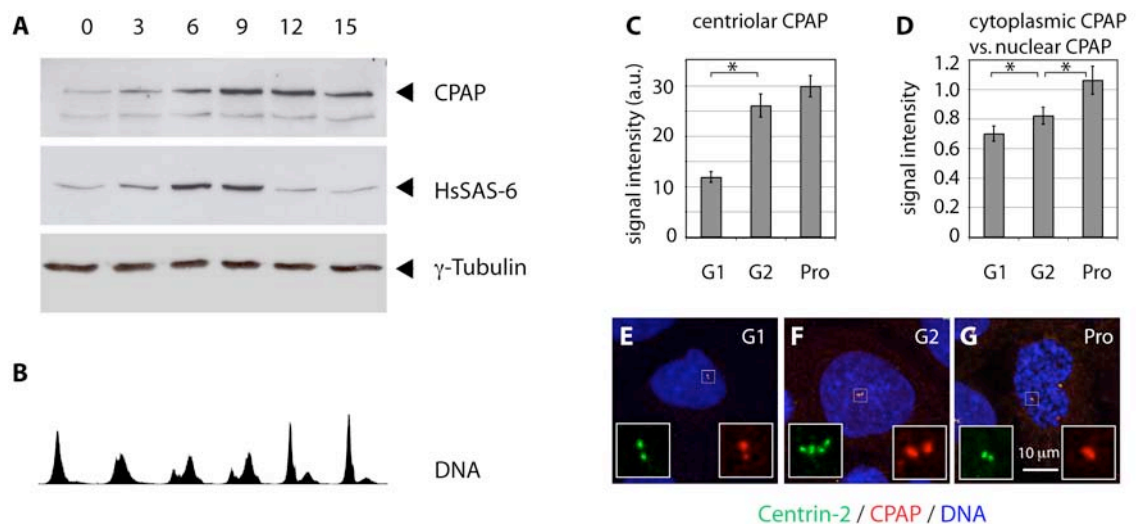


Figure 10: CPAP protein levels are cell cycle regulated

(A-B) HeLa cells released from a double thymidine block and analyzed at the indicated time points by Western blot using antibodies against CPAP, HsSAS-6 and γ -tubulin (A), as well as by flow cytometry for DNA content (B). Time points refer to 'hours after release' from the double thymidine block.

(C-G) Cycling U2OS cells were stained with antibodies against CPAP (red) and Centrin-2 (green). Signal intensities were quantified for 10 cells with two clear Centrin-2 foci (denoted as 'G1', E), two unseparated Centrin-2 pairs (denoted as 'G2', F) and two separated Centrin-2 pairs at the time of DNA condensation / Prophase (denoted as 'Pro', G), respectively. Intensities of regions of interest were normalized to background signals (C-D). Centriolar CPAP intensities are represented in arbitrary units (a.u.) (C), and cytoplasmic CPAP intensities are represented relative to nuclear CPAP intensities (D), which do not change throughout the cell cycle (data not shown). The increasing centriolar CPAP intensities in G2 and early mitosis (C) may either reflect the increase of procentriole size or an increased association with pericentriolar regions during these periods. A correlation with Centrin-2 signals would be needed to distinguish between these possibilities. Error bars represent 95% confidence intervals ($n = 10$ for each timepoint), and stars indicate that the values are significantly different (two-tailed Student's t-test, $p < 0.05$). CPAP^{C-term} antibodies were used in these (A, E-G) and upcoming experiments to reveal CPAP.

2.2.3 A centriole targeting domain of CPAP lies in the C-terminus

We next set out to identify which domain of CPAP targets the protein to centrioles. Immunostaining of Centrin-2 and GFP confirmed that ectopic GFP-tagged full-length CPAP (CPAP-FL) also localized at centrioles and in the cytoplasm (Figure 11A). Thus, we generated three GFP-tagged truncated mutants of CPAP covering its entire length (Table 1A, p.85) and analyzed their intracellular localization. We found that the C-terminal construct (CPAP-CT) comprising the CC4 and the TCP domain localized at centrioles and in the cytoplasm (Figure 11D), similar to the full-length protein. In contrast, the N-terminal (CPAP-NT) and central (CPAP-MI) constructs were never detected at centrioles but were predominantly present in the cytoplasm (CPAP-NT) or the nucleus (CPAP-MI) (Figure 11B-C). To further map the centriole targeting domain to the CC4 or the TCP domain, we generated deletions of either domain in GFP-tagged full-length CPAP (CPAP- Δ CC4 and CPAP- Δ TCP) as well as fragments containing each domain alone fused to GFP (CPAP-CC4 and CPAP-TCP) (Table 1B). We observed that the full-length construct lacking CC4 no longer localized to centrioles (Figure 11E), whereas the fragment containing CC4 alone was detected at that location (Figure 11G). By contrast, we could not detect centriolar signals with the fragment containing the TCP domain alone, whereas the full-length construct lacking this domain still localized to centrioles (Figure 11F, H). From these observations, we conclude that CC4 is both necessary and sufficient for targeting CPAP to centrioles. However, we also noted that the intensity of the CC4 construct at centrioles was in general lower than that of full-length CPAP. Thus, it appears that other parts of CPAP contribute to its robust centriolar localization.

We also generated GFP-tagged constructs of full-length CPAP with deletions removing the SAC-box (CPAP- Δ SAC) or the PN2-3 fragment (CPAP- Δ PN2-3) (Hung et al., 2004), and with a single amino acid mutation that is associated with primary microcephaly (CPAP-E>V) (Bond et al., 2005) (Table 1). The three resulting proteins were consistently detected at centrioles (Figure

11J-L), suggesting that the SAC-box, the PN2-3 region and the amino acid E1235 affected in the familial disease are not required for targeting CPAP to centrioles.

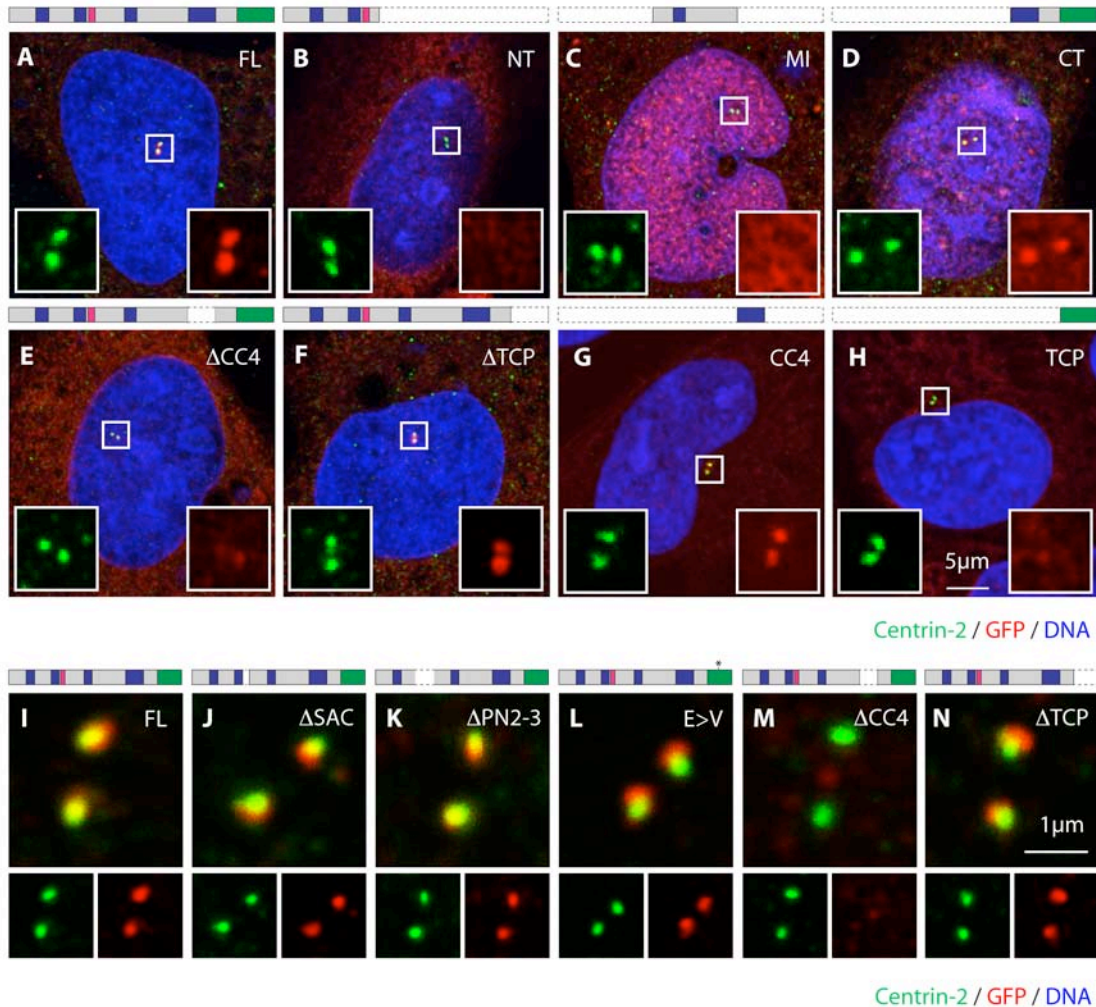


Figure 11: Centriole targeting of CPAP is mediated by the CC4 domain

(A-F) U2OS cells transiently transfected with GFP-tagged CPAP-FL (A), CPAP-NT (B), CPAP-MI (C), CPAP-CT (D), CPAP- Δ CC4 (E) and CPAP- Δ TCP (F) for 48 hours and stained with antibodies against Centrin-2 (green) and GFP (red). Note that a very low GFP signal was still detectable at centrioles in (E, H), whereas an asymmetric localization with one diffuse signal around one Centrin-2 focus was apparent in (F).

(G-H) U2OS cells harboring an inducible expression vector for GFP-tagged CPAP-CC4 (G) and CPAP-TCP (H) (Table 1), induced for 48 hours and stained with antibodies against Centrin-2 (green) and GFP (red). Note that the intensity of GFP at centrioles (G) was lower than for the full-length protein (A).

(I-N) High magnification view of centrioles in U2OS cells harboring an inducible expression vector for GFP-tagged CPAP-FL (I), CPAP- Δ SAC (J), CPAP- Δ PN2-3 (K), CPAP-E>V (L), CPAP- Δ CC4 (M) and CPAP- Δ TCP (N), induced for 38 hours and stained with antibodies against Centrin-2 (green) and GFP (red). Note that only unduplicated centrioles are shown (I-N), but similar staining patterns were observed at duplicated centrioles. Schematic representations of each construct are indicated above (A-N) according to Table 1.

2.2.4 GFP-CPAP shuttles between the cytoplasm and centrioles

Having established that CPAP localizes to centrioles and in the cytoplasm (see Figure 10C-D), we wanted to determine the dynamics of its centriolar recruitment. For this purpose, we performed fluorescence recovery after photobleaching (FRAP) experiments with cells overexpressing GFP-CPAP. Cells expressing GFP-Centrin-1 served as a control cell line (Piel et al., 2000). Strikingly, ~60% of the centrosome-associated GFP-CPAP fluorescence signal recovered within 3 minutes after photobleaching (Figure 12A-B), whereas the centrosomal GFP-Centrin-1 signal did not substantially recover after photobleaching within this time frame (Figure 12C). Analogous FRAP results for GFP-Centrin-1 were obtained by the laboratories of A. Khodjakov (pers. comm.) and A. Fry (Prosser et al., 2009). To test whether the dynamic behavior of GFP-CPAP is cell cycle regulated, we analyzed the recovery profiles of cells photobleached at various timepoints after release from a double thymidine block. Very similar recovery kinetics were observed in cells during S, G2 or the following G1 phase (Figure 12D), indicating that CPAP dynamics is not cell cycle regulated. We assessed whether GFP-tagged CPAP-CT or CPAP- Δ TCP could recapitulate the kinetics observed with the full-length protein. Indeed, similar recovery profiles were observed for both fusion proteins (Figure 12D). Given the rapid recovery of GFP-CPAP to ~60% of the initial fluorescence intensity within 3 minutes after photobleaching, we also wondered whether the signal would recover further at later timepoints. Therefore, we analyzed cells up to 60 minutes after photobleaching and observed a slow but steady increase to ~90% of the initial fluorescence intensity at centrosomes (Figure 12E). This long-term recovery curve could be fitted best with a bimodal distribution of data points (Figure 12E), hinting towards the existence of two independent centriolar CPAP populations, one with fast and one with slow recovery kinetics. Collectively, these data demonstrate that a sizeable fraction of CPAP at centrosomes is in dynamic exchange with the cytoplasmic pool.

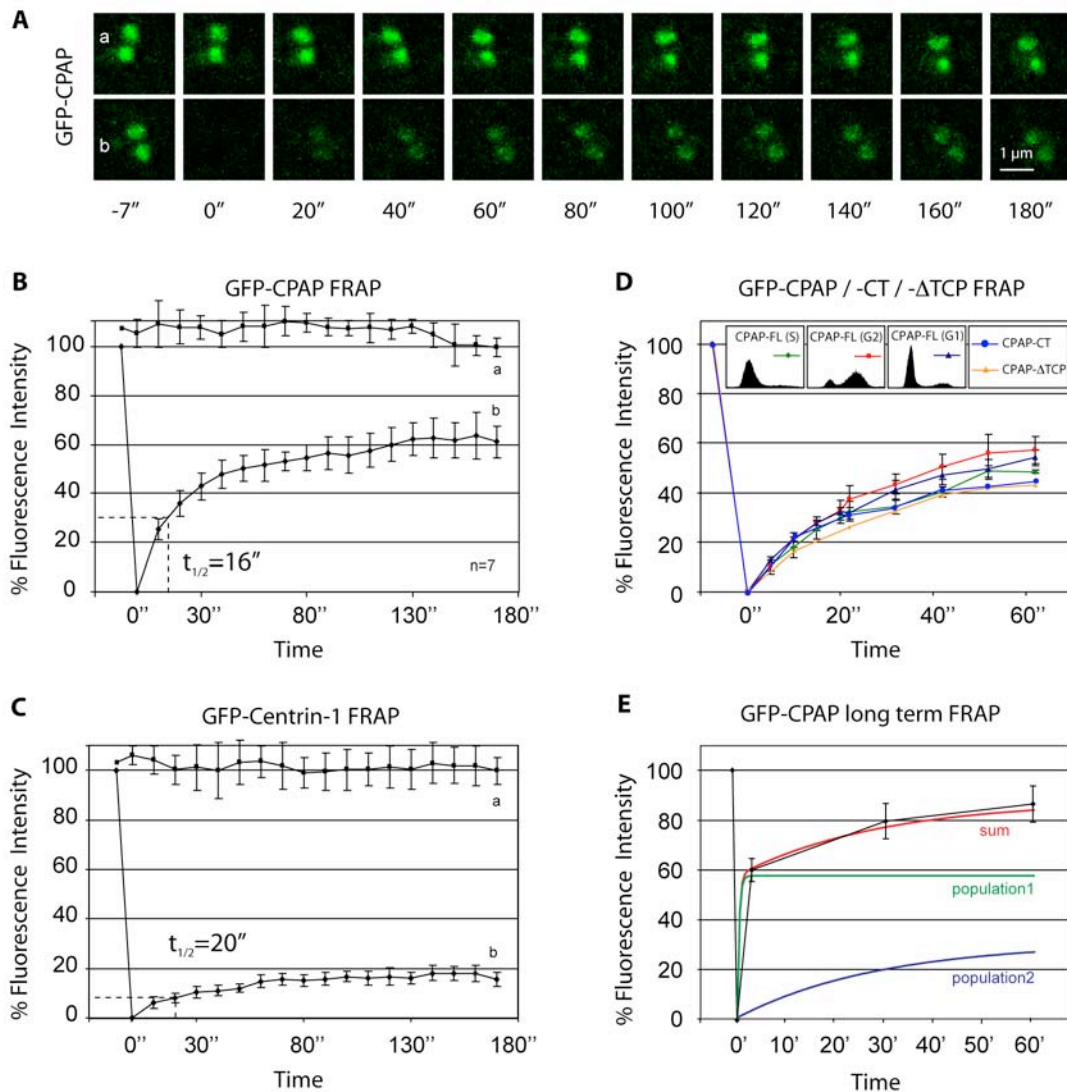


Figure 12: CPAP dynamically associates with centrioles

(A) HeLa cell transiently transfected with full-length GFP-CPAP for ~24 hours. Centriole-associated fluorescence was followed for 3 minutes before photobleaching (a) and for another 3 minutes after (b) photobleaching in the same cell.

(B-C) Centriole-associated fluorescence signals in HeLa cells expressing GFP-CPAP (B) or GFP-Centrin-1 (C) were recorded over 3 minutes before (a) and after photobleaching (b). Error bars represent 95% confidence intervals at each timepoint ($n = 7$ for B and $n = 9$ for C). The time of recovery to half of the plateau phase reached within the timeframe of the experiment ($t_{1/2}$) was determined as 16 seconds for (B) and 20 seconds for (C).

(D) 60 second FRAP profiles of HeLa cells expressing GFP-CPAP and released from a double thymidine block for 0 hours (S, green), 6 hours (G2, red) and 16 hours (G1, purple). Error bars represent 95% confidence intervals at each timepoint ($n = 5$ for each condition). HeLa cells expressing GFP-tagged CPAP-CT (blue) and CPAP-ΔTCP (orange) were also analyzed by FRAP for 60 seconds.

(E) Centriole-associated fluorescence signals in iGFP-CPAP U2OS cells (Table 1) analyzed at 3, 30 and 60 minutes after photobleaching. Error bars represent 95% confidence intervals at each timepoint ($n = 7$). The recovery profile could be fitted best with a curve representing the sum (red) of a fast (green, $t_{1/2} \sim 20$ seconds) and slowly (blue, $t_{1/2} \sim 16.5$ minutes) recovering population.

2.3 The Role of CPAP in Centrosome Duplication

Whereas CPAP has been reported to be implicated in regulating centrosome duplication as well as microtubule nucleation from centrosomes (see section 1.7), the published data and their interpretation are in part contradicting. In an attempt to clarify these observations, we examined in more detail the role of CPAP in centrosome duplication.

2.3.1 CPAP is required for centrosome overduplication during prolonged S phase

In various cell lines including U2OS cells, centrosomes repeatedly duplicate during prolonged S phase arrest (Balczon et al., 1995; Meraldi et al., 1999), a process that underlies similar but less stringent control mechanisms compared to centrosome duplication in proliferating cells (see section 1.5). To test whether CPAP is required for centrosome duplication, we first used siRNAs to downregulate CPAP expression during aphidicolin induced S phase arrest in U2OS cells and scored the number of centrosomal C-Nap1 and γ -tubulin foci, which overlapped. We found that ~56% of cells treated with control siRNAs contained more than two such centrosome foci (Figure 13A, C), whereas this was observed in only ~23% of cells treated with CPAP siRNA3 (Figure 13B, C). Similar findings were obtained with siRNAs targeting a different region within the CPAP coding sequence (Figure 13C, siRNA1), indicating that this phenotype is probably not caused by siRNA off-target effects. We conclude that CPAP is required for efficient centrosome overduplication in S phase arrested U2OS cells.

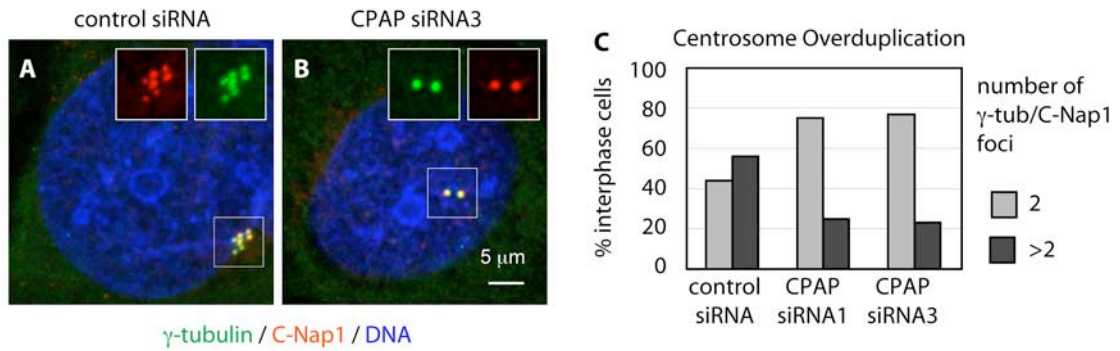


Figure 13: CPAP is required for repeated centrosome duplication during S phase arrest

(A-B) U2OS cells transfected with the indicated siRNAs for 72 hours, incubated with aphidicolin for the final 48 hours and stained with antibodies against γ -tubulin (green) and C-Nap1 (red).

(C) The number of γ -tubulin and C-Nap1 positive foci was scored ($n > 165$ for each siRNA).

2.3.2 CPAP is required for centriole duplication in proliferating cells

We next addressed whether CPAP is also required for centrosome duplication in proliferating cells. We therefore treated U2OS cells with CPAP siRNA3 for several cell cycles and scored the number of Centrin-3 foci during mitosis. More than 95% of mitotic cells treated with control siRNAs contained four Centrin-3 foci, two at each spindle pole (Figure 14A, E-F). Strikingly, upon treatment with CPAP siRNA3 for 48 hours, an increased number of mitotic cells contained only two Centrin-3 foci, mostly one at each spindle pole (Figure 14B), or only one Centrin-3 focus, either at one pole of a bipolar spindle (data not shown) or in the center of a monopolar spindle (Figure 14C, F). After 72 hours of siRNA3 treatment, the number of mitotic cells containing only one Centrin-3 focus increased to ~44% (Figure 14F). Analogous results were obtained with CPAP siRNA1 in U2OS cells (Figure 14E), as well as in HeLa cells treated with either siRNA species (Figure 14G-H). Both CPAP siRNA species also significantly reduced the specific signal in Western blot analysis (Figure 14I), demonstrating that CPAP was severely depleted.

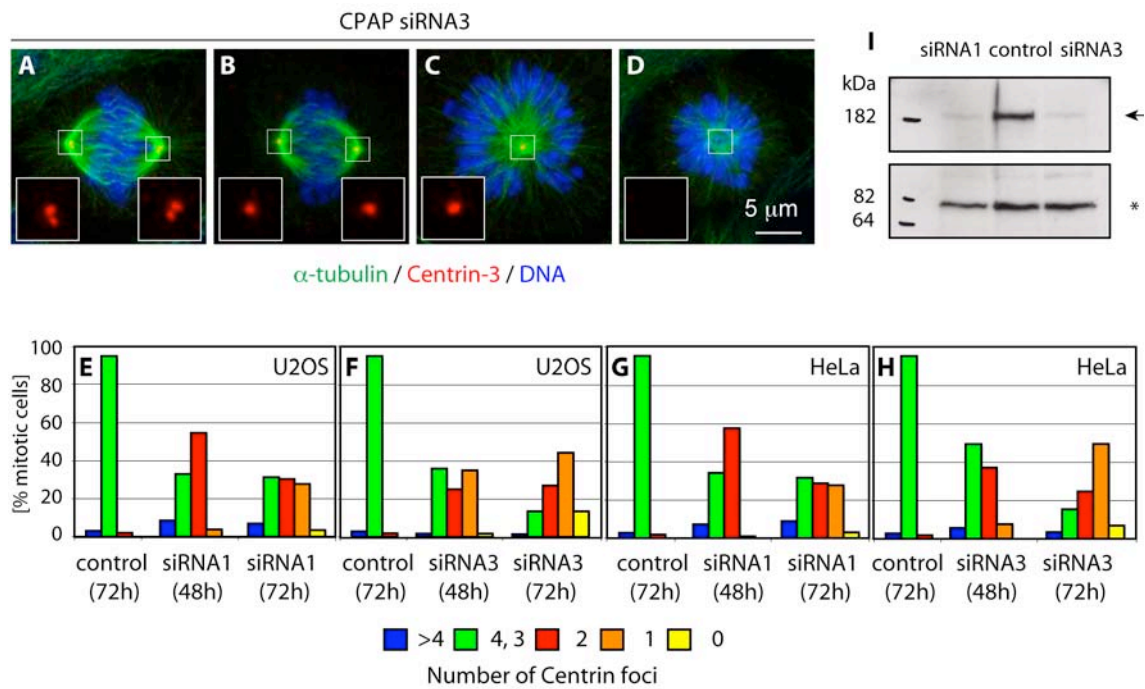


Figure 14: CPAP is required for centriole duplication in proliferating human cells

(A-D) U2OS cells transfected with CPAP siRNA3 for 72 hours and stained with antibodies against α -tubulin (green) and Centrin-3 (red). Two representative bipolar (A and B) and monopolar (C and D) figures are shown.

(E-H) U2OS (E and F) and HeLa (G and H) cells transfected with CPAP siRNA1 (E and G) and siRNA3 (F and H) for 48 and 72 hours and scored for the total number of Centrin-3 foci at spindle poles in mitotic cells ($n > 100$ for each time point).

(I) U2OS cells transfected with the indicated siRNAs for 72 hours and analyzed by Western blot using antibodies against CPAP. Arrow indicates specific band, star indicates unspecific band from the same antibody, which serves as loading control.

To exclude that the observed phenotype was caused by siRNA off-target effects, we generated a doxycycline-inducible cell lines for expressing GFP-CPAP (iGFP-CPAP, described in 2.5.1) and GFP-CPAP resistant to siRNA3 (iGFP-CPAP^R) (Table 1, p.85) and analyzed their mitotic spindles upon CPAP RNAi. While iGFP-CPAP cells treated with siRNA3 assembled monopolar spindles in ~25% of cases, this phenotype was observed only in ~5% of iGFP-CPAP^R cells treated with siRNA3, even in the uninduced condition (Figure 15A). Moreover, the percentage of monopolar spindles was reduced to background levels in iGFP-CPAP^R cells but not in iGFP-CPAP cells after induction (Figure 15A). The specific depletion of endogenous CPAP but not of the RNAi resistant transgene was also verified by Western blot analysis (Figure 15B). From these various lines of evidence, we conclude that the effect of CPAP siRNAs on centriole number is specific.

We investigated whether a block in cell cycle progression may cause the reduction of centriole numbers in CPAP RNAi. Therefore, we examined cells 70 hours after siRNA treatment by flow cytometry and immunofluorescence analysis with Centrin-2 and CPAP antibodies. While the CPAP centriolar signal was strongly reduced or absent in over 90% of interphase cells treated with CPAP siRNAs, FACS profiles of these cells were similar to that of cells treated with control siRNAs (Figure 15C-G, upper panels). A slight increase of ~10-15% in the G1 population was consistently detected in cells treated with siRNA3 (Figure 15E, upper panel). To further investigate this putative G1 arrest, we treated cells for 70 hours with siRNAs and added nocodazole for the final 17 hours to accumulate them in G2 and mitosis (Mikule et al., 2007). We found that cells treated with siRNA3 under these conditions shifted to the G2/M-peak, similar to cells treated with control or HsSAS-6 siRNAs (Figure 15C-F, lower panels). However, this was not the case for cells treated with CP110 siRNAs (Figure 15G, lower panel). We conclude that cells treated with siRNAs directed against CPAP proliferate normally for several cell cycles. Overall, these findings establish that CPAP is required for centriole duplication in proliferating cells.

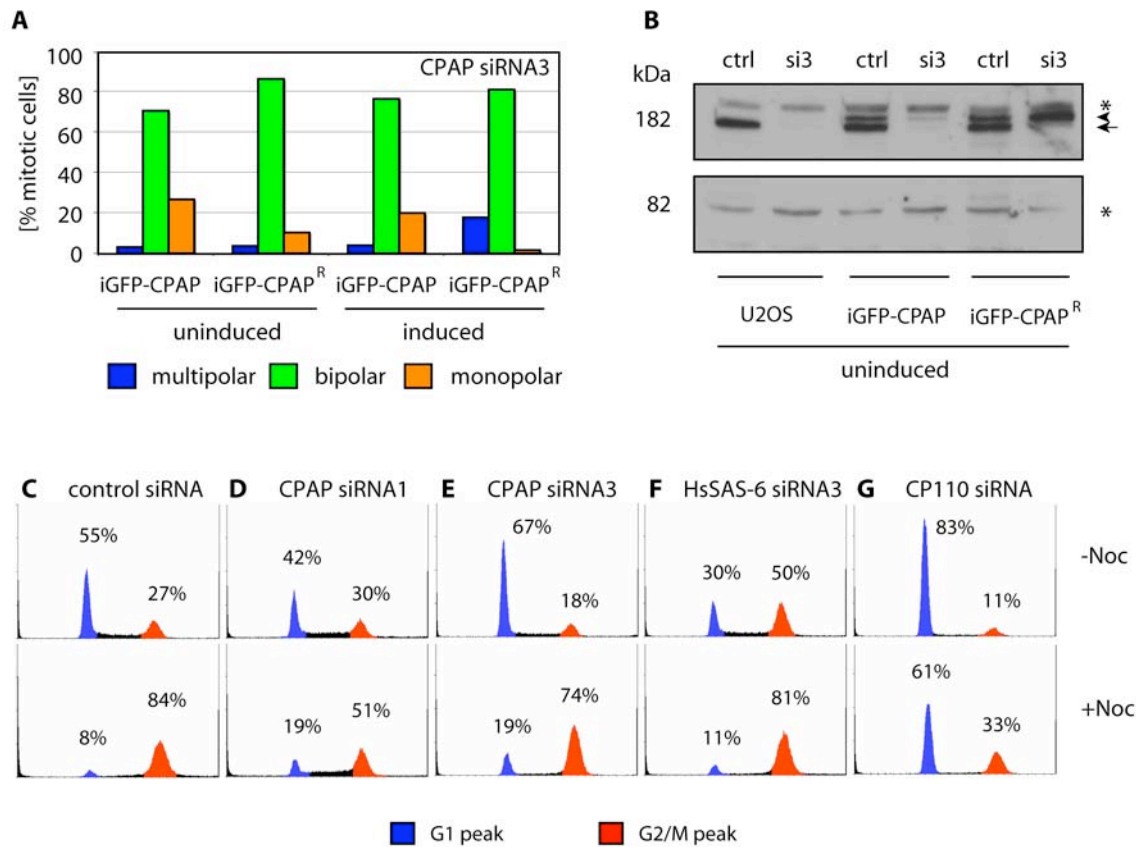


Figure 15: CPAP siRNAs do not cause a cell cycle arrest

(A) iGFP-CPAP and iGFP-CPAP^R U2OS cells were treated with CPAP siRNA3 in uninduced and induced conditions for 72 hours. Cells stained with Centrin-3 and α -tubulin were scored for the presence of bipolar or monopolar mitotic cells ($n > 125$ for each). Note that the percentage of monopolar spindles is reduced in cells harboring iGFP-CPAP^R even in the uninduced state, which is presumably due to leaky expression. Note also the formation of ~18% multipolar cells upon induction of iGFP-CPAP^R (see section 2.5.8).

(B) Normal U2OS cells and U2OS cells harboring iGFP-CPAP or iGFP-CPAP^R plasmids in uninduced conditions were treated with the indicated siRNAs (ctrl = control siRNA, si3 = CPAP siRNA3) for 72 hours. Whole cell extracts were analyzed by Western blot with CPAP antibodies. Arrow indicates endogenous CPAP, arrowhead indicates EGFP-tagged CPAP and asterisks mark unspecific bands from the same antibody. Note that control siRNAs were designed to target GFP (see section 4.4), leading to an underestimation of iGFP-CPAP levels. True levels of the GFP-tagged transgene in the uninduced condition can be estimated in cells harboring iGFP-CPAP^R and treated with CPAP siRNA3.

(C-G) U2OS cells treated with the indicated siRNAs for 70 hours (upper panels) and in addition with nocodazole for the final 17 hours (lower panels). Cells were analyzed by flow cytometry to measure DNA content. The fraction of cells in G1 (blue) and G2/M (red) are indicated. Cells treated with CPAP, HsSAS-6 and CP110 siRNAs were also analyzed by immunofluorescence with CPAP, HsSAS-6 and CP110 antibodies, respectively, to determine the efficiency of each RNAi. Centrin-2 served as a reference centriole marker. More than 90% of interphase cells treated with CPAP, HsSAS-6 or CP110 siRNAs exhibited strongly reduced centriolar signals with the respective antibodies as compared to control siRNA treated cells ($n > 100$ for each siRNA).

2.3.3 CPAP functions after centriolar recruitment of HsSAS-6

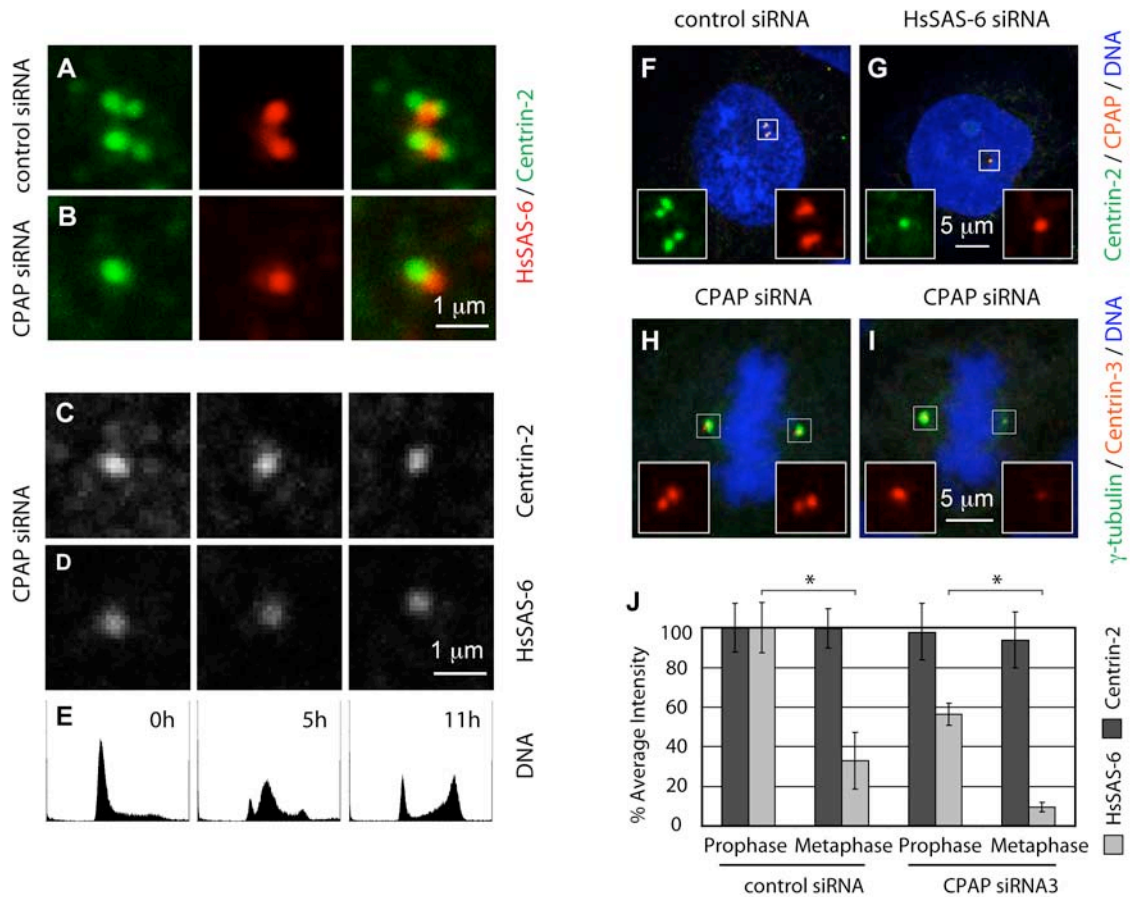
Next, we sought to investigate at which stage during the centrosome duplication cycle CPAP is required. To this end, we synchronized cells in S phase and then analyzed the recruitment of HsSAS-6, the earliest known marker of procentriole assembly (Strnad et al., 2007), to centrioles marked by Centrin-2. Importantly, we found that ~76% of CPAP siRNA3 treated interphase cells and containing only a single Centrin-2 focus also displayed a prominent HsSAS-6 focus in its close proximity (n = 54) (Figure 16B). Similarly, HsSAS-6 signals near Centrin-2 foci were detected in ~73% of interphase cells treated with control siRNAs (n = 226) (Figure 16A), suggesting that HsSAS-6 recruitment to procentriole assembly sites was not affected by CPAP RNAi. Moreover, Centrin-2 signals could not be detected distal to the HsSAS-6 foci, indicating that formation of procentrioles is blocked at a stage after HsSAS-6 incorporation but before Centrin-2 recruitment.

In order to confirm and extend our findings in proliferating cells, we examined HsSAS-6 recruitment in CPAP siRNA3 treated cells released from a single thymidine block and fixed at several time points throughout S, G2 and the following G1-phase. HsSAS-6 signals near single Centrin-2 foci could be detected in ~59% of cells arrested in S phase (Figure 16C-E, 0h). The fraction of cells containing such signals increased to ~71% and ~68%, respectively, when cells progressed through S (Figure 16C-E, 5h) and G2 (Figure 16C-E, 11h) (n > 100 for each time point). Upon entering the following G1-phase, the HsSAS-6 signals disappeared as expected (data not shown). We inspected the time of HsSAS-6 disappearance in CPAP-depleted cells more closely. Normally, HsSAS-6 levels at procentrioles are high during early mitosis, whereas they drop significantly before metaphase (Petr Strnad, pers. comm.) and decrease to undetectable levels during anaphase (Strnad et al., 2007). Interestingly, measurements of signal intensities revealed that the HsSAS-6 signal at procentrioles in CPAP siRNA3 treated prophase cells corresponded to ~60% of that in control siRNA treated prophase cells (Figure 16J, Prophase). At prometaphase / metaphase, the HsSAS-6 signals dropped to ~30% of the prophase signals in

control cells and to barely detectable levels in CPAP RNAi (Figure 16J, Metaphase). These data indicate that HsSAS-6 might be less efficiently recruited to or maintained at procentrioles in the absence of CPAP. Nevertheless, the CPAP signals were confined to the parental centriole in cells depleted of HsSAS-6 (Figure 16G). Weak HsSAS-6 signals near centrioles in the absence of CPAP were also detected in the Plk4 overexpression assay (Kleylein-Sohn et al., 2007). Although the authors conclude that this does not reflect bona fide recruitment to procentriole assembly sites, these data are reminiscent of our own, showing a less intense HsSAS-6 signal in the absence of CPAP. Together, we conclude that CPAP acts downstream of HsSAS-6 during procentriole formation in cycling human cells, in line with findings in *C. elegans* (Delattre et al., 2006; Pelletier et al., 2006).

On rare occasions, we noted that CPAP siRNA3 treated cells assembled asymmetric bipolar spindles (Figure 16H-I). These cells contained less γ -tubulin and Centrin-3 at the smaller spindle pole compared to the larger spindle pole. Similar asymmetry and structurally defective centrioles at the smaller spindle pole were observed after partial depletion of SAS-4 in *C. elegans* (Kirkham et al., 2003), raising the possibility that the amount of PCM is also proportional to centriole size in human cells.

Parts of this chapter were published in (Kohlmaier et al., 2009).



2.4 The Role of CPAP in Microtubule Regrowth from Centrosomes

Since the PN2-3 fragment within CPAP was shown to inhibit microtubule regrowth from purified centrosomes *in vitro* (Hung et al., 2004), we wanted to assess whether the full-length protein played a similar role at centrosomes in living cells. In a preliminary experiment, we therefore depleted cells of CPAP and analyzed their microtubule cytoskeleton after cold-treatment for 1 hour and regrowth for 4 minutes. Interestingly, no obvious microtubule regrowth could be detected around single Centrin-3 foci upon CPAP depletion (Figure 17C). By contrast, HsSAS-6 depletion did not significantly impair microtubule regrowth around single Centrin-3 foci (Figure 17B). Thus, the number of Centrin-3 foci at centrosomes per se does not appear to influence microtubule regrowth. We wondered whether the impairment of microtubule regrowth upon CPAP depletion might be explained by a specific loss of γ -tubulin, one of the major factors regulating microtubule nucleation (Joshi et al., 1992). Therefore, we determined whether γ -tubulin was still present at the MTOC in the absence of CPAP. As seen in Figure 17E-F, γ -tubulin was similarly present at the centrosome in cells depleted of HsSAS-6 or CPAP. Quantitative analysis revealed that the γ -tubulin signals at centrioles upon CPAP depletion are slightly but significantly lower than in control siRNA treated cells, but they are not significantly different from HsSAS-6 depleted cells (Figure 17G), indicating that the reduced capacity to regrow microtubules without CPAP cannot be explained by reduced γ -tubulin levels at centrioles only. Instead, these data raise the possibility that CPAP is required for efficient microtubule nucleation or growth from centrosomes independently of γ -tubulin. Alternatively, CPAP might be required for γ -tubulin function, rather than distribution, at the centrosome. Together, these results suggest that full-length CPAP plays a positive role in microtubule nucleation in living cells.

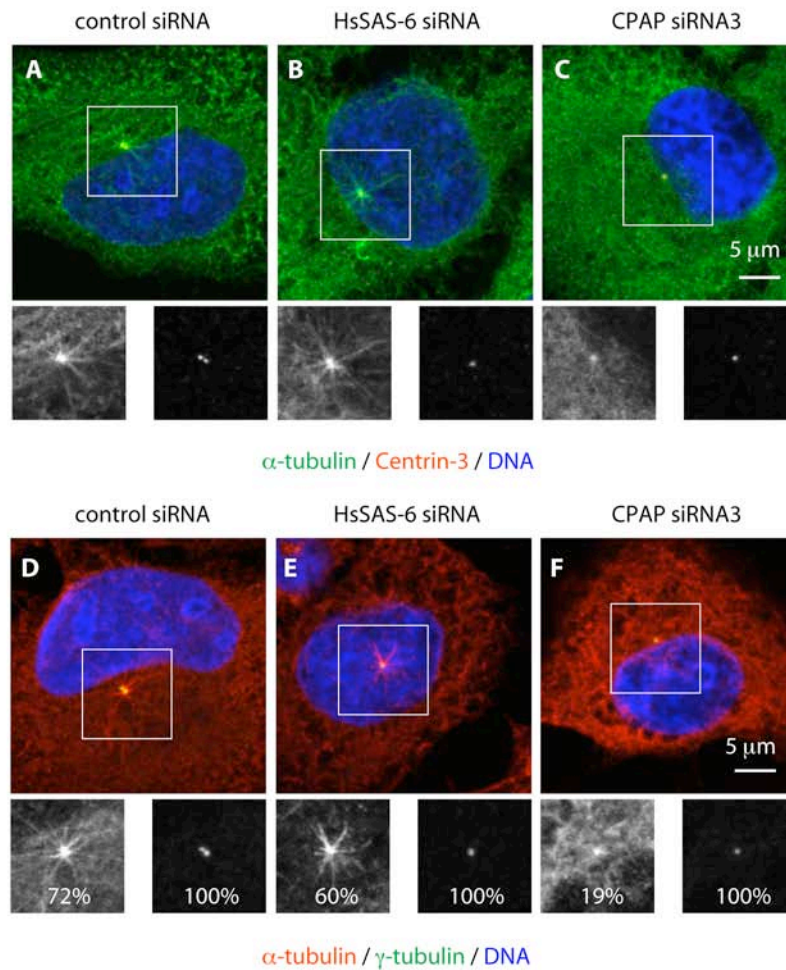


Figure 17: CPAP is required for efficient microtubule regrowth around centrosomes

(A-F) U2OS cells were treated with the indicated siRNAs for 72 hours, cold-treated for 1 hour, followed by 4 minutes incubation at 37°C and stained with antibodies against α -tubulin (green) and Centrin-3 (red) (A-C) or α -tubulin (red) and γ -tubulin (green) (D-F). The presence of a single Centrin-3 (B-C) or γ -tubulin (E-F) focus indicated that RNAi was efficient. Percentages in (D-F) refer to cells displaying clear asters or clear γ -tubulin signals at centrosomes (n>100 each). (G) Quantification of γ -tubulin signal intensities at single centrosomes from (D-F) normalized to the background. Error bars represent 95% confidence interval (n=15 each). The difference of γ -tubulin signal intensities between HsSAS-6 and CPAP RNAi is not statistically significant, but both values are significantly different from that of the control RNAi (two-tailed Student's t-test, $p < 0.05$).

2.5 Effects of Excess CPAP Levels on Centrosome Structure and Function

To gain more insights into the mechanisms by which CPAP functions, we transiently overexpressed GFP-tagged CPAP in U2OS cells. Close inspection of the GFP fluorescence revealed that ectopic CPAP not only localized near centrioles (Figure 11A), but also formed elongated threads in the vicinity of the nucleus (Figure 18B) and globular aggregates primarily in the cytoplasm (Figure 18C). Upon high expression levels, aggregates could be also detected inside of the nucleus (Figure 18D-E). Both phenotypes will be discussed in the following sections.

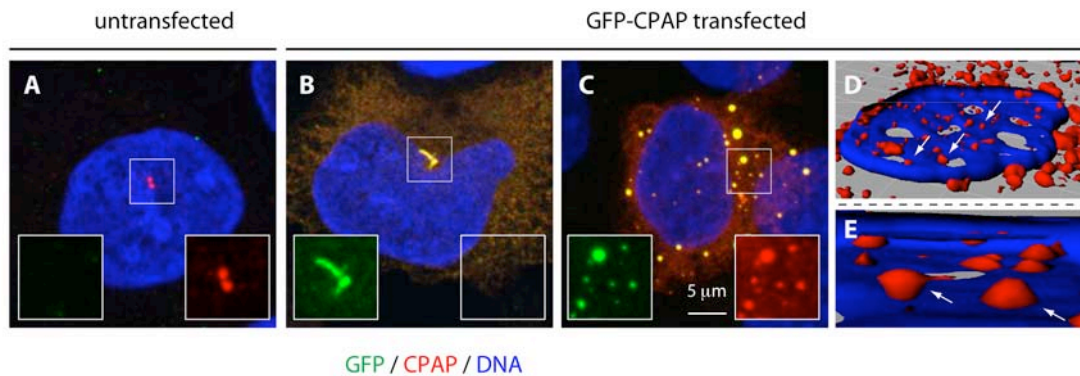


Figure 18: Excess CPAP results in formation of threads and aggregates

(A-C) Untransfected (A) and GFP-CPAP transfected (B-E) U2OS cells 72 hours after transfection stained with antibodies against GFP (green) and CPAP (red). Threads (B) were seen in 2%, 30% and 57% and aggregates (C) in 54%, 39% and 23% of strongly expressing cells at 24, 48 and 72 hours after transfection, respectively ($n > 100$ at each timepoint). Note that formation of aggregates was typically associated with high expression levels and preferentially occurred in the cytoplasm, where most GFP signal was detected. Note that few smaller aggregates could be also detected inside the nucleus.

(D-E) 3D reconstructions of two 293T cells (one in D and the other in E) were chosen to illustrate aggregates inside the nucleus (white arrows indicate some clear examples of nuclear aggregates; CPAP is shown in red and DNA in blue). Panel (E) shows a higher magnification of CPAP aggregates from a side view through the nucleus. Since formation of aggregates is likely caused by abnormally high protein levels, this indicates that overexpressed CPAP can also reach substantial levels in the nucleus. Reconstructions of confocal z-series through the depth of the nucleus were made in the program Imapris.

2.5.1 CPAP threads protrude from centrosomes and expand over time

We wanted to test whether thread formation was a result of the GFP-tag fused to CPAP, as well as whether it was observed only in U2OS cells. We found that overexpression of untagged or mCherry-tagged CPAP likewise resulted in the appearance of threads (data not shown). The same was observed in a number of cancer cell lines (Figure 19A-E) as well as nontransformed human

umbilical vein endothelial cells (HUVECs) (Figure 19F). Thus, the appearance of threads is a general response to elevated CPAP levels.

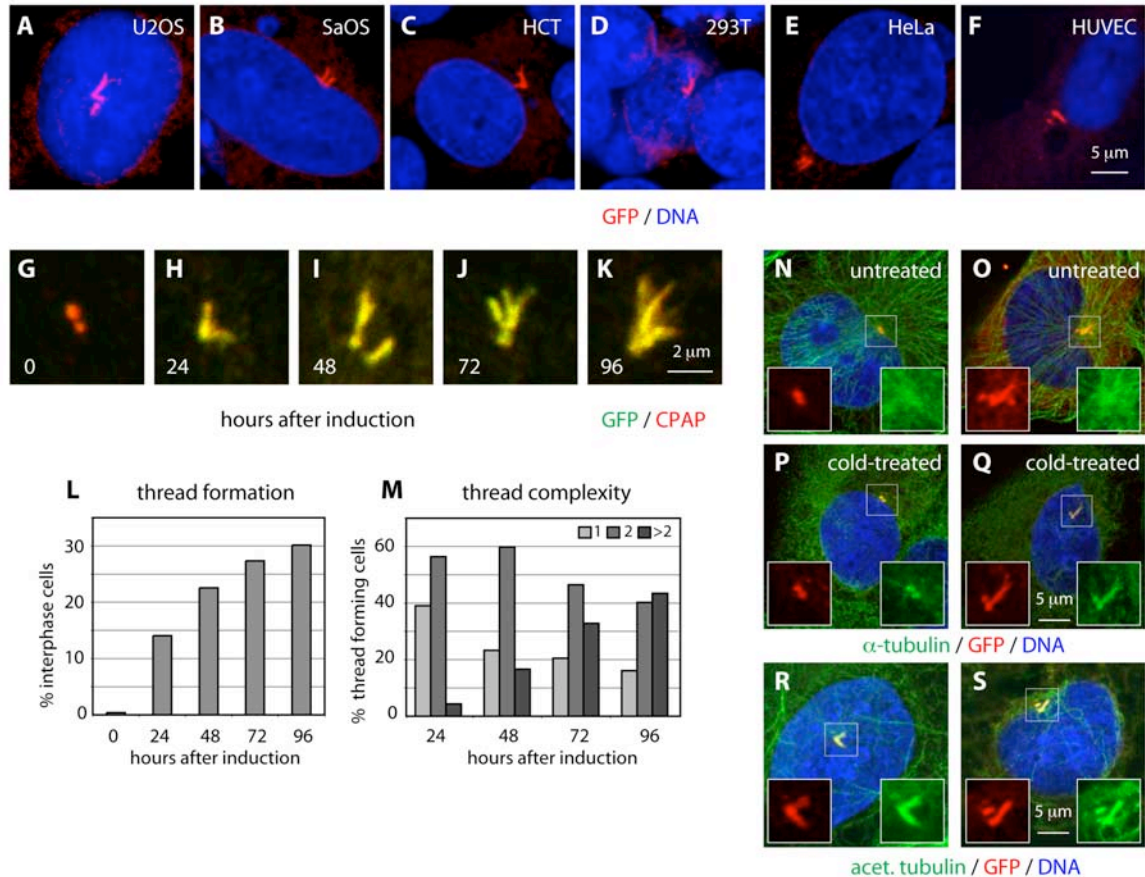


Figure 19: CPAP threads contain stable microtubules

(A-F) U2OS (A), SaOS (B), HCT (C), 293T (D), HeLa (E) and HUVEC (F) cells transiently transfected with GFP-CPAP for 72 hours and stained with antibodies against GFP (red). Threads formed in 21% (A), 12% (B) 9% (C) and 4% (F) of transfected cells. Due to very low transfection efficiencies, no quantification was performed in (D) and (E). Note that no threads were apparent following transient transfection of 3T3 cells and primary human keratinocytes (data not shown). Why threads in some cell lines are present at lower frequencies or altogether absent remains to be investigated.

(G-M) iGFP-CPAP cells induced with doxycycline for 0, 24, 48, 72 or 96 hours prior to fixation and stained with antibodies against GFP (green) and CPAP (red). Representative thread configurations are shown in (G-K). Panel (L) shows the frequency of threads ($n > 250$ at each time point), panel (M) their complexity, as determined by the number of free ends per thread ($n > 45$ at each time point).

(N-Q) U2OS cells transiently transfected with GFP-CPAP for 72 hours (untreated, N-O), or additionally incubated for 1 hour at 4°C (cold-treated, P-Q) and stained with antibodies against α -tubulin (green) and GFP (red). Transfected cells with GFP-CPAP at centrosomes (N-P) or at threads (O, Q) are shown. Note that the α -tubulin signal at centrosomes or threads (N-O) is hidden in the cytoplasmic signal in untreated cells.

(R-S) U2OS cells transiently transfected with GFP-CPAP for 72 hours and stained with antibodies against acetylated tubulin (green) and GFP (red).

To study this phenotype in more detail, we generated a U2OS cell line that stably maintains a plasmid allowing doxycycline inducible GFP-CPAP (iGFP-CPAP) expression. Consistent with results from transient transfection experiments, threads were also observed in this inducible expression system. We found that the frequency of iGFP-CPAP cells harboring threads steadily increased upon induction with doxycycline (Figure 19G-K). Moreover, threads tended to be longer and more complex at later time points (Figure 19L-M). On the other hand, cells harboring threads never displayed distinct centrosome foci in addition (Figure 18B). These observations raised the possibility that threads may emerge from centrosomes. To highlight the centrosome, we applied a pulse of nocodazole or cold-treatment which depolymerized microtubules in the cytoplasm but not at the centrosome that contains stable microtubules (Figure 19N, P and data not shown). Interestingly, pronounced threads marked by GFP were still detected under these conditions (Figure 19O, Q and data not shown). In addition, α -tubulin could be detected along threads (Figure 19Q), indicating that these structures might contain stable microtubules. Accordingly, threads stained positive for acetylated tubulin (Figure 19R-S), another hallmark of stable microtubules (Piperno and Fuller, 1985). Based on these observations, we assumed that threads protrude from centrosomes and continue to grow over time.

2.5.2 CPAP threads contain core centriolar proteins

Next, we investigated whether threads were related to centrioles. We found that threads contained polyglutamylated tubulin, Cep135 and Centrin-3 (Figure 20A-C), which are all characteristic of centriolar cylinders (Middendorp et al., 2000; Ohta et al., 2002; Wolff et al., 1992). CP110, which normally localizes to the distal part of procentrioles and centrioles (Spektor et al., 2007), was present at the end of threads (Figure 20D) or along their length (data not shown). In contrast, HsSAS-6 and C-Nap1, which marks the base of the centriole (Fry et al., 1998), were present at one end of the threads but never decorated all their length (Figure 20E-F). Odf2 and Ninein, which mostly mark the appendages of the mother centriole (Ishikawa et al., 2005; Mogensen et al., 2000), also associated with the threads but did not extend along their

length (Figure 20G-H). Overall, we conclude that threads formed upon CPAP overexpression bear proteins that are characteristic of centriolar cylinders.

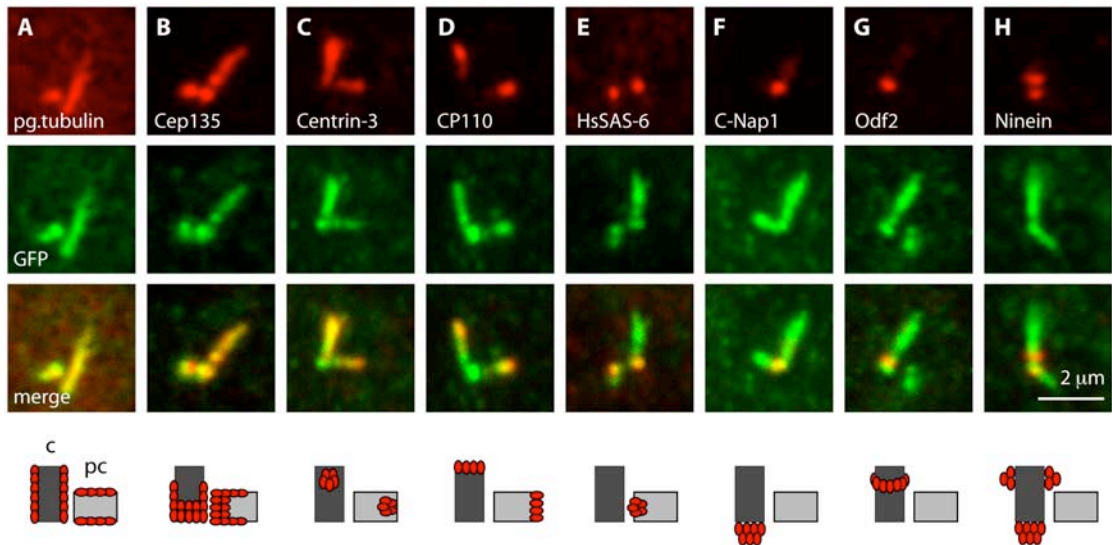


Figure 20: Threads incorporate proteins that are characteristic of centrioles

(A-H) Representative high magnification images of threads from iGFP-CPAP cells at different stages of the cell cycle induced with doxycycline for 48 hours and stained with antibodies against GFP (green) and polyglutamylated (pg.) tubulin (A), Cep135 (B), Centrin-3 (C), CP110 (D), HsSAS-6 (E), C-Nap1 (F), Odf2 (G) or Ninein (H), respectively (each in red). Centrioles (c) and procentrioles (pc) are drawn schematically below, with the approximate position of each marker relative to the normal centriole / procentriole pair.

2.5.3 CPAP threads resemble abnormally elongated centrioles

To determine whether threads resembled centrioles also at the ultrastructural level, we analyzed cells overexpressing GFP-tagged CPAP and that formed threads by combinatorial light microscopy (LM) / transmission electron-microscopy (TEM) in collaboration with Mette Mogensen. To this end, cells displaying prominent GFP-containing threads 72 hours after transfection were imaged by dual fluorescence and brightfield microscopy on a gridded coverslip, enabling us to unambiguously determine the position of these cells on the slide (Figure 21A). Upon fixation, the cells were sent to our collaborator who performed TEM analysis of the selected regions (Figure 21B). Importantly, we found that the selected cells sometimes contained centrioles with abnormally elongated ends (Figure 21D-E). These elongations were not symmetric at the centriole end (Figure 21E, F). Sometimes also, microtubule bundles were detected that resemble elongated centrioles but have a smaller diameter than expected for a

centriole (Figure 21G). We conclude that cells with threads contain centrioles with abnormally elongated ends.

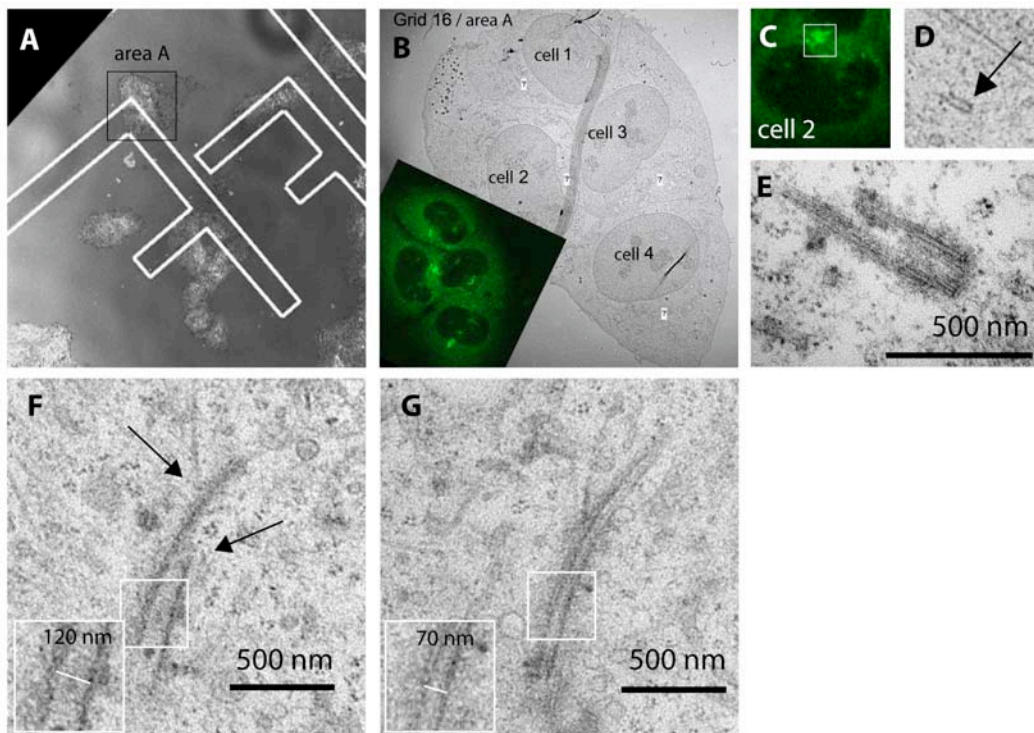


Figure 21: Thread forming cells harbor abnormally elongated centrioles

(A-E) U2OS cells transiently transfected with GFP-CPAP for 72 hours and analyzed by brightfield (A) and GFP fluorescence (B, inset) microscopy on a gridded coverslip before fixation. The position of thread-forming cells on the grid (area A) is indicated with a box (A). The four cells expressing GFP-CPAP in area A (B, inset) were analyzed by TEM (B). The centriole of a cell with threads (C) is shown in low (D, arrow) and high (E) magnification. Note that the centriole is asymmetrically elongated at its end, reaching ~700 nm (E).

(F-G) Examples of threads analyzed by TEM in U2OS cells overexpressing GFP-CPAP for 72 hours. The approximate size of a normal centriole is indicated next to each thread. Arrows in (F) indicate an asymmetrically elongated centriole end. Insets show magnified views of the squared boxes. Note that the thread in (F) corresponds approximately to the diameter of a centriole, whereas the thread in (G) does not.

To get a more detailed view of the centriole ultrastructure in thread-forming cells, we collaborated with Alexey Khodjakov who employed same-cell correlative LM / serial-section electron-microscopy (EM) on 12 iGFP-CPAP cells with prominent threads 72 hours after induction (Figure 22A-L). This analysis revealed that centrioles in all those cells were abnormally long (Figure 23D-F) and generally corresponded to the GFP-signal used to visualize threads (Figure 22A, L). This also demonstrates that threads are direct elongations of normal centrioles.

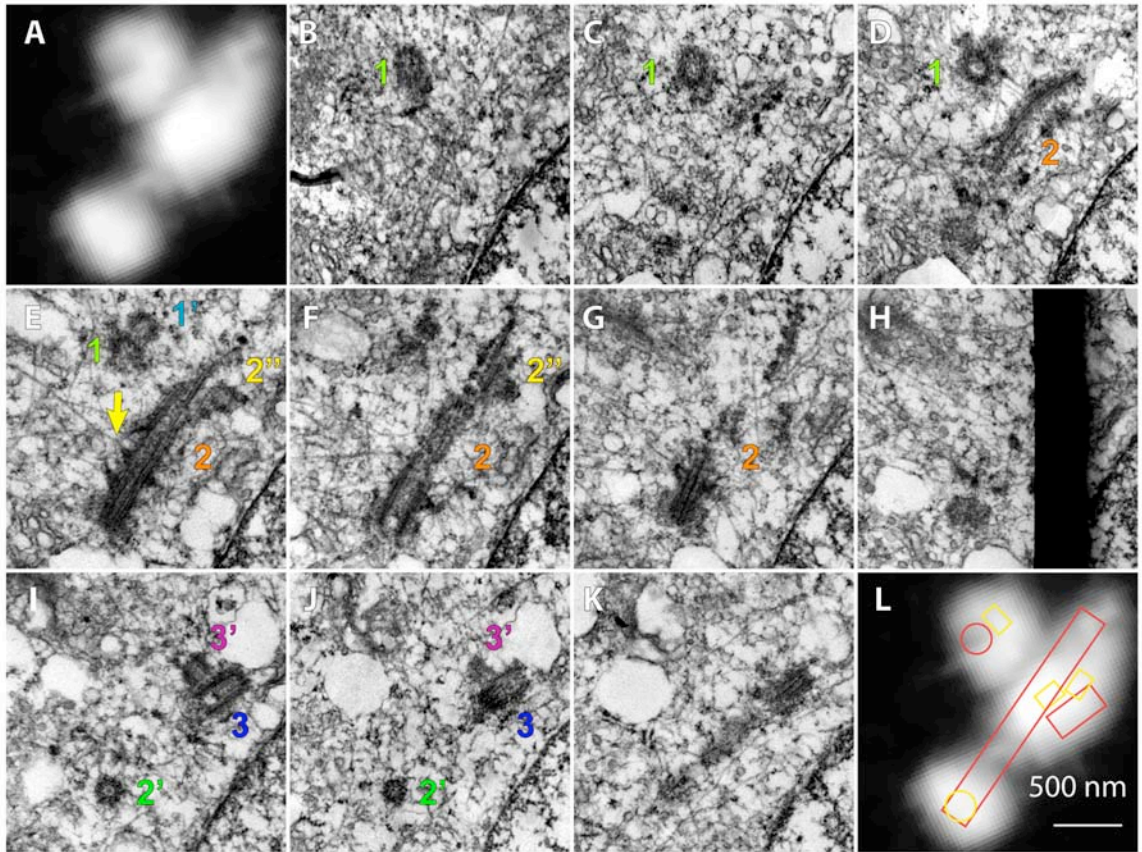


Figure 22: Threads are abnormally elongated centrioles

(A) CPAP-GFP threads in an iGFP-CPAP cell 72 hours after induction with doxycycline. Maximal-intensity projection of a through-focus series.

(B-K) Complete series of 100-nm sections through the centrosome in the same cell. Three centrioles and four procentrioles were present in this cell. Centrioles (1) and (3) were morphologically normal, while centriole (2) was significantly longer and distorted. Procentrioles (1', 2', and 3') resided near the proximal end of each centriole. A second, ectopic procentriole (2'') was found near the distal end of the long centriole.

(L) Contour traces of centriolar cylinders overlaid on the CPAP-GFP distribution. Notice that a morphologically-normal centriole (1) resides within a depression in CPAP-GFP signal. Also notice that the distribution of CPAP-GFP along centriole (2) is not uniform.

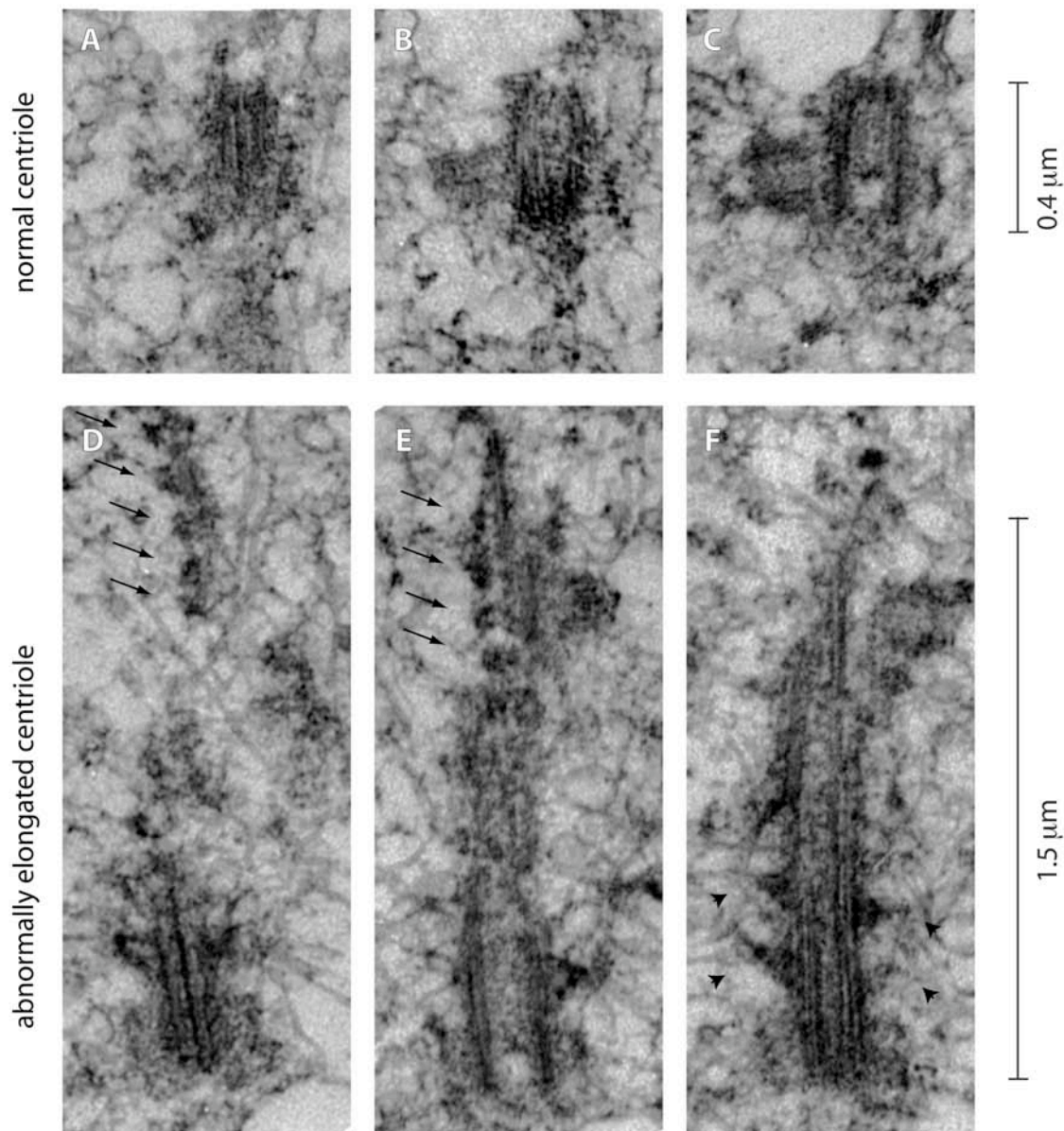


Figure 23: Structural comparison between a centriole and thread

(A-C) Higher magnification views of centriole (3) and (3') from the sections (Figure 22I-K). Note that this centriole / procentriole pair exhibits normal length and structure.

(D-F) Higher magnification views of the abnormally elongated centriole (2) from the sections (Figure 22E-G). Note that electron-dense patches decorate microtubule blades in regular spacing (arrows in D and E), as well as duplicated appendages on top of their expected position (arrowheads in F). Note also that the centriole cylinder is not elongated in one section (D), and that elongations are not symmetrical in other sections (E-F).

The structural organization of the proximal end of overly long centrioles appeared largely normal. However, we consistently detected that not all nine microtubule blades were equally elongated but terminated at different distances from the proximal end (Figure 23E-F and Figure 27C, marked with asterisks), with some blades not elongating at all (Figure 23D). Electron tomographic analysis in two of these cells revealed that these elongations consisted of microtubule doublets or singlets at their ends (data not shown). Serial-section EM analysis revealed additional abnormalities in the organization of elongated centrioles. Sub-distal appendages, which are normally organized in a tight ring around the mother centriole, appeared duplicated near their normal position on the elongated segment (Figure 23F, arrowheads). We also consistently found regularly spaced electron-dense foci decorating elongated microtubule blades (Figure 23D-E, arrows), as well as microtubule doublets decorated with electron-opaque material that are not directly connected to overly elongated centrioles (Figure 27C, arrowhead). Overall, we conclude that CPAP overexpression leads to abnormally elongated centrioles with severely disorganized architecture.

2.5.4 CPAP threads can elongate from procentrioles and centrioles

We addressed whether there is excess elongation strictly of the centriole or also of the procentriole. Since threads persist during mitosis (data not shown) and thus might be inherited from previous cell cycles, we examined prophase iGFP-CPAP cells 18 hours after induction to ensure analysis within the first cell cycle after overexpression. Using antibodies against HsSAS-6 to mark the proximal part of the procentriole and against Centrin-2 to label the distal part of procentrioles and centrioles, as well as threads, we assessed which centriolar cylinder underwent excess elongation. This analysis revealed excess elongation of the procentriole in ~30% of cases, of the centriole in ~35% of cases, and of both centriolar cylinders in the remaining ~35% (Figure 24A-D, n = 34). As expected for elongation stemming also from the centriole, depletion of HsSAS-6 did not prevent thread formation in cells overexpressing CPAP (Figure 24E-H). We

conclude that excess CPAP can result in abnormal elongation of the procentriole and the centriole in a single cell cycle.

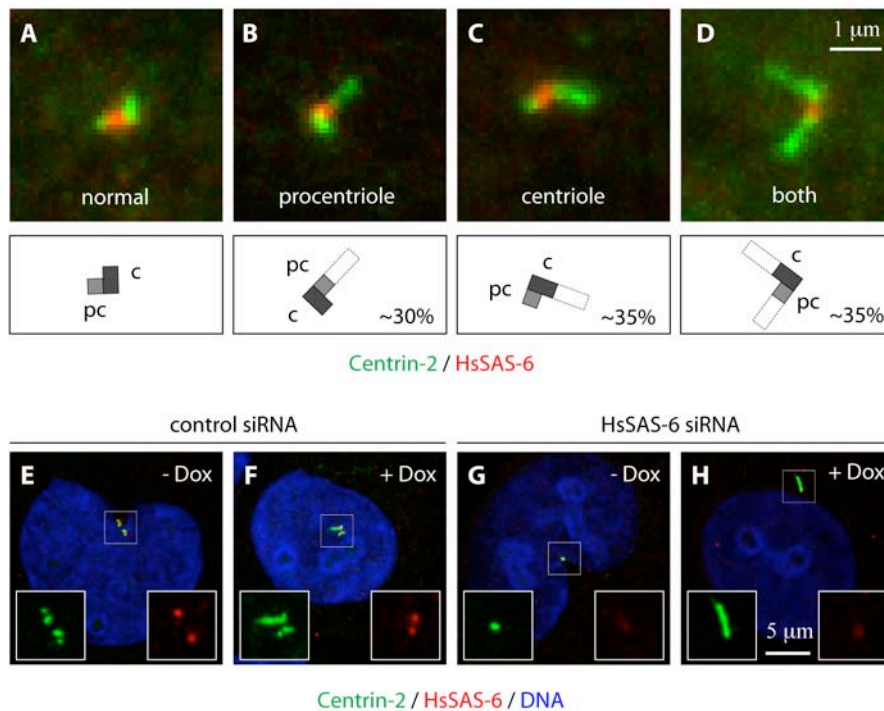


Figure 24: Excess CPAP induces elongation of procentrioles and centrioles

(A-D) iGFP-CPAP cells induced with doxycycline for 18 hours and stained with antibodies against Centrin-2 (green) and HsSAS-6 (red). Centrioles (c) and procentrioles (pc) are drawn schematically, and overly long centriolar cylinders are indicated in white (A'-D'). Percentages represent fraction of each type among centrosomes with threads. In 16/50 thread-bearing centrosomes, the single thread could not be unambiguously assigned to either procentriole or centriole, resulting in a slight underestimate of the frequency of single elongation events. Note also that 6% of uninduced prophase cells exhibited threads, all stemming from the centriole.

(E-H) iGFP-CPAP cells were treated with the indicated siRNAs (E-H) for 72 hours and induced with doxycycline (F, H) for the final 48 hours. Threads were observed in 19% of control siRNA treated (F) and 21% of HsSAS-6 siRNA treated interphase cells (H) ($n > 100$ for each). Accordingly, interphase cells with single centrioles were seen in 44% of cases upon treatment with HsSAS-6 siRNAs compared to 0 % upon treatment with control siRNAs in the uninduced state ($n > 100$ for each), demonstrating that RNAi was effective. Note that in this case, the different control siRNAs not targeting GFP were used.

2.5.5 CPAP threads elongate in G2 or shortly thereafter

We sought to determine when excess elongation initiates during the cell cycle. We generated a doxycycline-inducible U2OS cell line dubbed iCherry-CPAP that proved well suited for long-term live imaging due to lower phototoxicity compared to iGFP-CPAP. This cell line was sent to Jadranka Loncarek in the laboratory of Alexey Khodjakov, who imaged individual cells by combinational 3D fluorescence / DIC time-lapse microscopy starting 12-20 hours after

induction. 16 cells were analyzed in which centrosomes initially seemed normal but then underwent abnormal elongation. In 8 cells, the first signs of excess elongation were observed before mitosis, during late G2 (Figure 25A), with additional elongation during the ensuing G1 (data not shown). The other 8 cells entered mitosis with apparently normal centrosomes, but exhibited elongated structures immediately thereafter (Figure 25B). The limited resolution of light microscopy does not allow us to rule out that excess elongation always initiated during late G2 but was not always detected. Live imaging revealed also that threads usually did not form in cells arrested in S phase (Figure 25C). To confirm these results in fixed specimens, we induced expression of GFP-CPAP for 48 hours and simultaneously added mimosine, thymidine or nocodazole to arrest them in G1, S or G2/M, respectively. Cells arrested in G1 or S phase rarely formed threads (1% and 3%, respectively), whereas 8% of cells arrested in G2/M by nocodazole exhibited thread-like structures (Figure 25G). In comparison, 22% of untreated cells induced with doxycycline formed prominent threads (Figure 25D). This indicates that centrioles can, at least to some extent, elongate in G2 upon CPAP overexpression. Interestingly in addition, growth of centriolar microtubules takes place under microtubule depolymerizing conditions in the presence of excess CPAP, demonstrating that centriole elongation underlies different mechanisms than plain microtubule polymerization. It is noteworthy that in cycling cells the levels of endogenous CPAP increase as cells progress through G2 (Figure 10), when elongation of procentrioles normally takes place. Taken together, we propose that centrioles start abnormally elongating during G2 and continue so in G1 upon CPAP overexpression.

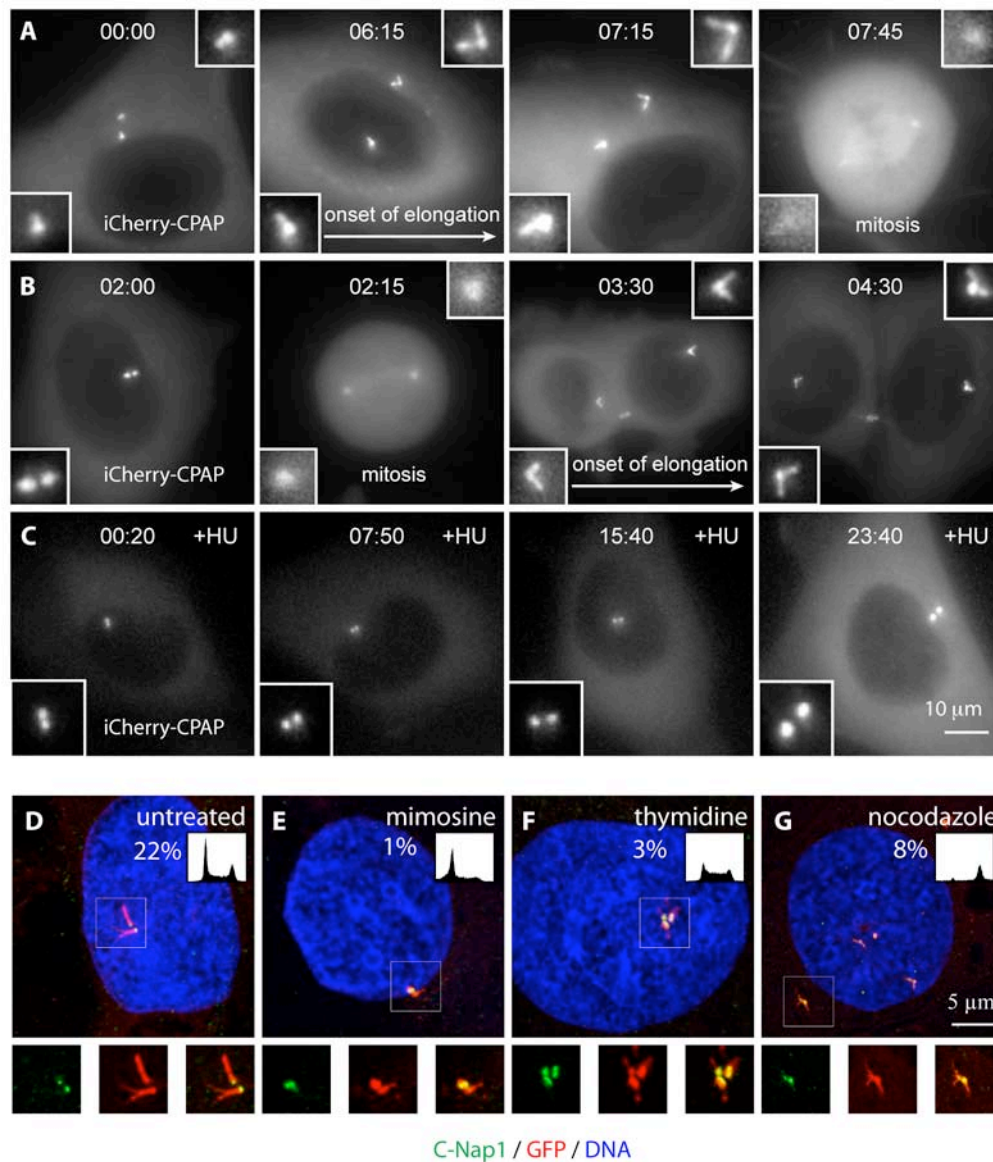


Figure 25: Centriole elongation starts in late G2 or shortly thereafter

(A-B) Live imaging of cycling iCherry-CPAP cells. In this and other live imaging panels, time is denoted in hours:minutes, with 00:00 corresponding to the onset of the time-lapse recording. Threads are first detected at 06:15 in (A), before mitosis, and at 03:30 in (B), after mitosis.

(C) Live imaging of iCherry-CPAP cell held in 2 mM hydroxyurea (HU) for 24 hours prior to incubation with both HU and doxycycline for 24 hours and onset of filming. Note that threads do not form during the entire duration of the recording, which also indicates that thread formation in cycling cells is not simply due to continued exposure to elevated CPAP levels. This results was observed in 4/5 cells held in HU, whereas 1/5 cell formed threads as CPAP levels became extremely elevated before cell death.

(D-G) iGFP-CPAP U2OS cells induced for 48 hours (D) and treated for the same time period with mimosine (E), thymidine (F) or nocodazole (G). A pronounced cell cycle arrest in G1 (E), S (F) and G2/M (G) was observed by flow cytometry (see insets). Cells were stained with C-Nap1 (green) and GFP (red) and scored for the presence of GFP-containing threads ($n > 100$ for each). The percentage of cells forming thread-like elongations is indicated for each condition. The low percentage of cells forming threads in thymidine-arrested cells might probably be explained by the incomplete S-phase arrest seen in the FACS profile in (F). Note that thread-like elongations clearly formed in nocodazole-arrest and were typically scattered throughout the cell (G).

2.5.6 CPAP threads associate with PCM and nucleate cytoplasmic microtubules

Given that regular centrioles recruit the PCM (Bobinnec et al., 1998a; Kirkham et al., 2003), we reasoned that overly long centrioles could also associate with PCM. Accordingly, we found that the PCM components γ -tubulin (Wiese and Zheng, 2006), pericentrin (Dichtenberg et al., 1998), NEDD1 (Lüders et al., 2006) and Cep192 (Gomez-Ferreria et al., 2007; Zhu et al., 2008) almost invariably decorated the threads formed upon GFP-CPAP overexpression in U2OS cells (Figure 26A-D), even at early time points after induction (data not shown). As anticipated from these observations, depolymerization / regrowth experiments established that microtubules can nucleate from threads (Figure 26E, arrows). Thus, functional PCM also decorates the overly elongated portion of centrioles.

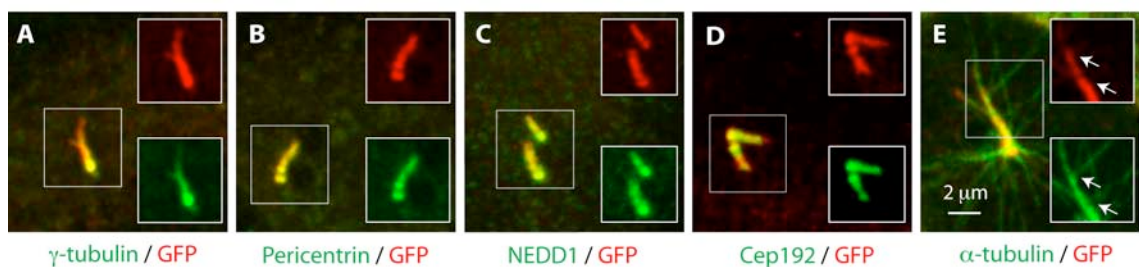


Figure 26: CPAP threads are decorated with functional PCM

(A-D) Representative high magnification images from iGFP-CPAP cells induced with doxycycline for 48 hours and stained with antibodies against GFP (red) and γ -tubulin (A), pericentrin (B), NEDD1 (C) or Cep192 (D) (each in green).

(E) U2OS cell transiently transfected with GFP-CPAP for 72 h, subjected to cold-induced depolymerization for 1 hour and warmed up to 37°C for 4 min prior to staining with antibodies against α -tubulin (green) and GFP (red). Arrows point to cytoplasmic microtubules emanating from threads.

2.5.7 CPAP threads template for more than one procentriole per cell cycle

Excess PCM facilitates procentriole formation in S phase arrested Chinese Hamster Ovary (CHO) cells (Loncarek et al., 2008), raising the possibility that overly long centrioles and their associated PCM could likewise promote procentriole formation. Intriguingly, our collaborators in the laboratory of Alexey Khodjakov observed that 6 of the 12 cells examined by serial-section EM contained more than the maximal number of two centrioles and two procentrioles normally

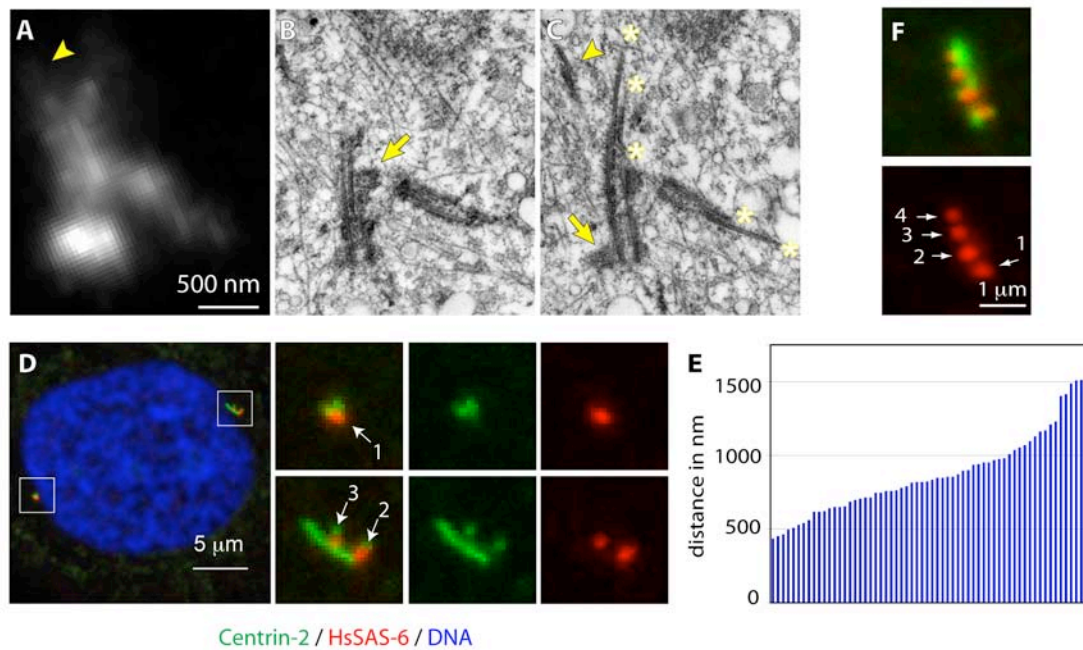


Figure 27: Supernumerary procentriole formation along overly elongated centrioles

(A) iGFP-CPAP cell 72 hours after induction with doxycycline. Maximal-intensity projection of a through-focus series.

(B-C) Two sequential 100-nm thin EM sections through the central part of the centrosome in the same cell. Both mother and daughter centrioles are elongated and their distal ends are distorted (asterisks in C mark distal ends of individual microtubule blades). Two procentrioles (arrows) associate with the mother centriole, one near the proximal end, one near the distal end. There is also an electron-dense thread located ~600 nm away from the distal end of the mother centriole (arrowhead in C), which corresponds to a lower-intensity CPAP-GFP signal (arrowhead in A).

(D) iGFP-CPAP cell induced with doxycycline for 72 hours and stained with antibodies against Centrin-2 (green) and HsSAS-6 (red). Arrows point to procentrioles (1 and 2 correspond to regular procentrioles and 3 to an ectopic procentriole formed in the vicinity of the overly long centriole).

(E) Distribution of distances between regular and ectopic HsSAS-6 foci on overly long centrioles marked by Centrin-2 ($n = 61$). Note that signals closer than 200 nm might have escaped detection due to the resolution limit of light microscopy.

(F) iGFP-CPAP cell induced with doxycycline for 72 hours and stained with antibodies against Centrin-2 (green) and HsSAS-6 (red). In 3/69 cases, two additional procentrioles formed next to the overly elongated centriole segment. Arrows point to procentrioles (1 and 2 correspond to regular procentrioles, 3 and 4 to two ectopic procentrioles formed in the vicinity of one overly long centriole). The distances of the two additional procentrioles to the regular procentriole were 0.43 μm and 0.87 μm (case 1, shown in F), 0.52 μm and 1.39 μm (case 2) and 0.69 μm and 1.57 μm (case 3). Thus, also the third procentriole from a single parental centriole respects the minimal distance of 400 nm to the neighboring procentriole, as depicted in (E).

present in a cell (Figure 22B-K). These were found either near the elongated centriole (Figure 22, procentriole 2' and 2'') or in broader regions surrounding threads (Figure 22, centriole pairs 1-1', 3-3'). In three cases, in addition to the procentriole at the expected position near the proximal end of the centriole, there was an ectopic procentriole in the vicinity of the overly elongated segment (Figure 27B-C, arrows). We confirmed the presence of supernumerary procentrioles by immunofluorescence analysis, with ectopic procentrioles emanating from the

side of threads being marked at their proximal end by HsSAS-6 (Figure 27D). We found also that such additional HsSAS-6 foci were present in 16% of cells with threads 48 hours after induction ($n = 74$) and in 36% of them 72 hours after induction ($n = 107$). This might be due to increasing expression levels over time. Since HsSAS-6 is only incorporated into newly forming procentrioles and degraded at the following mitosis, the presence of HsSAS-6 at both regular and ectopic procentrioles indicates that all HsSAS-6 positive procentrioles along an overly long mother formed within one cell cycle. We then wanted to determine where ectopic procentrioles could form along the overly long centriole segment. Therefore, we analyzed the distances between HsSAS-6 signals along threads marked by Centrin-2. Strikingly, we did not detect ectopic HsSAS-6 foci closer than 400 nm from the regular procentriole. Instead, they were found along the overly long centriole segment in a continuous distribution, starting from ~ 400 nm distal of the regular HsSAS-6 focus (Figure 27E). Thus, ectopic procentrioles seem to be excluded from a minimum distance near regular procentrioles. Furthermore, they do not seem to be enriched at any position of overly long centrioles. Intriguingly, the distance where extra procentrioles are formed corresponds approximately to the length of a normal centriole, raising the possibility that centriole length might be a general important parameter for restricting the number of procentrioles at each parent centriole to one (see section 1.5). Accordingly, in the rare occasions where three procentrioles were found on an overly elongated segment, they were never observed closer to each other than 400 nm (Figure 27F). Overall, these analyses establish that CPAP overexpression results in the formation of more than one procentriole per overly long centriole within one cell cycle.

2.5.8 CPAP overexpression promotes multipolar spindle formation

We next addressed the consequences of such abnormal figures for cell division. Fixed cell analysis established that $\sim 16\%$ of cells assemble a multipolar spindle 72 hours after induction of GFP-CPAP expression, in contrast to $\sim 2.5\%$ in control cells (Figure 28A-C). Accordingly, live cell imaging by Jadranka Loncarek revealed that mitosis in cells overexpressing iCherry-CPAP

and harboring threads were often multipolar (15/57 cells versus 2/35 in control cells). Furthermore, three cells with abnormal centrosomes did not complete mitosis and died (data not shown). Finally, although a bipolar spindle was assembled in the remaining 39 cells, cytokinesis failed in three of these (data not shown). Thus, overall, mitosis is defective in ~35% of cells with elongated centrosomes.

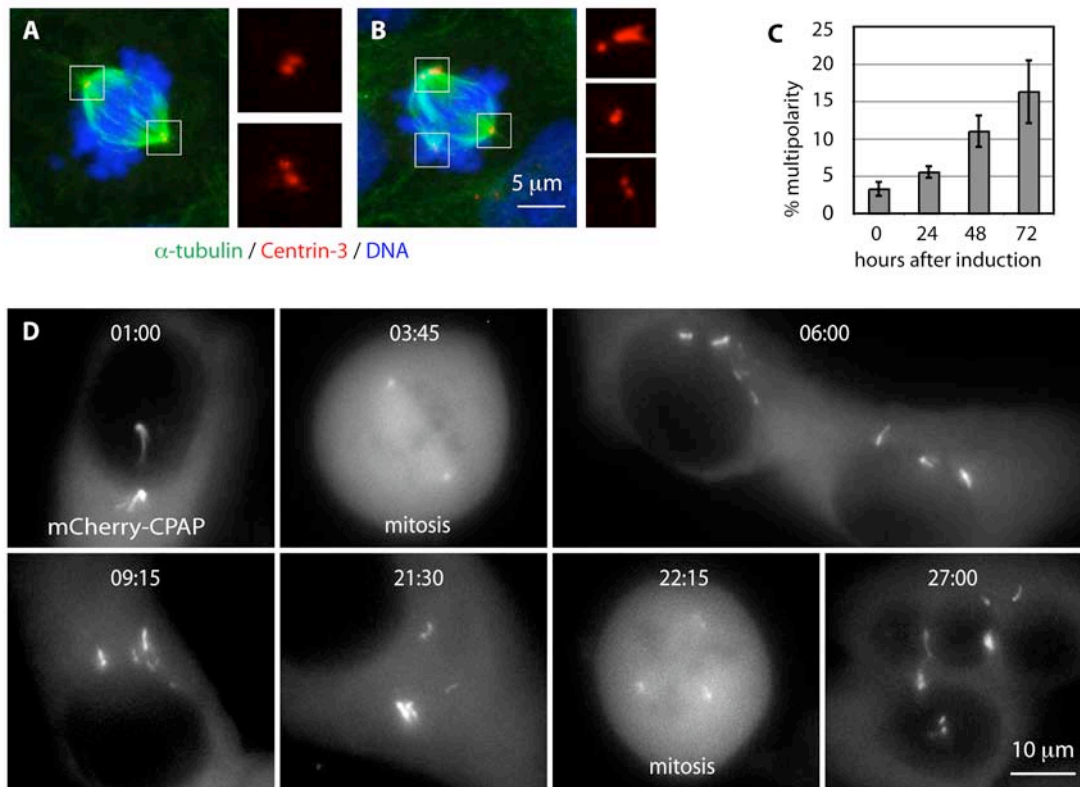


Figure 28: CPAP overexpression promotes multipolar spindle assembly

(A-B) iGFP-CPAP cell induced with doxycycline for 72 hours and stained with antibodies against α -tubulin (green), Centrin-3 (red). Note that some cells with threads assemble a bipolar spindle, and that some cells that do not harbor a thread assembled a multipolar spindle (data not shown).

(C) Fraction of multipolar spindles among iGFP-CPAP cells induced with doxycycline for 0, 24, 48, or 72 hours prior to fixation and staining with antibodies against α -tubulin. Data from two independent experiments were pooled ($n > 100$ for each).

(D) Selected fluorescence (maximal-intensity projections) frames from time-lapse recordings of iCherry-CPAP cell. Note bipolar spindle assembly at 03:45, presence of multiple individual threads in the ensuing G1 (06:00) and multipolar spindle assembly at the next cell division (22:15).

To gain further insight into the cause of these mitotic abnormalities, the progeny of single cells was followed for at least two consecutive cell cycles. In seven of ten such lineages, the first mitosis was bipolar even when both centrosomes comprised long and complex threads, presumably because they remain in two discrete complexes (Figure 28D, 03:45). However, during

the ensuing G1, threads were released from the common complexes, with each thread or fragment thereof behaving as an individual unit (Figure 28D, 06:00). These individualized units assembled a multipolar spindle during the subsequent mitosis (Figure 28D, 22:15). Since the overall levels of mCherry-CPAP are similar during bipolar and multipolar spindle assembly in such cells (Figure 28D and data not shown), multipolar spindle assembly does not appear to result merely from excess CPAP. Furthermore, since the preceding mitosis was bipolar despite threads, they alone cannot be responsible for multipolarity. Instead, this indicates that accumulation of supernumerary MTOCs, presumably due to the presence of ectopic procentrioles and the fragmentation of overly long centrioles, is at the root of multipolar spindle assembly upon CPAP overexpression.

2.5.9 CPAP and CP110 regulate centriole length

Formation of threads within the centrosome has been reported in U2OS cells following depletion of CP110 or of the CP110-associated protein Cep97 (Spektor et al., 2007). We confirmed this phenotype (Figure 29A-B) and noticed several similarities between the threads forming in U2OS cells in the absence of CP110 and upon overexpression of CPAP. For example, in both cases, threads formed in the vicinity of the nucleus and contained Centrin, a bona fide centriole marker. In an attempt to clarify the relationship between the structures formed in the absence of CP110 and upon excess of CPAP, we compared them by immunofluorescence analysis. First, we determined whether threads visualized by Centrin-2 in CP110 siRNA treated cells also recruited CPAP. Since CPAP can induce formation of threads and is itself strongly incorporated, we reasoned that it should also be incorporated in threads upon CP110 depletion. Unexpectedly, CPAP associated with threads at very low levels in CP110 depleted cells (Figure 29C). Also Cep135, which strongly associated with CPAP-induced threads, could hardly be detected at the elongated segment of CP110 threads (Figure 29D). However, γ -tubulin decorated elongated threads in CP110 siRNA treated cells (Figure 29E) as reported (Spektor et al., 2007). HsSAS-6 localized to the base of threads in ~20% of cases in CP110 siRNA treated cells (Figure

29F) as compared to ~70% in CPAP overexpressing cells ($n > 130$ for each). Ectopic HsSAS-6 foci near the elongated thread segment were rarely (~1%) detected upon CP110 RNAi. These differences between threads upon CPAP overexpression and CP110 RNAi might be explained by the strong G1 arrest that is evident upon depletion of CP110 (Figure 15G).

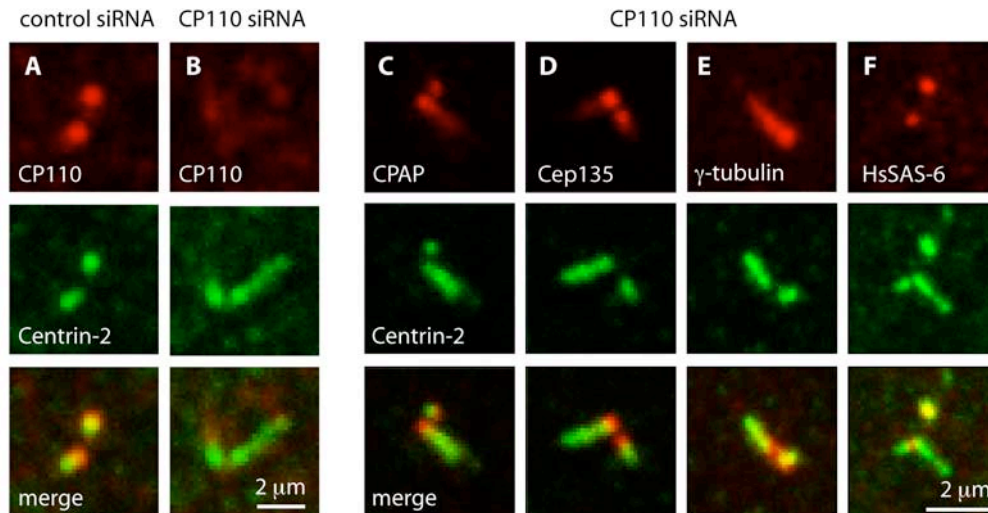


Figure 29: CP110 threads resemble CPAP threads

(A-B) U2OS cells treated with CP110 siRNAs for 72 hours and stained with antibodies against Centrin-2 (green) and CP110 (red). Upon depletion of CP110 (B), the Centrin-2 signal reveals an elongated shape similar to threads upon CPAP overexpression.

(C-F) U2OS cells treated with CP110 siRNAs for 72 hours and stained with antibodies against Centrin-2 (green) and CPAP (C), Cep135 (D), γ -tubulin (E) or HsSAS-6 (F) (each in red).

Then, we sought to find out whether excess CP110 would antagonize CPAP in elongating centrioles. To this end, we transiently transfected an empty Flag vector or Flag-CP110 (Spektor et al., 2007) in iGFP-CPAP cells and induced CPAP expression with doxycycline. After coexpression of the Flag-constructs and GFP-CPAP for 48 hours we stained the cells for Centrin-2 and the Flag epitope. We found that threads formed in 24% of cells coexpressing Flag and GFP-CPAP, compared to 31% of cells coexpressing Flag-CP110 and GFP-CPAP ($n > 100$ for each). Close inspection of the Flag-CP110 signal at CPAP-induced threads revealed that overexpressed CP110 associated with threads along their length in all cases (data not shown). This is in contrast to endogenous CP110, which localizes to the end of CPAP-induced threads or along their length (Figure 20D). Thus, it seems that endogenous CP110 has stronger affinity to associate with thread

ends than with thread walls in some cases, but that overexpressed CP110 tends to accumulate throughout threads. Overall, we conclude that overexpression of CP110 is not sufficient to inhibit CPAP-induced thread formation in our experimental conditions.

Threads formed in U2OS cells upon CP110 depletion were interpreted as primary cilia (Spektor et al., 2007). To test whether they resembled primary cilia, U2OS cells depleted of CP110 were serially sectioned for EM analysis in the laboratory of Alexey Khodjakov. This study revealed that U2OS cells depleted of CP110 also contained abnormally elongated centrioles (Figure 30A-B) and microtubule doublets not connected to them as well (Figure 30C-D), as in the case of CPAP overexpression. The overly long centrioles upon CP110 depletion were clearly located in the cytoplasm and did not possess a transition zone typically seen on primary cilia. Thus, threads formed upon overexpression of CPAP as well as depletion of CP110 in U2OS cells do not resemble primary cilia but overly long centrioles.

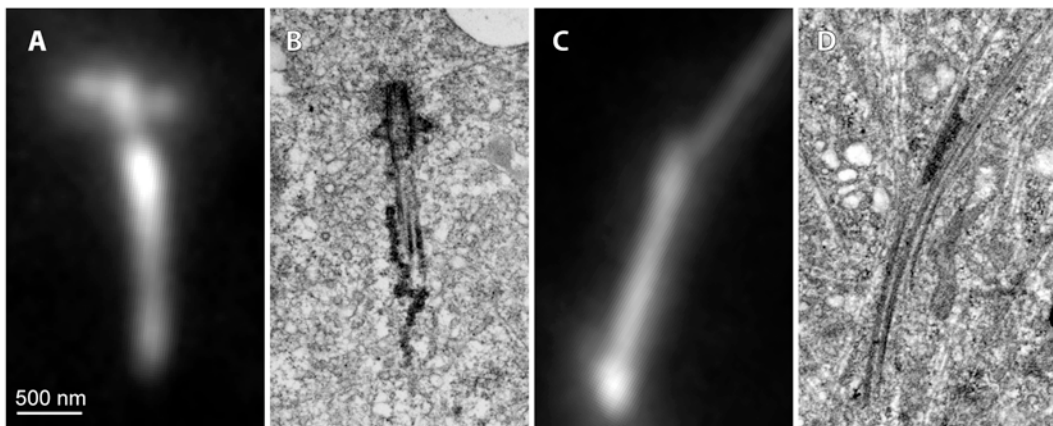


Figure 30: CP110 threads resemble overly elongated centrioles

(A-D) Formation of elongated centrioles and microtubule doublets in U2OS cells depleted of CP110 using siRNAs. Maximal projections of centrin-GFP (A and C) and corresponding 100-nm EM sections (B and D, selected from full series) illustrating the structure of elongated centrioles (A-B), and microtubule doublets that are not connected to centrioles (C-D).

CP110 also regulates formation of bona fide cilia in RPE-1 and 293T cells (Spektor et al., 2007), so we wondered whether CPAP would play an analogous role in such cells. We noted that CPAP localizes to basal bodies underlying cilia, but that neither its depletion nor overexpression changed the frequency or appearance of primary cilia in RPE-1 cells (Figure 31A-D). We

conclude that in contrast to CP110, CPAP does not regulate primary cilia formation in RPE-1 cells.

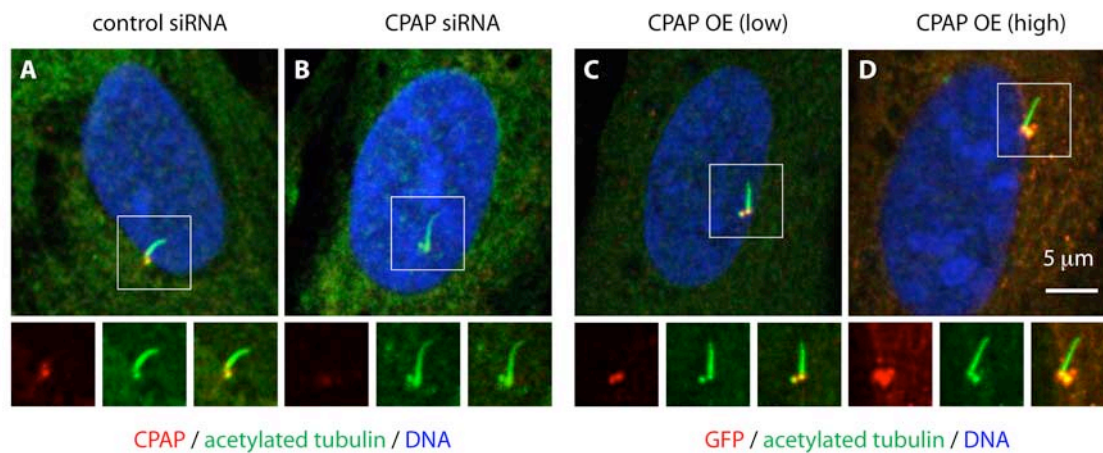


Figure 31: CPAP does not regulate primary cilia formation in RPE-1 cells

(A-B) RPE-1 cells transfected with control (A) and CPAP siRNAs (B) for 48 hours and serum starved for another 48 hours, fixed and stained with antibodies against CPAP (red) and acetylated tubulin (green). Primary cilia formed in ~74% of control siRNA- and ~72% of CPAP siRNA transfected cells ($n > 100$ for each). While ~73% of basal bodies underlying primary cilia exhibited a significant CPAP signal in control siRNA transfected cells, only ~33% showed such a staining upon CPAP depletion, demonstrating that RNAi was effective. In a similar experimental setup, primary cilia formed in ~83% of control siRNA- but only in ~23% of Cep164 siRNA transfected cells, consistent with its known role in primary cilia formation (Graser et al., 2007).

(C-D) RPE-1 cells transfected with a control GFP plasmid (not shown) or GFP-CPAP (C-D) for 72 hours, fixed and stained with antibodies against GFP (red) and acetylated tubulin (green). Primary cilia formed in ~41% of cells transfected with the control plasmid and in ~35% of GFP-CPAP transfected cells ($n > 100$ for each). Note that a population of cycling cells is analyzed here, leading to a generally lower number of primary cilia compared to (A-B). Both weakly (C) and strongly expressing (D) cells similarly displayed primary cilia without an apparent change in their frequency or morphology. CPAP was never incorporated in the axoneme of primary cilia, and no other thread-like structures were present in those cells. OE=overexpression

2.5.10 CPAP aggregates are assemblies of α -Tubulin, γ -Tubulin and Pericentrin

Besides threads, cells overexpressing untagged, GFP- and mCherry-tagged CPAP also form globular aggregates preferentially in the cytoplasm (Figure 18C and data not shown). Live imaging of GFP-CPAP revealed that GFP-containing aggregates appeared when GFP levels increased (data not shown), suggesting that formation of threads is a result of very high GFP-CPAP expression levels. We investigated whether proteins associating with threads were also recruited to these aggregates. Notably, we found that aggregates invariably colocalized with α -tubulin, acetylated tubulin, polyglutamylated tubulin, γ -tubulin and pericentrin, whereas Cep135, Centrin-3, CP110, HsSAS-6, C-Nap1, Odf-2 and Ninein were consistently absent ($n > 50$ for

each) (Figure 32A-D and data not shown). Accordingly, aggregates resisted cold-treatment for one hour (data not shown), suggesting that tubulin is present at aggregates in a stabilized form or is somehow trapped. Low-intensity imaging revealed that the GFP-CPAP signals were concentrated at the aggregate edges, while the other proteins localizing to the aggregates were found throughout interior regions (Figure 32E-H and data not shown). Thus, it appears that aggregates consist of two domains with different protein content.

To assess whether these aggregates contained microtubules or fragments thereof, we analyzed cells overexpressing GFP-CPAP and forming aggregates by combinatorial LM / serial-section EM together with Graham Knott (EPFL BIO-EM facility). In brief, cells with aggregates were selected post fixation by dual fluorescence (Figure 32J) and differential interference contrast (DIC) microscopy on a marked coverslip (Figure 32I). The selected cells were identified relative to the mark after embedding (Figure 32K) and analyzed by serial-section EM (Figure 32L). This analysis revealed electron-dense particles with a diameter of 0.5 – 2 μm that were not present in cells without aggregates (Figure 32M-P and data not shown). Such particles were more intensely stained in their outer regions (Figure 32M, *) than in their interior (Figure 32M, **) in all cases (9/9 serially sectioned aggregates). Thus, it might be possible that the outer shell corresponds to the GFP-CPAP signal seen by immunofluorescence (Figure 32E-H). The interior sometimes appeared to contain an organized substructure composed of small rings and rod-like filaments (Figure 32N, arrowheads), although these structures did not exactly match the diameter or shape of microtubules. The particles also exhibited thin protrusions from the outer shell into the surrounding cytoplasm (Figure 32M, arrows). Similar particles containing microtubules and centriole precursors were recently found to form upon coexpression of Plk4, HsSAS-6 and CPAP in CHO cells (Kuriyama, 2009). It remains possible that CPAP aggregates contain centriole assembly intermediates that are not detectable by standard EM methods, and transform into recognizable centriolar microtubules only in synergy with excess levels of other centriole assembly regulators.

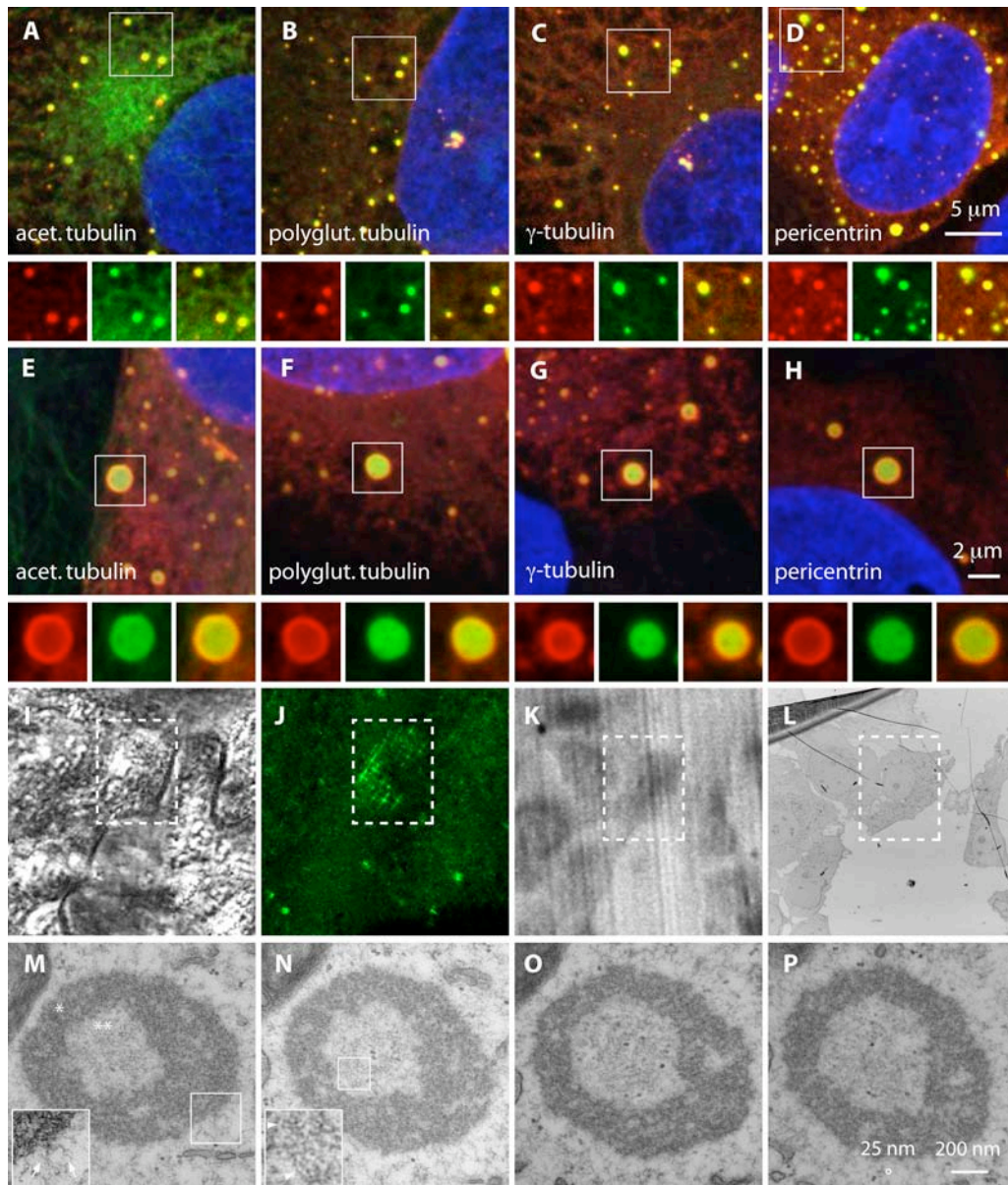


Figure 32: CPAP aggregates are hollow, electron-dense structures

(A-D) iGFP-CPAP cells induced with doxycycline for 48 hours and stained with the antibodies as indicated (red) and GFP (green). Note that the fluorescence signals at the aggregates are overexposed in all cases.

(E-H) Low-intensity and higher magnification pictures from the same experiment as shown in (A-D).

(I-L) iGFP-CPAP cells induced with doxycycline for 48 hours on a marked coverslip, fixed and analyzed by DIC (I), GFP fluorescence (J) (both before embedding), brightfield (K, after embedding) and EM (L, after sectioning). The position of a cell forming GFP-aggregates is indicated with a dashed box. Note that the diffraction of the GFP-signal (J) is due to imaging through the plastic coverslip in a glass-bottom dish.

(M-P) Serial sections of approximately 50 nm distance through one aggregate from the cell selected in (I-L). The particle is composed of an inner (**) and outer (*) domain (see M). Thin protrusions (inset with arrows in M) are found to radiate from the particle. Ring- and rod-like structures (inset with arrowheads in N) with a seemingly regular pattern are found in the inner domain. Note that the contrast was enhanced for the insets (M-N). A circle with 25 nm diameter corresponding to a microtubule diameter is represented next to the side bar. Black particles are ribosomes.

Parts of this chapter were published in (Kohlmaier et al., 2009).

2.6 Initial Structure-Function Analysis

We explored which regions of CPAP are required for abnormal centriole elongation. Therefore, we generated doxycycline-inducible U2OS cell lines for GFP-tagged CPAP constructs lacking the SAC-box (CPAP- Δ SAC), the PN2-3 region (CPAP- Δ PN2-3), CC4 (CPAP- Δ CC4) and TCP (CPAP- Δ TCP) or changing amino acid E1235 to V (CPAP-E>V) (Table 1). Cells were induced with doxycycline for 48 hours and stained with GFP and Centrin-2 to visualize regular or elongated centrioles. Cells with excess CPAP- Δ SAC or CPAP- Δ PN2-3 still formed threads as the full-length protein (Figure 33C-D, G). Thus, the region associated with tubulin heterodimer binding (Hsu et al., 2008) and microtubule depolymerization *in vitro* (Cormier et al., 2009; Hung et al., 2004) is not required for abnormal centriole elongation. Unexpectedly, cells overexpressing CPAP-E>V exhibited threads that were more prominent and were formed in a higher proportion of cells (Figure 33B, G). We assume that the change of glutamate to valine at position 1235, which is associated with primary microcephaly (Bond et al., 2005), might render CPAP more active towards centriole elongation. By contrast, cells overexpressing CPAP- Δ CC4 or CPAP- Δ TCP formed significantly less threads (Figure 33E-F, G), indicating that the protein C-terminus which is important for centriole targeting (2.2.3) is also required for efficient centriole overelongation. We also investigated whether overexpression of those constructs had a dominant effect on bipolar spindle formation. While multipolar spindles were found to variable levels, a clear increase in monopolar spindles was observed in cells overexpressing CPAP- Δ SAC or CPAP- Δ PN2-3 (Figure 33H). We assume that constructs lacking the SAC-box or PN2-3 fragment exert a dominant negative effect on endogenous CPAP in this assay. Thus, the regions associated with tubulin heterodimer binding and microtubule destabilization *in vitro* (Cormier et al., 2009; Hsu et al., 2008; Hung et al., 2004) might be required for regular centrosome duplication.

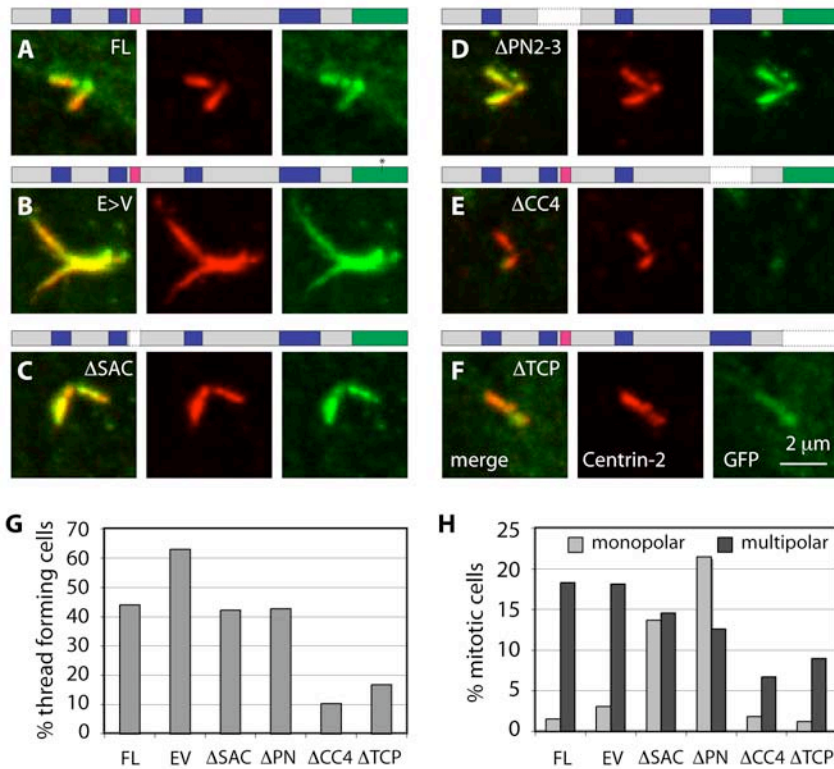


Figure 33: Initial structure-function analysis

(A-F) U2OS cells harboring iGPF-CPAP FL (A), iGFP-CPAP-E>V (B), iGFP-CPAP-ΔSAC (C), iGFP-CPAP-ΔPN2-3 (D), iGFP-CPAP-ΔCC4 (E) or iGFP-CPAP-ΔTCP (F) plasmids, induced for 48 hours and stained against Centrin-2 (red) and GFP (green). Schematic representations of each construct are indicated above (A-F) according to Table 1.

(G-H) The same cell lines (A-F) were induced for 72 hours, stained against Centrin-2 and α -tubulin and scored for the presence of Centrin-2 containing threads during mitosis ($n > 150$) (G). Mitotic cells were also scored according to their spindle polarity visualized by α -tubulin in the same experiment ($n > 150$) (H) Note that bipolar spindles are not shown in (H).

3 Discussion

We have characterized in detail the human protein CPAP. Using high-resolution fluorescence microscopy and FRAP analysis we showed that CPAP concentrates at centrioles, but that it is not stably incorporated there. The protein levels in the cytoplasm and at centrioles gradually increase from S phase to mitosis.

We performed loss and gain of function experiments to determine the role of this protein. We demonstrated that CPAP is required for centriole duplication and efficient microtubule growth from centrosomes. CPAP functions in centriole duplication after recruitment of HsSAS-6 but before that of Centrin, suggesting that it is an important regulator of early stages of procentriole assembly. The regulation of microtubule growth from centrosomes is independent of γ -tubulin centrosomal localization, raising the possibility that CPAP regulates γ -tubulin activity. Notably, we found that excess levels of CPAP result in excessive elongation of procentrioles and centrioles, in assembly of supernumerary procentrioles, and ultimately in defective cell division.

Overall, we determined that CPAP is a multifunctional protein that regulates centriole and PCM functions. In addition, we identified a novel regulation of centriole length in human cells and propose that setting a proper centriole length is crucial for restricting procentriole number and allowing faithful cell division.

3.1.1 The role of CPAP in procentriole assembly

It was initially reported that HeLa cells depleted of CPAP build up multipolar spindles (Cho et al., 2006), suggesting that this protein might play a negative role in centrosome duplication. In contrast to this suggestion, several other studies including our own indicate that CPAP instead plays a positive role in centrosome duplication. We showed here that CPAP is required both for centrosome overduplication in HU-arrested U2OS cells and regular centrosome duplication in proliferating U2OS and HeLa cells. Consistent with this, CPAP is required for Plk4-induced centriole overduplication in U2OS cells (Kleylein-Sohn et al., 2007). A positive role in Plk4- and HU-induced overduplication was recently also confirmed by another laboratory (Tang et al., 2009). Collectively, converging evidence from different experimental conditions, including proliferating culture cells, indicates that CPAP is a positive regulator of centrosome duplication.

We also found that HsSAS-6 but not Centrin is recruited to procentrioles in the absence of CPAP. HsSAS-6 is similarly detected before Centrin very early during procentriole formation in proliferating cells (Strnad et al., 2007), suggesting that CPAP functions early in procentriole assembly. Depletion of the Centrin-binding protein hPOC5 also blocks procentriole assembly, but this clearly happens at a later stage, after Centrin incorporation (Azimzadeh et al., 2009). Such partially assembled procentrioles are composed only of short microtubule doublets corresponding to ~40% of their normal final length. Serial-section EM analysis of cells depleted of CPAP would be needed to address whether procentrioles that form in the absence of CPAP exhibit even shorter microtubule doublets, microtubule singlets or no microtubules at all. EM analyses of mammalian centrioles/basal bodies showed the presence of electron-dense granules near the proximal base of parental centrioles before the assembly of procentriolar microtubules (Anderson and Brenner, 1971; Kalnins and Porter, 1969; Sorokin, 1968). However, it is not known whether the initial HsSAS-6 recruitment to procentrioles corresponds to this or even earlier stages of procentriole development. Ciliated unicellular organisms often exhibit a radial symmetric cartwheel structure

very early during basal body assembly (reviewed in Strnad and Gönczy, 2008), and evidence suggests that SAS-6 is a structural component of this cartwheel in *Chlamydomonas* (Nakazawa et al., 2007) and *Tetrahymena* (Kilburn et al., 2007). Comparable structures in mammalian centrioles have been very rarely reported so far (reviewed in Alvey, 1986), which might be due to unfavorable fixation conditions and their probably transient nature in duplicating centrioles. Since CPAP-depleted cells recruit HsSAS-6 but not Centrin to procentrioles, their assembly may be blocked at this transient stage. Thus, such cells might provide a means to enrich and identify those structures also in human cells.

What might be the mechanism by which CPAP functions in such early stages of procentriole assembly in human cells? It was previously shown that CPAP binds α/β tubulin dimers in a 1:1 ratio *in vitro* (Cormier et al., 2009; Hung et al., 2004). Together with our observation that CPAP rapidly shuttles between the cytoplasm and centrioles, the simplest model would be that CPAP recruits α/β tubulin dimers to procentriole assembly sites and somehow promotes their incorporation in centriolar microtubules (Figure 34A). In favor of this model, we found that overexpression of a CPAP construct lacking the α/β tubulin binding domain significantly increases the number of monopolar spindles, which probably is the result of a dominant negative effect on the wild-type protein. In addition, mutations in aa 377 and 378 (KR>EE), which significantly decrease α/β tubulin dimer binding (Hsu et al., 2008), also impair Plk4-induced centriole amplification (Tang et al., 2009). It will be important to test whether the tubulin-binding domain within CPAP is required to rescue centriole duplication in the absence of endogenous CPAP. A second model would be that CPAP somehow assembles α/β tubulin multimers in the cytoplasm and promotes their incorporation in procentrioles (Figure 34B). Such a mechanism is suggested for the elongation of cytoplasmic microtubules through the microtubule plus-end binding proteins (+TIPs) XMAP215, CLIP-170 and EB1 (Slep and Vale, 2007). Each of these proteins carries multiple tubulin-binding domains, which might favor the formation of tubulin multimers in the cytoplasm (discussed in Cassimeris, 2007). Since CPAP only carries a single tubulin-binding domain, several CPAP molecules might need to assemble in the cytoplasm

to assemble such tubulin multimers. However, it is not known whether CPAP self-interacts or whether it is able to form multimers that assemble with tubulin multimers. A third model would be that CPAP promotes the assembly of centriolar microtubule fragments at some distance from centrioles and then delivers the products to procentrioles (Figure 34C). The analysis of centriole assembly by electron tomography in *C. elegans* revealed that centriolar microtubules always become visible as units of a certain length (Pelletier et al., 2006), indicating indeed that whole microtubules might be assembled at some distance from procentrioles before their attachment around the central tube. Compatible with this hypothesis, we consistently detected microtubule doublets not directly associated with elongated centrioles in the case of CPAP overexpression and CP110 depletion. In the case of excess CPAP levels, perhaps an overload of preformed microtubule fragments would compete for their incorporation in centriolar microtubules, leading to the disorganized ends seen by EM. In any case, these models predict that CPAP at some point directly interacts with centriolar microtubule plus ends during early stages of their assembly. However, no data exist so far that would support such localization. It remains to be determined by immuno-EM or superresolution microscopy techniques such as Stochastic Optical Reconstruction Microscopy (STORM) or Stimulated Emission Depletion Microscopy (STED), where exactly CPAP molecules localize during procentriole assembly. Alternative models are conceivable where CPAP only indirectly functions in the assembly of centriolar microtubules. For example, it might stabilize already formed centriolar microtubules by lateral interactions. However, the FRAP profiles of GFP-CPAP indicate that it probably does not play a structural role at centrioles.

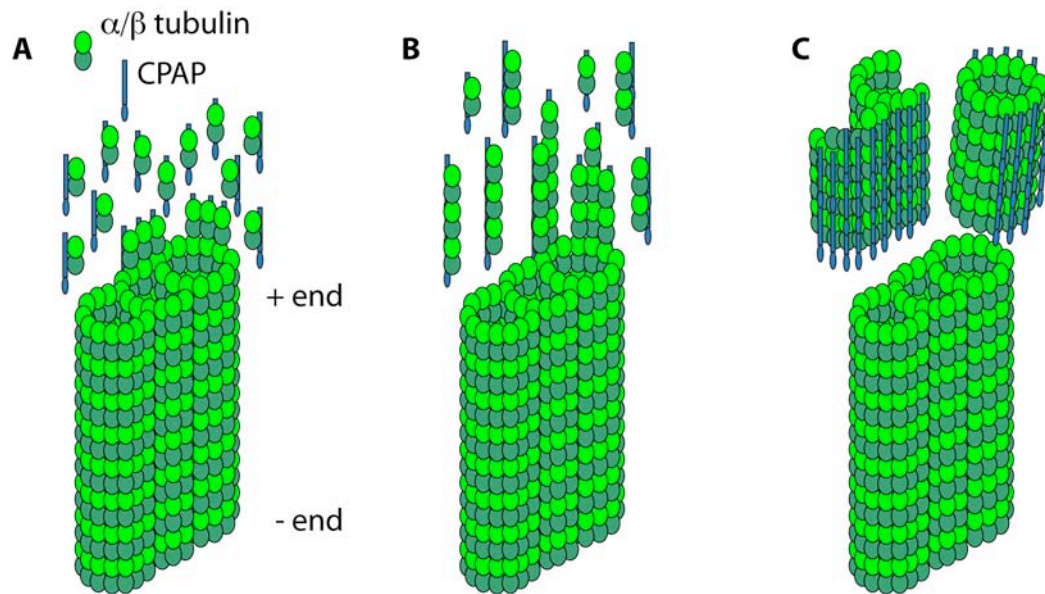


Figure 34: Hypothetical models of CPAP action at centriole ends

(A-C) Microtubule triplet blades are shown representative for the growing centriole end. CPAP is drawn to attach tubulin dimers (A), multimers (B) or preformed microtubule fragments (C) to the growing plus end. Note that CPAP probably also interacts with centriolar microtubule walls, but this is not represented here. CPAP head-to-tail interactions forming CPAP multimers are predicted in (B) and (C).

3.1.2 A common mechanism for SAS-4, DSas-4 and CPAP?

CPAP and DSas-4 were found by BLAST searches with a fragment of *C. elegans* SAS-4 (Leidel and Gönczy, 2003). However, the region with highest similarity between these proteins is restricted to only ~16 amino acids (SAC-box). The probability that 16 out of 20 building blocks are placed in the correct order by pure chance lies in the range of 10^{-20} , strongly suggesting that the SAC-box is evolutionary conserved or a product of convergent evolution. Given the little overall sequence relatedness, it is remarkable that CPAP also functions during centriole duplication after HsSAS-6 recruitment in human cells, like SAS-4 in *C. elegans* (Leidel et al., 2005). DSas-4 shares higher homology with CPAP in the C-terminus and is also required for centriole duplication in flies (Basto et al., 2006), presumably after DSas-6 recruitment. The question arises whether CPAP and DSas-4 work through a similar mechanism as SAS-4, or whether these proteins evolved different mechanisms for a similar function.

Some lines of evidence suggest that there are considerable mechanistic differences between SAS-4 and CPAP. First, we showed that CPAP is targeted to the centrioles via its CC4. Although it is not known which regions target SAS-4 to centrioles, at least the CC4 does not appear to be conserved in SAS-4 (Leidel and Gönczy, 2003). SAS-4 also localizes to human centrosomes when it is overexpressed in U2OS cells, but this probably reflects an unspecific localization to the PCM and also does not induce formation of threads (data not shown). Second, we detected that the majority of centrosomal CPAP continuously exchanges with the cytoplasmic CPAP pool during G1, S and G2. This is in contrast to SAS-4, which does not exchange with the cytoplasmic SAS-4 pool after its incorporation in centrioles (Leidel and Gönczy, 2003). Third, we report here a role for CPAP in microtubule nucleation or growth from centrosomes, whereas a similar function was not reported for SAS-4 in *C. elegans*.

Other data point towards mechanistic similarities between both proteins. First, α/β tubulin binding seems to be important for CPAP to regulate centriole assembly upon Plk4 overexpression (Tang et al., 2009). Two residues (aa 377 and 378) that are critical for α/β tubulin binding are part of the SAC-box, which is conserved in SAS-4. Since SAS-4 is required for assembly of centriolar microtubules in *C. elegans* (Pelletier et al., 2006), it is tempting to speculate that the SAC-box might play an important role for SAS-4 in recruiting tubulin to procentrioles. In contrast to CPAP, SAS-4 does not shuttle between centrioles and the cytoplasm (Leidel and Gönczy, 2003). However, FRAP analyses during early stages of procentriole assembly detected some fluorescence recovery also for SAS-4 (Dammermann et al., 2008; Leidel and Gönczy, 2003), indicating that this protein similarly exchanges with the cytoplasmic pool during some time of procentriole assembly. Moreover, it is possible that a small fraction of centrosomal CPAP is also stably incorporated in centrioles, as slight centriolar CPAP signals remained after RNAi (data not shown). The continuous shuttling of the majority of centrosomal CPAP might reflect other functions of this protein that are probably not conserved in SAS-4, such as the regulation of microtubule growth from centrosomes. Furthermore, partial depletion of SAS-4 correlates with the assembly of shorter and structurally defective centrioles, which in turn recruit less PCM

(Kirkham et al., 2003). We similarly find partially assembled centrioles and a lesser amount of associated PCM upon partial depletion of CPAP. We assume that such centrioles were blocked at a slightly later stage of their assembly than upon complete protein depletion, since a weak Centrin signal could be detected in such cases. These findings raise the possibility that the extent of elongation and the structural integrity of centrioles depend on correct SAS-4 / CPAP protein levels during centriole duplication in both worms and humans. Moreover, these results suggest that the length of centrioles determines the amount of associated PCM in both cases.

Overall, it seems possible that CPAP and SAS-4 function through a similar mechanism early in procentriole assembly, probably in the regulation of centriolar microtubule assembly. The notable absence of related proteins from centriole/basal body containing protozoan species like *Tetrahymena* or *Chlamydomonas* indicates either that procentriole assembly is based on different mechanisms than in humans and worms, or that other proteins play analogous roles in these systems.

3.1.3 Normal vs. abnormal centriole elongation

It was previously reported that elevated levels of upstream regulators of centriole assembly, such as HsSAS-6 and Plk4, can induce the initiation of supernumerary procentrioles from a parental centriole in a flower-like configuration in human cells (Kleylein-Sohn et al., 2007; Strnad et al., 2007). We provide evidence that elevated levels of CPAP can induce abnormal elongation of both procentrioles and centrioles, and two other laboratories independently reported similar results (Schmidt et al., 2009; Tang et al., 2009).

Does abnormal centriole elongation upon CPAP overexpression reflect its regular role during normal procentriole elongation? And if so, does this provide novel insights into the mechanism by which CPAP acts during regular centriole assembly? In this context, it is interesting to compare the protein levels in both conditions. CPAP levels associated with abnormal centriole elongation are 10-15 fold above the ones in normal cells. What exactly is the concentration of CPAP necessary for centriole duplication requires further study. But it appears

that centriole length is relatively insensitive against excess CPAP levels, since excess centriole elongation does not happen during the regular cell cycle and also not in all cells that overexpress CPAP. This raises the possibility that inhibitory mechanisms exist which normally protect centriolar microtubules from excess elongation and counteract length-promoting factors such as CPAP. We and others showed that CP110, which localizes to the distal tip of procentrioles and centrioles, plays such an inhibitory role for centriole length (Schmidt et al., 2009). How exactly CP110 functions to counteract the length-promoting role of CPAP is not fully understood. CP110 also regulates primary cilia formation in 3T3 and RPE-1 cells, and it is removed from the mother centriole to allow axoneme elongation (Spektor et al., 2007). Elevated CP110 levels are sufficient to inhibit axoneme elongation during primary cilia formation (Spektor et al., 2007), probably via increased localization to the centriole end. We and others found that endogenous CP110 is not displaced from centriole ends upon excess centriole elongation (Schmidt et al., 2009), and we furthermore showed that excess CP110 is also not sufficient to inhibit this overelongation. On the other hand, depletion of CP110 can act synergistically with CPAP overexpression to produce extra long centrioles (Schmidt et al., 2009). These results indicate that the regulation of centriole length underlies different regulations than that of primary cilia formation. In addition, centriolar microtubules elongate beneath a CP110 cap, which might provide a microenvironment for tubulin incorporation.

We analyzed the importance of several regions of CPAP for promoting centriole elongation. The PN2-3 region which includes the conserved SAC-box was previously implicated in α/β tubulin binding (Cormier et al., 2009; Hsu et al., 2008; Hung et al., 2004) and regulating Plk4-induced centriole overduplication (Tang et al., 2009). Thus, we were surprised to find that overexpression of CPAP constructs lacking either domain still localized to centrioles and induced centriole elongation at similar frequency as the wild type protein. These data strongly suggests that the PN2-3 region and SAC-box are not required for abnormal centriole elongation. However, these experiments were performed in the presence of endogenous CPAP, so it is possible that centriole elongation may be caused by the recruitment of this pool of wild type protein. Of special

note, we analyzed a CPAP mutation (E1235V) that is associated with MCPH (Bond et al., 2005). MCPH usually correlates with truncations of several centrosomal proteins including CPAP, which may cause defects in neuronal mitoses (reviewed in Bond and Woods, 2006). In fact, flies lacking DSas-4 do exhibit problems in asymmetric divisions of larval neuroblasts, although their brain size appears undistinguishable from that of wild type flies (Basto et al., 2006). However, the resulting adult flies lack flagella and cilia, leading to their death shortly after birth. The primary cilium in vertebrates plays an essential role during development as a center of Hedgehog (Hh) and Wnt signaling (reviewed in Wong and Reiter, 2008), and disruption of the primary cilia leads to an early developmental arrest with an open neural tube in mice (Huangfu et al., 2003). Therefore, microcephaly patients probably do not totally lack primary cilia. However, it might be possible that primary cilia function is compromised during some stages of development, especially in the brain. Importantly, we found that the E1235V mutant protein also localizes to centrioles and induces their elongation when overexpressed. Furthermore, centriole overelongation happens even at higher frequency and in a more pronounced manner compared to the wild type protein. This phenotype could be due to a higher activity in centriole elongation, to higher expression levels or to less turnover of the protein. How can this have the same effect on brain growth as a protein truncation? Perhaps centriole overelongation does not allow centrioles to properly function as basal bodies and ciliary signaling any more. It would be important to analyze whether microcephaly patients exhibit ciliary defects in the brain or other tissues. Transgenic mice expressing CPAP or the E1235V variant might allow studying the function of this protein in brain development in more detail.

Little is known about other proteins that might contribute to the regulation of centriole length. The binding of CP110 with the coiled-coil protein CEP290 and the small GTPase Rab8a regulate primary cilia formation (Tsang et al., 2008), but it is unclear whether such interactions are important also for centriole elongation. Interestingly, depletion of γ -tubulin from *Drosophila* S2 cells also results in elongation of centriolar microtubules (Raynaud-Messina et al., 2004), indicating that γ -tubulin might also play a protective role in centriole length like CP110. γ -tubulin

also interacts with CPAP in centrosomal fractions of human cells (Hung et al., 2000), but this could also reflect the function of both proteins to regulate microtubule nucleation and growth from the PCM. Overexpression of the centrosomal protein POC-1 also induces formation of elongated structures that harbor centriolar proteins in U2OS cells, but an ultrastructural analysis was not performed (Keller et al., 2009). POC-1 localizes to similar centriole regions as CPAP and is also required for HU-induced centrosome overduplication. This raises the possibility that CPAP and POC-1 collaborate in regulating centriole length.

It is not known whether overexpression of SAS-4 in *C. elegans* would similarly lead to centriole elongation. Due to the lack of transcription in the early embryo it is generally not possible to reach high expression levels at this time. The situation is different in later stages of development, and it would be interesting to analyze SAS-4 overexpression in postembryonic proliferating cells, such as seam cells. Signs of abnormal centriole elongation were also not reported upon overexpression of DSas-4 *in vivo* (Peel et al., 2007), although depletion of the *Drosophila* homologue of CP110 in the fly also seems to slightly increase centriole length (J. Raff, pers. comm.). It would be interesting to overexpress SAS-4 and DSas-4 in *Drosophila* S2 cells or human cells to determine whether it would behave similarly as CPAP in proliferating tissue culture cells. Conversely, CPAP could be expressed in *Drosophila* S2 cells. Thus, further analysis is required to determine whether DSas-4 or SAS-4 can also induce abnormal centriole elongation.

Overall, the centriole overelongation observed upon excess CPAP might be interpreted as enhanced tubulin incorporation in centriolar microtubules, which probably also happens at endogenous levels in normal cells. Why then do centrioles elongate during late G2 upon CPAP overexpression, whereas endogenous CPAP is required during centriole duplication at very early stages between G1 and S phase? There is no definite answer to this question, but it is possible that the late G2 phase represents a window of opportunity where centrioles are specially labile and accessible to structural changes. Furthermore, we cannot exclude that a substantial elongation

initiates already earlier in S phase, but that our detection methods allow clear visualization of abnormal elongation only during G2.

3.1.4 Regulation of procentriole number

The current concept of centriole duplication holds that early regulators like HsSAS-6 and Plk4 are essential to initiate formation of new procentrioles and restrict their number to one per parent centriole (reviewed in Strnad and Gönczy, 2008). The recent observation that excess levels of the PCM component pericentrin are sufficient to enhance centriole overduplication during S-phase arrest provided further insights in the mechanisms underlying initiation of centriole assembly (Loncarek et al., 2008). This finding was unexpected, since the accumulation of pericentrin is thought to be a downstream event not directly involved in centriole assembly (discussed in Loncarek and Khodjakov, 2009). Although it is not understood how exactly pericentrin overexpression contributes to initiation of new procentrioles, excess pericentrin levels create an enlarged PCM that possibly favors accumulation of early regulators of procentriole assembly.

We found that CPAP overexpression also induces centriole overduplication. Strikingly, additional procentrioles were detected along the overly elongated centriole segment with increasing frequency over time. What might be the mechanisms by which such additional procentrioles form? First, enhanced CPAP levels are unlikely to directly initiate new procentriole assembly like enhanced levels of HsSAS-6 or Plk4. Indeed, supernumerary procentrioles were not detected around parental centrioles in a flower-like configuration, as is the case in HsSAS-6 or Plk4 overexpression (Kleylein-Sohn et al., 2007; Strnad et al., 2007). This goes in line with the requirement of CPAP downstream of HsSAS-6 in regular centriole duplication. Instead, our findings raise the possibility that centriole length contributes to the regulation of procentriole number. We always detected the recruitment of PCM components such as γ -tubulin and pericentrin to the overly long centriole segments, suggesting that the ectopic PCM found in those places might somehow contribute to additional procentriole formation as in the case of pericentrin

overexpression (Loncarek et al., 2008). It will be interesting to determine whether ectopic γ -tubulin or pericentrin is necessary for centriole overduplication or whether abnormal centriole length is sufficient. However, this is not easy to address experimentally since strong depletion of these PCM components leads to cell cycle arrest (pers.comm. A. Khodjakov). Furthermore, we do not know whether these proteins are necessary for the abnormal elongation of centrioles in the first place. Depletion of Cdk5Rap2 was reported to displace γ -tubulin from the PCM without interfering with cell cycle progression (Fong et al., 2008). However, in a preliminary experiment we could not reproduce these results. Therefore, it remains to be determined what is the contribution of the PCM for CPAP-induced centriole overduplication.

Normally, procentrioles exert an inhibitory effect for the formation of additional procentrioles in their vicinity. This inhibitory effect is believed to act *in cis* for each parent centriole, since procentrioles reform after laser ablation in the presence of a neighboring centriole/procentriole pair (Loncarek et al., 2008). We used ectopic procentriole formation on overly long centrioles as an assay to determine the range over which such an inhibitory effect works. Interestingly, we rarely observed more than one ectopic procentriole per elongated structure and moreover found that such additional procentrioles are present starting at \sim 400 nm away from the regular procentrioles. This information provides further evidence that the inhibitory effect associated with procentrioles acts in a locally restricted manner at parent centrioles. Furthermore, the range of this effect correlates with the length of normal centrioles. This raises the exciting possibility that controlling centriole length represents a novel mechanism by which the number of procentrioles can be regulated. Thus, proteins like HsSAS-6 and Plk4 would directly regulate the initiation event of procentriole formation, whereas proteins like CPAP would establish the size of the platform on which such procentrioles can form.

We addressed the consequence of CPAP overexpression for cell division and observed thread formation, multipolar spindle formation and cell division defects. Based on data from fixed cell analyses and live cell imaging, we propose a mechanistic model explaining how multipolarity and cell division defects can arise from enhanced levels of the centrosomal protein CPAP (Figure 35). Overall, it seems that centriole overelongation is an early effect of excess CPAP levels that is followed by the formation of extra centrioles, but that does not directly hinder bipolar spindle formation (Figure 35, cell cycle I). In favor of this, up to 2.6 μm long centrioles in primary spermatocytes also build up two meiotic spindles without apparent problems (González et al., 1998). It is not clear why no extra procentrioles form in this case, but one explanation might be that the centriole duplication machinery is generally shut off at these stages of meiosis. It would be interesting to test whether this case of centriole elongation is associated with excess DSas-4 or insufficient CP110. POC1 is another protein that was implicated in the control of centriole length in humans (Keller et al., 2009) . An ortholog also exists in *Drosophila*, indicating that it could also play a role in the regulation of centriole length in spermatocytes. It was postulated that centrioles play a crucial role in cytokinesis (Piel et al., 2001). Although we identified a highly distorted centriole structure at the overelongated segment by EM, we only observed 8% cytokinesis errors in U2OS cells harboring threads. Thus, an intact distal centriole end is not essential for cytokinesis in this cell line. It was also postulated that loss of centrosome integrity upon depletion of several centrosomal proteins leads to a G1 arrest in RPE-1 cells (Mikule et al., 2007). We did not detect such an arrest upon CPAP induction for up to 96 hours (FACS analysis, data not shown), indicating that the disrupted centriole structure seen in threads is probably not sufficient to induce such an arrest. Multipolar spindle formation seems to happen in a later step as a consequence of having too many centrosomes (Figure 35, cell cycle II). We cannot exclude that excess CPAP directly induces centrosome overduplication, but extra procentriole formation along elongated centrioles clearly contributes to centrosome overduplication. Too many centrosomes were recently linked to chromosome missegregation even when they cluster in bipolar spindles

(Ganem et al., 2009), indicating that this might also happen in the case of CPAP overexpression and might further contribute to genomic instability.

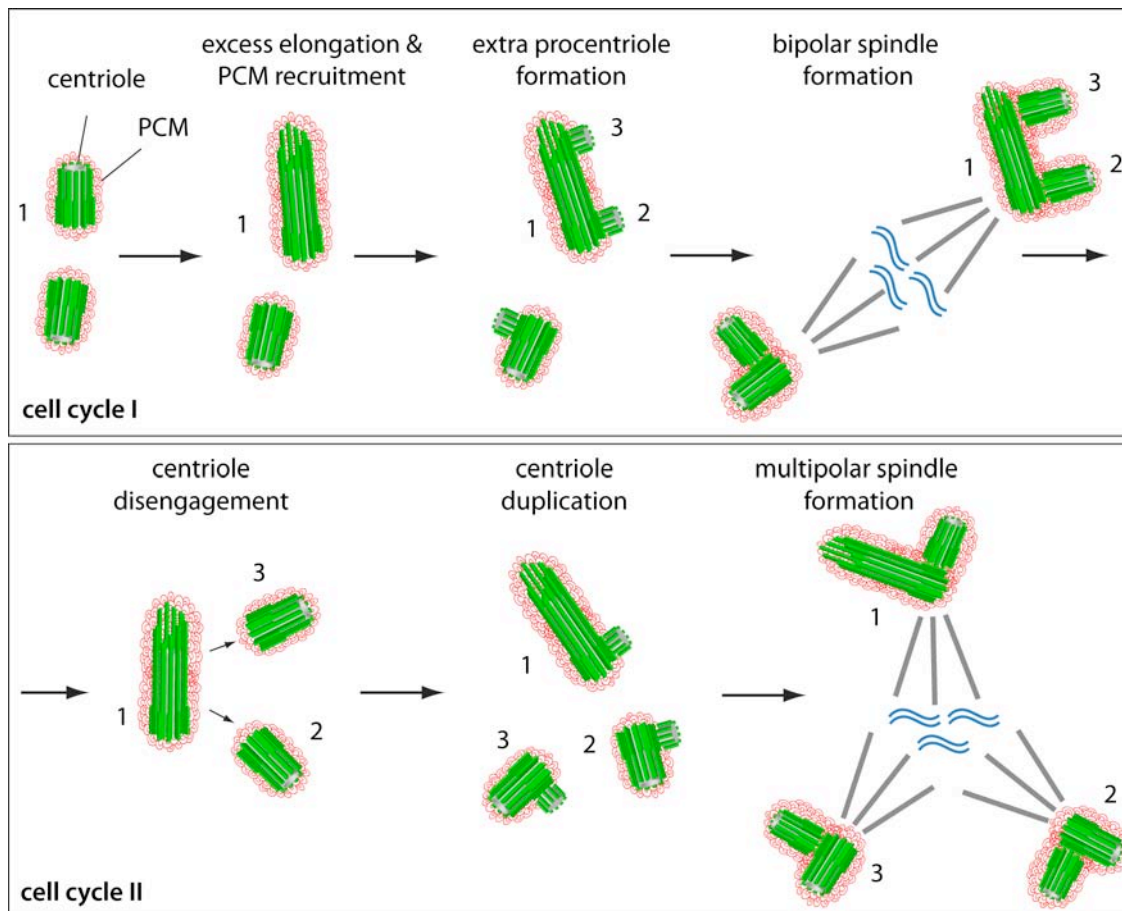


Figure 35: Proposed sequence of events upon excess CPAP

Excess CPAP levels are believed to initially induce excess centriole elongation and PCM recruitment, which can happen from centrioles (as indicated here) or from procentrioles (not shown here). The centriole which underwent excess elongation (1) can produce multiple procentrioles (2 and 3), which does not impair bipolar spindle formation in cell cycle I. Cell division occurs normally, and the extra procentrioles (2 and 3) disengage from their parent centriole (1) shortly thereafter, allowing each of them to undergo another round of centriole duplication. The multiple centrioles stemming from the previous cell cycle then set up a multipolar spindle (shown here) or cluster at two spindle poles (not shown here). Overall, CPAP is believed to initiate this cascade of events by providing an overly elongated parent centriole. Centrioles are shown in green, PCM in red, the mitotic spindle in grey and DNA in blue.

Several centrosomal defects including disrupted centriole structure and excess PCM are associated with human tumors (Lingle and Salisbury, 1999), and increasing evidence points towards a causal relationship between supernumerary centrosomes and the development of genetic instability which is often seen in cancer (reviewed in Godinho et al., 2009). The simultaneous formation of multiple procentrioles on overly long parent centrioles may provide

one way by which multiple centrosomes are generated also in tumors. CPAP is expressed in many human tissues, but highest levels are detected in haematopoietic organs, heart, brain, lung and skeletal muscle (Peng et al., 2002). Therefore, it will be interesting to test whether CPAP is upregulated in tumors of such tissues or whether centrioles are unusually long in such cases. Centriole length variations are also seen under physiological conditions, not only within tissues but also within species (discussed in Delattre and Gönczy, 2004; González et al., 1998). It will be furthermore important to dissect whether relatives of CPAP, CP110 or POC1 are involved in the regulation of centriole length in such systems.

Despite the crucial roles of centrosomes in physiological and pathological conditions in humans, the mechanisms regulating centrosome structure and function are only starting to be understood. We have shed light on the regulation of centriole length, which has received little attention thus far. A better understanding of how centriole length is regulated will be relevant also to better understand the role of centrosomes in the development of cancer and other diseases.

4 Materials and Methods

4.1 Molecular Biology and Antibody Generation

Full-length CPAP in pEGFP-C1 was kindly provided by T.K.Tang (Hung et al., 2000). Three overlapping fragments covering the full-length cDNA (Table 1, A) were cloned into pEGFP-C1 (Clontech, Mountain View, CA). For further overexpression experiments, two codons (129 and 1333) were reverted to fully correspond to the NCBI reference sequence NM_018451 (Table 1, B). In addition, four silent nucleotide changes were introduced in the siRNA3 target region (nt 2862 – 2880) to make the construct RNAi resistant (Table 1, B). From this modified CPAP cDNA, candidate regions were removed or changed (Table 1, C). The various constructs were then cloned into the pENTR 1A vector (Invitrogen) and subsequently transferred into the pEBTet-EGFP and pEBTet-mCherry vectors (modified from Bach et al., 2007) for inducible expression (Table 1, D).

The C-terminal region of CPAP (from RZPD clone IRAUp969C1177D, GenBank entry AF139625) corresponding to amino acids 1070 – 1338 of the full-length protein was cloned into pGEX-6P-3 (Amersham Pharmacia Biotech, Freiburg, Germany) to express a GST-CPAP^{C-term} fusion. In addition, the PN2-3 fragment of CPAP (Hung et al., 2004) was cloned into pET-30a+ (EMD Biosciences, Novagen, San Diego, CA) and pGEX-4T1 (Amersham Pharmacia Biotech, Freiburg, Germany) to express HIS-CPAP^{PN2-3} and GST-CPAP^{PN2-3} fusions, respectively. Polyclonal rabbit antibodies were raised against the affinity purified GST-CPAP^{C-term} and HIS-CPAP^{PN2-3} proteins (Eurogentec, Seraing, Belgium). CPAP^{C-term} antibodies were affinity purified with the antigenic CPAP^{C-term} protein that was cleaved from GST using Precision Protease (Amersham Pharmacia Biotech) and coupled to Affi-Gel-15 (Bio-Rad Laboratories, Hercules, CA). CPAP^{PN2-3} antibodies were similarly affinity purified with GST-CPAP^{PN2-3} fusion protein. Both CPAP antibodies were batch eluted in 200 mM glycine (pH 2.2) / 500 mM NaCl, neutralized with 1.5M Tris-HCl (pH 9.2), dialysed in phosphate-buffered saline (PBS) with 10%

glycerol and concentrated to 1 μ g/ μ l using Centrprep columns (Millipore, 10kD exclusion volume).

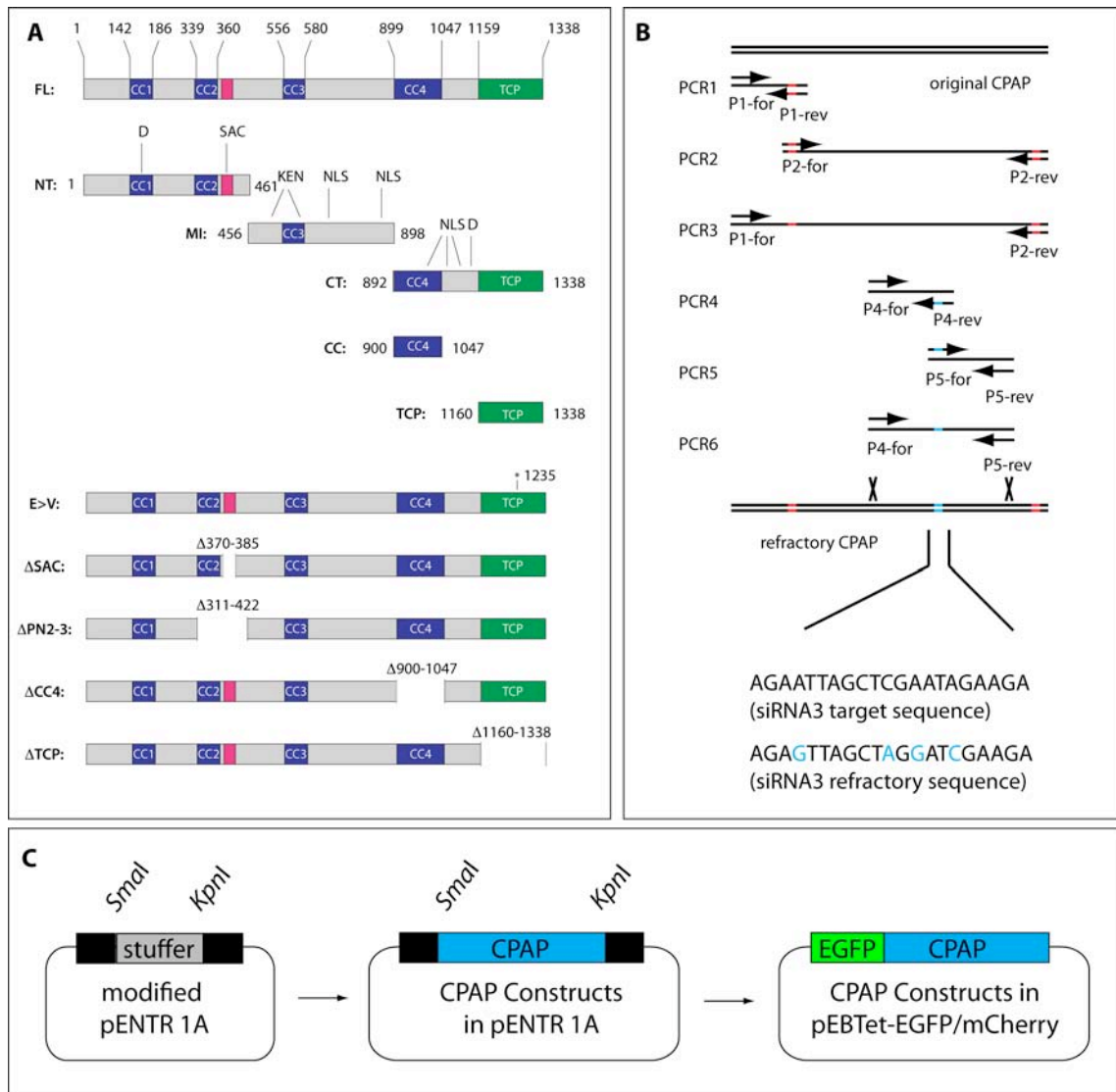


Table 1: Molecular Cloning of CPAP and CPAP Fragments

(A) Three CPAP fragments (NT=N-terminus, MI=Middle, CT=C-terminus) were amplified from pEGFP-C1-CPAP with the primers NT-For (CCGGGATCCATGTTCTGATGCCAACCTC) and NT-Rev (GCTCTAGAGAATTCTCATTACAGCATTTTCGGCTTCTG), MI-For (CCGGGATCCAGAAGCCGAAAATGCTGAAG) and MI-Rev (GCTCTAGAGAATTCTCACCAGGTGGTTGGTCTTGACT), and CT-For (CCGGGATCCAGTCAAGACCAACCACCTGG) and CT-Rev (GCTCTAGAGAATTCTCACAGCTCCGTGTCCATTG), respectively. The PCR products were cloned with *Bam*HI and *Xba*I into pBluescript II KS (+), sequenced (Microsynth, Balgach, CH) and then cloned with *Sal*I and *Sac*I into pEGFP-C1.

Several changes and deletions were introduced into the refractory CPAP cDNA (from B) by PCR splicing. The respective primers P1-for and P1-rev (PCR1), P2-for and P2-rev (PCR2), and P1-for and P2-rev (PCR3) were as following - for CPAP-E>V: P1-for (CAGCAAATAGCAGATTTACG), P1-rev (ATCTGGGTAATGTTTCACTATTTGTCCACT), P2-for (AGTGGACAAATAGTGAAACATTACCCAGAT), P2-rev (CGGGGTACCTCACAGCTCCGTGTCCATTGACACATT); for CPAP-ΔSAC: P1-for (ACTACAGAGACTCATGGAAG), P1-rev (CTTAGATTTGGCATTAGTTGCTTTGATTGGCAATGG), P2-for (CCATTGCCAATCAAAGCAACTAATGCCAAATCTAAG), P2-rev (CGGCTGGTCTCGGAAGTGCTC); for CPAP-ΔPN2-3: P1-for (ACTACAGAGACTCATGGAAG), P1-rev (CACAGCTCTTTATTTTAAAGAGCGGTTTTAAGTTCTTATCATTGCTTC), P2-for (GAAGCAAATGATAAGAACTTAAAAACCGCTCTTAAAAATAAAGAGCTGTG), P2-rev (CGGCTGGTCTCGGAAGTGCTC); for CPAP-ΔCC: P1-for (AAGATTGCACCAGTCAAGAG), P1-rev (CCAGGCATCCAGTCCGGAAGTCAACCAGGTGGTTGGTC), P2-for (GACCAACCACCTGGTGACTTCGACTGGATGCCTGG), P2-rev (GGATCTTCGAGGTGGATTGC); for CPAP-ΔTCP: P1-for (GACCAACCACCTGGTGACTTCCGACTGGATGCCTGG), P1-rev (CGGGGTACCTCACTTTCCATCAGGATGACTGATTTTC); Internal CPAP restriction sites were used to exchange endogenous regions with the PCR products harboring the respective changes. The constructs were then transferred with *Sma*I and *Kpn*I into pENTR 1A (see D) and sequenced. Two additional C-terminal regions of CPAP were amplified - the coiled coil region with P-for (CGCGGATATACCCCGGGGATGAATGCTCGATCCCAGGTTTTGAG) and P-rev (GCGCGAATTCGGTACCTTATCTTTCCACTTTTATTTTC), and the TCP10 domain with P-for (CGCGGATATACCCCGGACCATGGTGGAAAAGGTTTATAAGAATGGG) and P-rev (GCGCGAATTCGGTACCTCACAGCTCCGTGTCCATTGACAC). The PCR products were directly cloned with *Sma*I and *Kpn*I into pENTR 1A (see D) and sequenced.

(B) The original CPAP cDNA was modified by PCR splicing to revert two codons according to NM_018451 and make the construct refractory to siRNA3. Two PCR reactions (PCR1 and 2) introducing point mutations (red, changing amino acid R129L and S1333L) were performed with the primers P1-for (AAAAGTGCAGATGTTCTGATGCCAACCTC) and P1-rev (GAATTCACCTCGCAAGATCTGGGATGAAATGTC), and P2-for (GACTTCATCCCAGATCTTGCAGTGAATTC) and P2-rev (CGGGGTACCTCACAGCTCCGTGTCCATTAGCACATT). In a third PCR reaction (PCR3) these fragments were joined by overlap extension and amplified with the primers P1-for and P2-rev. The final PCR product was cloned with *Pst*I and *Kpn*I into pBluescript II KS (+) (Stratagene, La Jolla, CA) and sequenced. With two additional PCR reactions (PCR4 and 5) using the primers P4-for (GAAAATGTAAGTGTGCTC) and P4-rev (TTCGATCCTAGCTAACTCTTT), and P5-for (AAAGAGTTAGCTAGGATCGAA) and P5-rev (GGATCTTCGAGGTGGATTGC), four silent nucleotide changes between the position 2862 – 2880 (blue) were generated. In a sixth PCR reaction (PCR6) with the primers P4-for and P5-rev these fragments were joined and amplified. The resulting PCR product was used to exchange the region between *Bst*EII and *Hind*III in the so far generated CPAP cDNA in pBluescript II KS (+) and sequenced. Arrows indicate primers. PCR reactions were performed with the respective forward (for) and reverse (rev) primers using the Expand High Fidelity PCR System (Roche, Mannheim, Germany).

(C) The various CPAP constructs were transferred to the Gateway system. Therefore, *Sma*I and *Kpn*I restriction sites were introduced in the pENTR 1A plasmid by PCR with the primers P-for (CGCGGATATACCCCGGGACCATGGTGAAGGCGAGGAG) and P-rev (GCGCGAATTCGGTACCTTACTTGTACAGCTCGTCCAT). After cloning the CPAP constructs into this pENTR 1A vector, they were transferred to the Gateway compatible pEBTet-EGFP and -mCherry destination vectors according to the manufacturer's protocol (Invitrogen). Black bars indicate sequences needed for recombination.

4.2 Cell Culture and Cell Lines

Human cultured cells were grown in high-glucose DMEM with GlutaMAX (Invitrogen, Carlsbad, CA) supplemented with 10% fetal calf serum (FCS) in a humidified 5% CO₂ incubator at 37°C. Cells were split every 3-4 days or when reaching confluency. To generate inducible cell lines, U2-OS cells were transiently transfected with pEBTet-EGFP-CPAP or pEBTet-mCherry-

CPAP at 80-90% confluency. 24 h after transfection, cells were exposed to selective medium containing 1 µg/ml puromycin, which lead to substantial death of nontransfected cells over 4-5 days. After amplification of the transfected cell population under selective conditions for 1-2 weeks, cells were frozen in 10% DMSO and stored at -80°C. Expression was induced for the indicated time intervals using 1 µg/ml doxycyclin.

Primary human cell culture work was conducted in collaboration with Gaetana Restivo and Natsuko Imaizumi as described (Ruegg et al., 1998). Human umbilical vein endothelial cells (HUVECs) and human keratinocytes were obtained from the Centre Hospitalier Universitaire Vaudois (CHUV, Lausanne). HUVECS were electroporated and cultured for 72 hours thereafter. Human keratinocytes were transfected with Lipofectamine 2000 (Invitrogen, Carlsbad, CA) as described below and also cultured for 72 hours after transfection.

4.3 Cell Cycle Synchronization and FACS Analysis

Cells were synchronized at the G1/S transition by a double thymidine block and then released into G2 phase, mitosis and the subsequent G1 phase. At the indicated timepoints during the release, samples were taken, stained with Propidium Iodide and the DNA content measured by flow cytometry (FACScan, BD Biosciences). To perform the double thymidine block, cells were incubated in medium containing 2 mM thymidine for 18 h, released for 6 h and again incubated in thymidine containing medium for 18 h.

4.4 RNAi and Transient Plasmid Transfection

For RNAi experiments, ~100.000 cells were seeded on 18 mm sterile glass coverslips in 6-well plates. 6 µl of 20 µM siRNA in 100 µl OptiMEM medium (Invitrogen, Carlsbad, CA) and 3 µl of Oligofectamine (Invitrogen) in 27 µl OptiMEM were incubated in parallel for 5 minutes, mixed for 15 minutes and then added to 1 ml medium per well. 1 ml medium was added to each well after 24 h, and cells were analyzed after 48 or 72 h. Double stranded siRNA oligonucleotides were synthesized with 3'-UU overhangs (Dharmacon, Lafayette, CO) with the sequences

GGACUGACCUUGAAGAGAA (CPAP-siRNA1), AGAAUUAGCUCGAAUAGAA (CPAP-siRNA3) and UCUAUAUCAUGGCCGACAA (control-siRNA). Note that the control-siRNA targets GFP as described (Strnad et al., 2007). siRNA against CP110 and HsSAS-6 were as described (Spektor et al., 2007; Strnad et al., 2007). For generating a GFP-CPAP construct resistant to siRNA3, four silent nucleotide changes were introduced in the corresponding region of CPAP (AGAGTTAGCTAGGATCGAA) to render the construct resistant to these siRNAs. The corresponding sequence-verified cDNA (CPAP-R) was cloned into pEBTet as above. For the centrosome overduplication assay, 4 μ l aphidicolin (1.6 mg/ml) were added to the medium 24 hours after siRNA transfection and fixed 48 hours thereafter.

For plasmid transfections, cells were seeded on 18 mm sterile glass coverslips in 6 well plates at 80-90% confluency. 1 μ g of plasmid DNA in 50 μ l OptiMEM and 2 μ l of Lipofectamine 2000 (Invitrogen, Carlsbad, CA) in 50 μ l were incubated in parallel for 10 minutes, mixed for 10 minutes and added to each well. The medium was changed after 12-24 h to reduce toxicity of the reaction mix.

4.5 Fluorescence Recovery After Photobleaching

Fluorescence Recovery After Photobleaching (FRAP) was performed on the Leica TCS SP2 inverted confocal microscope with a 63x oil immersion objective in an equilibrated chamber with 37°C and 5% CO₂. The medium was replaced by prewarmed colorless DMEM (Invitrogen, Carlsbad, CA) supplemented with FCS before the experiment. A small region of interest (ROI) around the centrosomal GFP signal was bleached three times with maximum laser intensity, and single confocal sections were then recorded within 3, 30 and 60 minutes. The centrosomal signal could be usually followed without refocussing for 3 minutes. Due to centrosome movements, the imaging plane with highest centrosomal fluorescence had to be identified by refocussing at later time points. Signal intensities of the ROI were integrated in ImageJ and normalized between the highest (prebleached) and lowest (bleached) signals.

4.6 Multi-Mode Time-Lapse Microscopy

Multi-mode time-lapse microscopy was conducted by Jadranka Loncarek and Alexey Khodjakov as described (Loncarek et al., 2008). In brief, cells were grown on coverslips and mounted in Rose chambers. Full Z-series through the cell (0.7 μm steps) were recorded at 15 min intervals using either 60x1.4 or 100x1.4 PlanApo lens. Images were captured on Andor iXon back-illuminated EM CCD. The system was driven by IPLab software. During the experiment, cells were maintained at 37°C, and using shutters directly synchronized with the camera minimized the light exposure.

4.7 Immunoblotting and Immunofluorescence Microscopy

To determine total CPAP levels, cells from different timepoints after G1/S phase release from a thymidine block were lysed in buffer containing 50 mM HEPES (pH 7.4), 250 mM NaCl, 5 mM EDTA, 1% NP-40 and protease inhibitors (P8340, Sigma-Aldrich) by three freeze-thaw cycles in liquid N₂ and centrifugation at 13,000 rpm for 10 minutes to remove cell debris. Protein concentration was determined by Bradford analysis. 80 μg of lysate were resolved by SDS-PAGE on a 8-13% gradient gel and immunoblotted on Immobilon-P transfer membrane (Millipore Corporation, Bedford, MA). Primary antibodies were 1:500 rabbit anti-CPAP (this study), 1:1000 mouse anti- γ -tubulin (GTU88, Sigma-Aldrich) and 1:500 rabbit anti-HsSAS-6 (Strnad et al., 2007) diluted in 3% non-fat dry milk in PBS. Secondary antibodies were 1:5000 HRP-conjugated anti rabbit or mouse IgG (Promega, Madison, WI). Washes were performed in tris-buffered saline (TBS) containing 0.05% Triton X-100 (TBST).

For immunofluorescence (IF) analysis, cells were fixed in -20°C methanol for 10 minutes and washed in PBS containing 0.05% Triton X-100 (PBST). After blocking in 1% bovine serum albumin (BSA) in PBS for 1 hour, cells were incubated with primary antibodies over night at 4°C. Following three washes in PBST for 5 minutes, cells were incubated with secondary antibodies and 1 $\mu\text{g}/\text{ml}$ Hoechst 33258 for 1 hour at room temperature, washed four times for 5 minutes in PBST and mounted. Primary antibodies were 1:1000 rabbit anti-CPAP (this study), 1:200 mouse

anti- α -tubulin (DM1A, Sigma-Aldrich), 1:2000 mouse anti- γ -tubulin (GTU88, Sigma-Aldrich), 1: 25 goat anti-pericentrin (E17, Santa-Cruz), 1:1000 rabbit anti-NEDD1 (Lüders et al., 2006), 1:500 rabbit anti-Cep192 (Zhu et al., 2008), 1:1000 mouse anti-acetylated tubulin (6-11B-1, Abcam, UK), 1:1000 mouse anti-polyglutamylated tubulin (gift from B. Eddé), 1:1000 mouse '20H5' anti-Centrin-2 (Errabolu et al., 1994) (gift from J.L. Salisbury), 1:2000 rabbit anti-Centrin-3 (Middendorp et al., 2000) (gift from M. Bornens), 1:1000 rabbit anti-Cep135 (gift from R. Kuriyama), 1:200 rabbit anti-CP110 (Chen et al., 2002), 1:200 rabbit anti-Odf2 (Ishikawa et al., 2005; Nakagawa et al., 2001) (gift from H. Ishikawa), 1:20'000 rabbit anti-Ninein (Mogensen et al., 2000) (gift from M. Bornens), 1:2000 rabbit anti-C-Nap1 (Mayor et al., 2000) (gift from E. Nigg), 1:200 rabbit anti-HsSAS-6 (Strnad et al., 2007) and 1:200 rabbit anti-GFP (gift from V. Simanis). Secondary antibodies were 1:1000 Alexa488-coupled anti-mouse, Alexa568-coupled anti-rabbit, Alexa488-coupled anti-goat (Molecular Probes, Eugene, OR), Cy3-coupled anti-rabbit (Dianova) and 1:400 Cy5-coupled anti-mouse antibodies (Dianova). Images were taken on the Leica TCS SP2 inverted confocal microscope using a 63x oil immersion objective (Zeiss, Germany). Sequential line scanning and line averaging of 4 were generally applied to avoid fluorescence cross talk and reduce electronic noise, respectively. Images of relevant structures were taken as Z-series with 0.2 μm – 0.4 μm intervals at zoom 5 (low resolution) or zoom 15 (high resolution) and maximum intensity projected using the Leica LCS Lite software (Leica Microsystems, Germany). Images were postprocessed in Adobe Photoshop or Imaris for 3D reconstructions.

For quantitative immunofluorescence microscopy, cells were imaged with identical laser and detector settings in one session. In other cases where quantification was not performed, the settings were optimized for each cell separately. For quantification of thread complexity, confocal Z-series of these structures were imaged as described, and the end of each elongated segment marked with a ~ 300 nm radius. Thread complexity was defined as the number of free ends per

thread. Non-overlapping radii were counted as one free end, whereas multiple ends located in a single radius were counted as one (branched) end.

4.8 Electron Microscopy (EM)

Single section EM analyses of CPAP threads marked with GFP were carried out in a collaborative approach with Mette Mogensen. Cells expressing GFP-CPAP were grown on gridded glass coverslips in glass bottom dishes (both from MatTek, Ashland, MA). Shortly before fixation, the medium was changed for colorless DMEM medium supplemented with 10% FCS and membrane permeable Hoechst 33342 (1 ug/ml). Cells were then imaged using dual fluorescent (GFP) and brightfield microscopy on the Leica TCS SP2 inverted microscope with a 63x oil immersion objective. Cells were fixed in 2.5% glutaraldehyde in cacodylate buffer (0.1 M sodium cacodylate, 2 M calcium chloride). The coverslips were then transferred to 15 ml Falcon tubes in cacodylate buffer and sent to our collaborator, who retrieved the position of selected cells on the grid for TEM analysis as described (Moss et al., 2007).

Serial section EM analyses of CPAP aggregates marked with GFP were performed in collaboration with Graham Knott (EPFL BioEM Facility). Cells expressing GFP-CPAP were grown on marked plastic coverslips (Thermanox, Nunc) in glass bottom dishes (MatTek, Ashland, MA) and fixed in 2% paraformaldehyde mixed with 0.2% glutaraldehyde in phosphate buffer (0.1M, pH 7.4) to reduce autofluorescence of the GFP signal. Dual fluorescent (GFP) and differential interference contrast (DIC) microscopy on the Leica TCS SP2 inverted microscope with a 10x dry objective allowed us to identify the position of cells. After imaging, cells were post-fixed in 2.5% glutaraldehyde in phosphate buffer (0.1M, pH 7.4), and serial section EM analysis was performed.

Correlative Light Microscopy (LM) / serial section Electron Microscopy (EM) analyses were conducted by Jadranka Loncarek and Alexey Khodjakov as described (Loncarek et al., 2008). Cells expressing GFP-CPAP were fixed by perfusion with 2.5% glutaraldehyde. Spinning-disk confocal Z-series of selected cells were collected immediately before and shortly after

fixation. After standard embedment (Rieder and Cassels, 1999), full series of 100-nm sections were obtained for each cell. The sections were examined in a Zeiss 910 electron microscope at 80 kV. Images were recorded on film and subsequently scanned.

5 References

- Adams, I. R. and Kilmartin, J. V.** (2000). Spindle pole body duplication: a model for centrosome duplication? *Trends in Cell Biology* **10**, 329-35.
- Albertson, D. G. and Thomson, J. N.** (1993). Segregation of holocentric chromosomes at meiosis in the nematode, *Caenorhabditis elegans*. *Chromosome Res* **1**, 15-26.
- Alvey, P. L.** (1986). Do adult centrioles contain cartwheels and lie at right angles to each other? *Cell Biol Int Rep* **10**, 589-98.
- Andersen, J. S., Wilkinson, C. J., Mayor, T., Mortensen, P., Nigg, E. A. and Mann, M.** (2003). Proteomic characterization of the human centrosome by protein correlation profiling. *Nature* **426**, 570-4.
- Anderson, R. G. and Brenner, R. M.** (1971). The formation of basal bodies (centrioles) in the Rhesus monkey oviduct. *J Cell Biol* **50**, 10-34.
- Azimzadeh, J. and Bornens, M.** (2004). The Centrosome in Evolution. *Centrosomes in Development and Disease (Book)*, 93 - 122.
- Azimzadeh, J. and Bornens, M.** (2007). Structure and duplication of the centrosome. *Journal of Cell Science* **120**, 2139-42.
- Azimzadeh, J., Hergert, P., Delouvé, A., Euteneuer, U., Formstecher, E., Khodjakov, A. and Bornens, M.** (2009). hPOC5 is a centrin-binding protein required for assembly of full-length centrioles. *J Cell Biol* **185**, 101-14.
- Bach, M., Grigat, S., Pawlik, B., Fork, C., Utermöhlen, O., Pal, S., Banczyk, D., Lazar, A., Schömig, E. and Gründemann, D.** (2007). Fast set-up of doxycycline-inducible protein expression in human cell lines with a single plasmid based on Epstein-Barr virus replication and the simple tetracycline repressor. *FEBS J* **274**, 783-90.
- Bahe, S., Stierhof, Y. D., Wilkinson, C. J., Leiss, F. and Nigg, E. A.** (2005). Rootletin forms centriole-associated filaments and functions in centrosome cohesion. *J Cell Biol* **171**, 27-33.
- Balczon, R., Bao, L., Zimmer, W. E., Brown, K., Zinkowski, R. P. and Brinkley, B. R.** (1995). Dissociation of centrosome replication events from cycles of DNA synthesis and mitotic division in hydroxyurea-arrested Chinese hamster ovary cells. *J Cell Biol* **130**, 105-15.
- Basto, R., Brunk, K., Vinadogrova, T., Peel, N., Franz, A., Khodjakov, A. and Raff, J. W.** (2008). Centrosome amplification can initiate tumorigenesis in flies. *Cell* **133**, 1032-42.
- Basto, R., Lau, J., Vinogradova, T., Gardiol, A., Woods, C. G., Khodjakov, A. and Raff, J. W.** (2006). Flies without centrioles. *Cell* **125**, 1375-86.
- Beaudouin, J., Gerlich, D., Daigle, N., Eils, R. and Ellenberg, J.** (2002). Nuclear envelope breakdown proceeds by microtubule-induced tearing of the lamina. *Cell* **108**, 83-96.
- Bellett, G., Carter, J. M., Keynton, J., Goldspink, D., James, C., Moss, D. K. and Mogensen, M. M.** (2009). Microtubule plus-end and minus-end capture at adherens junctions is involved in the assembly of apico-basal arrays in polarised epithelial cells. *Cell Motil Cytoskeleton (ahead of print)*.
- Bettencourt-Dias, M., Rodrigues-Martins, A., Carpenter, L., Riparbelli, M., Lehmann, L., Gatt, M. K., Carmo, N., Balloux, F., Callaini, G. and Glover, D. M.** (2005). SAK/PLK4 is required for centriole duplication and flagella development. *Curr Biol* **15**, 2199-207.
- Bobinnec, Y., Khodjakov, A., Mir, L. M., Rieder, C. L., Eddé, B. and Bornens, M.** (1998a). Centriole disassembly in vivo and its effect on centrosome structure and function in vertebrate cells. *J Cell Biol* **143**, 1575-89.
- Bobinnec, Y., Moudjou, M., Fouquet, J. P., Desbruyères, E., Eddé, B. and Bornens, M.** (1998b). Glutamylation of centriole and cytoplasmic tubulin in proliferating non-neuronal cells. *Cell Motil Cytoskeleton* **39**, 223-32.

- Boisvieux-Ulrich, E., Lainé, M. C. and Sandoz, D.** (1990). Cytochalasin D inhibits basal body migration and ciliary elongation in quail oviduct epithelium. *Cell Tissue Res* **259**, 443-54.
- Bond, J., Roberts, E., Springell, K., Lizarraga, S. B., Lizarraga, S., Scott, S., Higgins, J., Hampshire, D., Morrison, E., Leal, G. et al.** (2005). A centrosomal mechanism involving CDK5RAP2 and CENPJ controls brain size. *Nat Genet* **37**, 353-5.
- Bond, J. and Woods, C. G.** (2006). Cytoskeletal genes regulating brain size. *Curr Opin Cell Biol* **18**, 95-101.
- Brown, R. C., Lemmon, B. E. and Horio, T.** (2004). Gamma-tubulin localization changes from discrete polar organizers to anastral spindles and phragmoplasts in mitosis of *Marchantia polymorpha* L. *Protoplasts* **224**, 187-93.
- Callaini, G., Riparbelli, M. G. and Dallai, R.** (1999). Centrosome inheritance in insects: fertilization and parthenogenesis. *Biol Cell* **91**, 355-66.
- Callaini, G., Whitfield, W. G. and Riparbelli, M. G.** (1997). Centriole and centrosome dynamics during the embryonic cell cycles that follow the formation of the cellular blastoderm in *Drosophila*. *Exp Cell Res* **234**, 183-90.
- Cassimeris, L.** (2007). Tubulin delivery: polymerization chaperones for microtubule assembly? *Developmental Cell* **13**, 455-6.
- Castellanos, E., Dominguez, P. and Gonzalez, C.** (2008). Centrosome dysfunction in *Drosophila* neural stem cells causes tumors that are not due to genome instability. *Curr Biol* **18**, 1209-14.
- Cavalier-Smith, T.** (2002). The phagotrophic origin of eukaryotes and phylogenetic classification of Protozoa. *Int J Syst Evol Microbiol* **52**, 297-354.
- Chapman, M. J., Dolan, M. F. and Margulis, L.** (2000). Centrioles and kinetosomes: form, function, and evolution. *The Quarterly review of biology* **75**, 409-29.
- Chen, C. H., Howng, S. L., Cheng, T. S., Chou, M. H., Huang, C. Y. and Hong, Y. R.** (2003). Molecular characterization of human ninein protein: two distinct subdomains required for centrosomal targeting and regulating signals in cell cycle. *Biochemical and Biophysical Research Communications* **308**, 975-83.
- Chen, Z., Indjeian, V. B., McManus, M., Wang, L. and Dynlacht, B. D.** (2002). CP110, a cell cycle-dependent CDK substrate, regulates centrosome duplication in human cells. *Developmental Cell* **3**, 339-50.
- Cho, J. H., Chang, C. J., Chen, C. Y. and Tang, T. K.** (2006). Depletion of CPAP by RNAi disrupts centrosome integrity and induces multipolar spindles. *Biochemical and Biophysical Research Communications* **339**, 742-7.
- Chrétien, D., Buendia, B., Fuller, S. D. and Karsenti, E.** (1997). Reconstruction of the centrosome cycle from cryoelectron micrographs. *J Struct Biol* **120**, 117-33.
- Clute, P. and Pines, J.** (1999). Temporal and spatial control of cyclin B1 destruction in metaphase. *Nat Cell Biol* **1**, 82-7.
- Cormier, A., Clément, M. J., Knossow, M., Lachkar, S., Savarin, P., Toma, F., Sobel, A., Gigant, B. and Curmi, P. A.** (2009). The PN2-3 domain of CPAP implements a novel mechanism for tubulin sequestration. *J Biol Chem* **284**, 6909-17.
- D'Assoro, A. B., Barrett, S. L., Folk, C., Negron, V. C., Boeneman, K., Busby, R., Whitehead, C., Stivala, F., Lingle, W. L. and Salisbury, J. L.** (2002). Amplified centrosomes in breast cancer: a potential indicator of tumor aggressiveness. *Breast Cancer Res Treat* **75**, 25-34.
- Dammermann, A., Maddox, P. S., Desai, A. and Oegema, K.** (2008). SAS-4 is recruited to a dynamic structure in newly forming centrioles that is stabilized by the gamma-tubulin-mediated addition of centriolar microtubules. *J Cell Biol* **180**, 771-85.
- Dammermann, A., Müller-Reichert, T., Pelletier, L., Habermann, B., Desai, A. and Oegema, K.** (2004). Centriole assembly requires both centriolar and pericentriolar material proteins. *Developmental Cell* **7**, 815-29.
- Daudeker, C., Schliwa, M. and Gräf, R.** (1999). Dictyostelium discoideum: a promising centrosome model system. *Biol Cell* **91**, 313-20.

- Dawe, H., Farr, H. and Gull, K.** (2007). Centriole/basal body morphogenesis and migration during ciliogenesis in animal cells. *Journal of Cell Science* **120**, 7-15.
- Debec, A., Détraves, C., Montmory, C., Géraud, G. and Wright, M.** (1995). Polar organization of gamma-tubulin in acentriolar mitotic spindles of *Drosophila melanogaster* cells. *Journal of Cell Science* **108 (Pt 7)**, 2645-53.
- Delattre, M., Canard, C. and Gönczy, P.** (2006). Sequential protein recruitment in *C. elegans* centriole formation. *Curr Biol* **16**, 1844-9.
- Delattre, M. and Gönczy, P.** (2004). The arithmetic of centrosome biogenesis. *Journal of Cell Science* **117**, 1619-30.
- Delattre, M., Leidel, S., Wani, K., Baumer, K., Bamat, J., Schnabel, H., Feichtinger, R., Schnabel, R. and Gönczy, P.** (2004). Centriolar SAS-5 is required for centrosome duplication in *C. elegans*. *Nat Cell Biol* **6**, 656-64.
- Dictenberg, J. B., Zimmerman, W., Sparks, C. A., Young, A., Vidair, C., Zheng, Y., Carrington, W., Fay, F. S. and Doxsey, S. J.** (1998). Pericentrin and gamma-tubulin form a protein complex and are organized into a novel lattice at the centrosome. *J Cell Biol* **141**, 163-74.
- Dix, C. I. and Raff, J. W.** (2007). *Drosophila* Spd-2 recruits PCM to the sperm centriole, but is dispensable for centriole duplication. *Curr Biol* **17**, 1759-64.
- Doxsey, S., Zimmerman, W. and Mikule, K.** (2005). Centrosome control of the cell cycle. *Trends in Cell Biology* **15**, 303-11.
- Doxsey, S. J., Stein, P., Evans, L., Calarco, P. D. and Kirschner, M.** (1994). Pericentrin, a highly conserved centrosome protein involved in microtubule organization. *Cell* **76**, 639-50.
- Duensing, A., Liu, Y., Tseng, M., Malumbres, M., Barbacid, M. and Duensing, S.** (2006). Cyclin-dependent kinase 2 is dispensable for normal centrosome duplication but required for oncogene-induced centrosome overduplication. *Oncogene* **25**, 2943-9.
- Errabolu, R., Sanders, M. A. and Salisbury, J. L.** (1994). Cloning of a cDNA encoding human centrin, an EF-hand protein of centrosomes and mitotic spindle poles. *Journal of Cell Science* **107 (Pt 1)**, 9-16.
- Fong, K. W., Choi, Y. K., Rattner, J. B. and Qi, R. Z.** (2008). CDK5RAP2 Is a Pericentriolar Protein That Functions in Centrosomal Attachment of the {gamma}-Tubulin Ring Complex. *Mol Biol Cell* **19**, 115-25.
- Fry, A. M., Mayor, T., Meraldi, P., Stierhof, Y. D., Tanaka, K. and Nigg, E. A.** (1998). C-Nap1, a novel centrosomal coiled-coil protein and candidate substrate of the cell cycle-regulated protein kinase Nek2. *J Cell Biol* **141**, 1563-74.
- Ganem, N. J., Godinho, S. A. and Pellman, D.** (2009). A mechanism linking extra centrosomes to chromosomal instability. *Nature* **460**, 278-82.
- Giansanti, M. G., Bucciarelli, E., Bonaccorsi, S. and Gatti, M.** (2008). *Drosophila* SPD-2 is an essential centriole component required for PCM recruitment and astral-microtubule nucleation. *Curr Biol* **18**, 303-9.
- Godinho, S. A., Kwon, M. and Pellman, D.** (2009). Centrosomes and cancer: how cancer cells divide with too many centrosomes. *Cancer Metastasis Rev* **28**, 85-98.
- Golsteyn, R. M., Mundt, K. E., Fry, A. M. and Nigg, E. A.** (1995). Cell cycle regulation of the activity and subcellular localization of Plk1, a human protein kinase implicated in mitotic spindle function. *J Cell Biol* **129**, 1617-28.
- Gomez-Ferreria, M. A., Rath, U., Buster, D. W., Chanda, S. K., Caldwell, J. S., Rines, D. R. and Sharp, D. J.** (2007). Human Cep192 is required for mitotic centrosome and spindle assembly. *Curr Biol* **17**, 1960-6.
- Gonzalez, C.** (2007). Spindle orientation, asymmetric division and tumour suppression in *Drosophila* stem cells. *Nat Rev Genet* **8**, 462-72.
- González, C., Tavosanis, G. and Mollinari, C.** (1998). Centrosomes and microtubule organisation during *Drosophila* development. *J Cell Sci* **111 (Pt 18)**, 2697-706.

- Graser, S., Stierhof, Y. D., Lavoie, S. B., Gassner, O. S., Lamla, S., Le Clech, M. and Nigg, E. A.** (2007). Cep164, a novel centriole appendage protein required for primary cilium formation. *J Cell Biol* **179**, 321-30.
- Guarguaglini, G., Duncan, P. I., Stierhof, Y. D., Holmström, T., Duensing, S. and Nigg, E. A.** (2005). The forkhead-associated domain protein Cep170 interacts with Polo-like kinase 1 and serves as a marker for mature centrioles. *Mol Biol Cell* **16**, 1095-107.
- Habedanck, R., Stierhof, Y. D., Wilkinson, C. J. and Nigg, E. A.** (2005). The Polo kinase Plk4 functions in centriole duplication. *Nat Cell Biol* **7**, 1140-6.
- Hachet, V., Canard, C. and Gönczy, P.** (2007). Centrosomes promote timely mitotic entry in *C. elegans* embryos. *Developmental Cell* **12**, 531-41.
- Hagan, I. and Palazzo, R. E.** (2006). Warming up at the poles. *EMBO Rep* **7**, 364-71.
- Hanahan, D. and Weinberg, R. A.** (2000). The hallmarks of cancer. *Cell* **100**, 57-70.
- Haren, L., Remy, M. H., Bazin, I., Callebaut, I., Wright, M. and Merdes, A.** (2006). NEDD1-dependent recruitment of the gamma-tubulin ring complex to the centrosome is necessary for centriole duplication and spindle assembly. *J Cell Biol* **172**, 505-15.
- Heald, R., Tournebize, R., Blank, T., Sandaltzopoulos, R., Becker, P., Hyman, A. and Karsenti, E.** (1996). Self-organization of microtubules into bipolar spindles around artificial chromosomes in *Xenopus* egg extracts. *Nature* **382**, 420-5.
- Higginbotham, H. R. and Gleeson, J. G.** (2007). The centrosome in neuronal development. *Trends in Neurosciences* **30**, 276-83.
- Hinchcliffe, E. H., Miller, F. J., Cham, M., Khodjakov, A. and Sluder, G.** (2001). Requirement of a centrosomal activity for cell cycle progression through G1 into S phase. *Science* **291**, 1547-50.
- Hsu, W. B., Hung, L. Y., Tang, C. J., Su, C. L., Chang, Y. and Tang, T. K.** (2008). Functional characterization of the microtubule-binding and -destabilizing domains of CPAP and d-SAS-4. *Exp Cell Res* **314**, 2591-602.
- Huang, S. C., Liu, E. S., Chan, S. H., Munagala, I. D., Cho, H. T., Jagadeeswaran, R. and Benz, E. J.** (2005). Mitotic regulation of protein 4.1R involves phosphorylation by cdc2 kinase. *Mol Biol Cell* **16**, 117-27.
- Huangfu, D., Liu, A., Rakeman, A. S., Murcia, N. S., Niswander, L. and Anderson, K. V.** (2003). Hedgehog signalling in the mouse requires intraflagellar transport proteins. *Nature* **426**, 83-7.
- Hung, L. Y., Chen, H. L., Chang, C. W., Li, B. R. and Tang, T. K.** (2004). Identification of a novel microtubule-destabilizing motif in CPAP that binds to tubulin heterodimers and inhibits microtubule assembly. *Mol Biol Cell* **15**, 2697-706.
- Hung, L. Y., Tang, C. J. and Tang, T. K.** (2000). Protein 4.1 R-135 interacts with a novel centrosomal protein (CPAP) which is associated with the gamma-tubulin complex. *Mol Cell Biol* **20**, 7813-25.
- Ibrahim, R., Messaoudi, C., Chichon, F. J., Celati, C. and Marco, S.** (2008). Electron tomography study of isolated human centrioles. *Microsc Res Tech* **72**, 42-8.
- Ishikawa, H., Kubo, A., Tsukita, S. and Tsukita, S.** (2005). Odf2-deficient mother centrioles lack distal/subdistal appendages and the ability to generate primary cilia. *Nat Cell Biol* **7**, 517-24.
- Jackman, M., Lindon, C., Nigg, E. A. and Pines, J.** (2003). Active cyclin B1-Cdk1 first appears on centrosomes in prophase. *Nat Cell Biol* **5**, 143-8.
- Joshi, H. C., Palacios, M. J., McNamara, L. and Cleveland, D. W.** (1992). Gamma-tubulin is a centrosomal protein required for cell cycle-dependent microtubule nucleation. *Nature* **356**, 80-3.
- Kalnins, V. I. and Porter, K. R.** (1969). Centriole replication during ciliogenesis in the chick tracheal epithelium. *Zeitschrift für Zellforschung und mikroskopische Anatomie (Vienna, Austria : 1948)* **100**, 1-30.
- Karsenti, E. and Vernos, I.** (2001). The mitotic spindle: a self-made machine. *Science* **294**, 543-7.

- Keller, L. C., Geimer, S., Romijn, E., Yates, J., Zamora, I. and Marshall, W. F.** (2009). Molecular architecture of the centriole proteome: the conserved WD40 domain protein POC1 is required for centriole duplication and length control. *Mol Biol Cell* **20**, 1150-66.
- Keller, L. C., Romijn, E. P., Zamora, I., Yates, J. R. and Marshall, W. F.** (2005). Proteomic analysis of isolated chlamydomonas centrioles reveals orthologs of ciliary-disease genes. *Curr Biol* **15**, 1090-8.
- Kemp, C. A., Kopish, K. R., Zipperlen, P., Ahringer, J. and O'Connell, K. F.** (2004). Centrosome maturation and duplication in *C. elegans* require the coiled-coil protein SPD-2. *Developmental Cell* **6**, 511-23.
- Keryer, G., Witczak, O., Delouvé, A., Kemmner, W. A., Rouillard, D., Tasken, K. and Bornens, M.** (2003). Dissociating the centrosomal matrix protein AKAP450 from centrioles impairs centriole duplication and cell cycle progression. *Mol Biol Cell* **14**, 2436-46.
- Khodjakov, A., Cole, R. W., Oakley, B. R. and Rieder, C. L.** (2000). Centrosome-independent mitotic spindle formation in vertebrates. *Curr Biol* **10**, 59-67.
- Khodjakov, A. and Rieder, C. L.** (1999). The sudden recruitment of gamma-tubulin to the centrosome at the onset of mitosis and its dynamic exchange throughout the cell cycle, do not require microtubules. *J Cell Biol* **146**, 585-96.
- Khodjakov, A. and Rieder, C. L.** (2001). Centrosomes enhance the fidelity of cytokinesis in vertebrates and are required for cell cycle progression. *J Cell Biol* **153**, 237-42.
- Khodjakov, A., Rieder, C. L., Sluder, G., Cassels, G., Sibon, O. and Wang, C. L.** (2002). De novo formation of centrosomes in vertebrate cells arrested during S phase. *J Cell Biol* **158**, 1171-81.
- Kilburn, C. L., Pearson, C. G., Romijn, E. P., Meehl, J. B., Giddings, T. H., Culver, B. P., Yates, J. R. and Winey, M.** (2007). New Tetrahymena basal body protein components identify basal body domain structure. *J Cell Biol* **178**, 905-12.
- Kirkham, M., Müller-Reichert, T., Oegema, K., Grill, S. and Hyman, A.** (2003). SAS-4 is a *C. elegans* centriolar protein that controls centrosome size. *Cell* **112**, 575-87.
- Kleylein-Sohn, J., Westendorf, J., Le Clech, M., Habedanck, R., Stierhof, Y. D. and Nigg, E. A.** (2007). Plk4-induced centriole biogenesis in human cells. *Developmental Cell* **13**, 190-202.
- Ko, M., Rosario, C. O., Hudson, J., Kulkarni, S., Pollett, A., Dennis, J. and Swallow, C.** (2005). Plk4 haploinsufficiency causes mitotic infidelity and carcinogenesis. *Nat Genet* **37**, 883-8.
- Kohlmaier, G., Lončarek, J., Meng, X., McEwen, B. F., Mogensen, M. M., Spektor, A., Dynlacht, B. D., Khodjakov, A. and Gönczy, P.** (2009). Overly long centrioles and defective cell division upon excess of the SAS-4-related protein CPAP. *Curr Biol* **19**, 1012-8.
- Koyanagi, M., Hijikata, M., Watashi, K., Masui, O. and Shimotohno, K.** (2005). Centrosomal P4.1-associated protein is a new member of transcriptional coactivators for nuclear factor-kappaB. *J Biol Chem* **280**, 12430-7.
- Krauss, S. W., Chasis, J. A., Rogers, C., Mohandas, N., Krockmalnic, G. and Penman, S.** (1997). Structural protein 4.1 is located in mammalian centrosomes. *Proc Natl Acad Sci USA* **94**, 7297-302.
- Krauss, S. W., Spence, J. R., Bahmanyar, S., Barth, A. I., Go, M. M., Czerwinski, D. and Meyer, A. J.** (2008). Downregulation of protein 4.1R, a mature centriole protein, disrupts centrosomes, alters cell cycle progression, and perturbs mitotic spindles and anaphase. *Mol Cell Biol* **28**, 2283-94.
- Kuriyama, R.** (1982). Effect of colcemid on the centriole cycle in Chinese hamster ovary cells. *Journal of Cell Science* **53**, 155-71.
- Kuriyama, R.** (2009). Centriole assembly in CHO cells expressing Plk4/SAS6/SAS4 is similar to centriogenesis in ciliated epithelial cells. *Cell Motil Cytoskeleton*.
- Kuriyama, R. and Borisy, G. G.** (1981). Centriole cycle in Chinese hamster ovary cells as determined by whole-mount electron microscopy. *J Cell Biol* **91**, 814-21.

- La Terra, S., English, C. N., Hergert, P., McEwen, B. F., Sluder, G. and Khodjakov, A.** (2005). The de novo centriole assembly pathway in HeLa cells: cell cycle progression and centriole assembly/maturation. *J Cell Biol* **168**, 713-22.
- Lacey, K. R., Jackson, P. K. and Stearns, T.** (1999). Cyclin-dependent kinase control of centrosome duplication. *Proc Natl Acad Sci USA* **96**, 2817-22.
- Lancaster, M. A. and Gleeson, J. G.** (2009). The primary cilium as a cellular signaling center: lessons from disease. *Current Opinion in Genetics & Development* **19**, 220-9.
- Leidel, S., Delattre, M., Cerutti, L., Baumer, K. and Gönczy, P.** (2005). SAS-6 defines a protein family required for centrosome duplication in *C. elegans* and in human cells. *Nat Cell Biol* **7**, 115-25.
- Leidel, S. and Gönczy, P.** (2003). SAS-4 is essential for centrosome duplication in *C. elegans* and is recruited to daughter centrioles once per cell cycle. *Developmental Cell* **4**, 431-9.
- Leidel, S. and Gönczy, P.** (2005). Centrosome duplication and nematodes: recent insights from an old relationship. *Developmental Cell* **9**, 317-25.
- Lingle, W. L. and Salisbury, J. L.** (1999). Altered centrosome structure is associated with abnormal mitoses in human breast tumors. *Am J Pathol* **155**, 1941-51.
- Loncarek, J., Hergert, P., Magidson, V. and Khodjakov, A.** (2008). Control of daughter centriole formation by the pericentriolar material. *Nat Cell Biol* **10**, 322-8.
- Loncarek, J. and Khodjakov, A.** (2009). Ab ovo or de novo? Mechanisms of centriole duplication. *Mol Cells* **27**, 135-42.
- Lüders, J., Patel, U. and Stearns, T.** (2006). GCP-WD is a gamma-tubulin targeting factor required for centrosomal and chromatin-mediated microtubule nucleation. *Nat Cell Biol* **8**, 137-47.
- Marshall, W. F.** (2007). What is the function of centrioles? *J. Cell. Biochem.* **100**, 916-22.
- Matsumoto, Y., Hayashi, K. and Nishida, E.** (1999). Cyclin-dependent kinase 2 (Cdk2) is required for centrosome duplication in mammalian cells. *Curr Biol* **9**, 429-32.
- Mattagajasingh, S. N., Huang, S. C., Hartenstein, J. S., Snyder, M., Marchesi, V. T. and Benz, E. J.** (1999). A nonerythroid isoform of protein 4.1R interacts with the nuclear mitotic apparatus (NuMA) protein. *J Cell Biol* **145**, 29-43.
- Matthies, H. J., McDonald, H. B., Goldstein, L. S. and Theurkauf, W. E.** (1996). Anastral meiotic spindle morphogenesis: role of the non-claret disjunctional kinesin-like protein. *J Cell Biol* **134**, 455-64.
- Mayor, T., Stierhof, Y. D., Tanaka, K., Fry, A. M. and Nigg, E. A.** (2000). The centrosomal protein C-Nap1 is required for cell cycle-regulated centrosome cohesion. *J Cell Biol* **151**, 837-46.
- Meraldi, P., Lukas, J., Fry, A. M., Bartek, J. and Nigg, E. A.** (1999). Centrosome duplication in mammalian somatic cells requires E2F and Cdk2-cyclin A. *Nat Cell Biol* **1**, 88-93.
- Merdes, A., Ramyar, K., Vechio, J. D. and Cleveland, D. W.** (1996). A complex of NuMA and cytoplasmic dynein is essential for mitotic spindle assembly. *Cell* **87**, 447-58.
- Middendorp, S., Küntziger, T., Abraham, Y., Holmes, S., Bordes, N., Paintrand, M., Paoletti, A. and Bornens, M.** (2000). A role for centrin 3 in centrosome reproduction. *J Cell Biol* **148**, 405-16.
- Middendorp, S., Paoletti, A., Schiebel, E. and Bornens, M.** (1997). Identification of a new mammalian centrin gene, more closely related to *Saccharomyces cerevisiae* CDC31 gene. *Proc Natl Acad Sci USA* **94**, 9141-6.
- Mikule, K., Delaval, B., Kaldis, P., Jurczyk, A., Hergert, P. and Doxsey, S.** (2007). Loss of centrosome integrity induces p38-p53-p21-dependent G1-S arrest. *Nat Cell Biol* **9**, 160-70.
- Mogensen, M. M., Malik, A., Piel, M., Bouckson-Castaing, V. and Bornens, M.** (2000). Microtubule minus-end anchorage at centrosomal and non-centrosomal sites: the role of ninein. *Journal of Cell Science* **113 (Pt 17)**, 3013-23.

- Morris, N. R.** (2003). Nuclear positioning: the means is at the ends. *Curr Opin Cell Biol* **15**, 54-9.
- Moss, D. K., Bellett, G., Carter, J. M., Liovic, M., Keynton, J., Prescott, A. R., Lane, E. B. and Mogensen, M. M.** (2007). Ninein is released from the centrosome and moves bi-directionally along microtubules. *Journal of Cell Science* **120**, 3064-74.
- Nakagawa, Y., Yamane, Y., Okanou, T., Tsukita, S. and Tsukita, S.** (2001). Outer dense fiber 2 is a widespread centrosome scaffold component preferentially associated with mother centrioles: its identification from isolated centrosomes. *Mol Biol Cell* **12**, 1687-97.
- Nakazawa, Y., Hiraki, M., Kamiya, R. and Hirono, M.** (2007). SAS-6 is a cartwheel protein that establishes the 9-fold symmetry of the centriole. *Curr Biol* **17**, 2169-74.
- Nigg, E. A.** (2002). Centrosome aberrations: cause or consequence of cancer progression? *Nat Rev Cancer* **2**, 815-25.
- Nigg, E. A.** (2006). Origins and consequences of centrosome aberrations in human cancers. *Int J Cancer* **119**, 2717-23.
- O'Connell, K. F., Caron, C., Kopish, K. R., Hurd, D. D., Kemphues, K. J., Li, Y. and White, J. G.** (2001). The *C. elegans* *zyg-1* gene encodes a regulator of centrosome duplication with distinct maternal and paternal roles in the embryo. *Cell* **105**, 547-58.
- O'Toole, E. T., McDonald, K. L., Mäntler, J., McIntosh, J. R., Hyman, A. A. and Müller-Reichert, T.** (2003). Morphologically distinct microtubule ends in the mitotic centrosome of *Caenorhabditis elegans*. *J Cell Biol* **163**, 451-6.
- Ohba, T., Nakamura, M., Nishitani, H. and Nishimoto, T.** (1999). Self-organization of microtubule asters induced in *Xenopus* egg extracts by GTP-bound Ran. *Science* **284**, 1356-8.
- Ohta, T., Essner, R., Ryu, J. H., Palazzo, R. E., Uetake, Y. and Kuriyama, R.** (2002). Characterization of Cep135, a novel coiled-coil centrosomal protein involved in microtubule organization in mammalian cells. *J Cell Biol* **156**, 87-99.
- Paintrand, M., Moudjou, M., Delacroix, H. and Bornens, M.** (1992). Centrosome organization and centriole architecture: their sensitivity to divalent cations. *J Struct Biol* **108**, 107-28.
- Paoletti, A., Moudjou, M., Paintrand, M., Salisbury, J. L. and Bornens, M.** (1996). Most of centrin in animal cells is not centrosome-associated and centrosomal centrin is confined to the distal lumen of centrioles. *Journal of Cell Science* **109** (Pt 13), 3089-102.
- Peel, N., Stevens, N. R., Basto, R. and Raff, J. W.** (2007). Overexpressing centriole-replication proteins in vivo induces centriole overduplication and de novo formation. *Curr Biol* **17**, 834-43.
- Pelletier, L., O'Toole, E., Schwager, A., Hyman, A. and Müller-Reichert, T.** (2006). Centriole assembly in *Caenorhabditis elegans*. *Nature* **444**, 619-23.
- Pelletier, L., Ozlü, N., Hannak, E., Cowan, C., Habermann, B., Ruer, M., Müller-Reichert, T. and Hyman, A. A.** (2004). The *Caenorhabditis elegans* centrosomal protein SPD-2 is required for both pericentriolar material recruitment and centriole duplication. *Curr Biol* **14**, 863-73.
- Peng, B., Sutherland, K. D., Sum, E. Y., Olayioye, M., Wittlin, S., Tang, T. K., Lindeman, G. J. and Visvader, J. E.** (2002). CPAP is a novel stat5-interacting cofactor that augments stat5-mediated transcriptional activity. *Mol Endocrinol* **16**, 2019-33.
- Pennisi, E.** (2003). Modernizing the tree of life. *Science* **300**, 1692-7.
- Pfleger, C. M. and Kirschner, M. W.** (2000). The KEN box: an APC recognition signal distinct from the D box targeted by Cdh1. *Genes & Development* **14**, 655-65.
- Piel, M., Meyer, P., Khodjakov, A., Rieder, C. L. and Bornens, M.** (2000). The respective contributions of the mother and daughter centrioles to centrosome activity and behavior in vertebrate cells. *J Cell Biol* **149**, 317-30.
- Piel, M., Nordberg, J., Euteneuer, U. and Bornens, M.** (2001). Centrosome-dependent exit of cytokinesis in animal cells. *Science* **291**, 1550-3.

- Pihan, G. A., Purohit, A., Wallace, J., Knecht, H., Woda, B., Quesenberry, P. and Doxsey, S. J.** (1998). Centrosome defects and genetic instability in malignant tumors. *Cancer Research* **58**, 3974-85.
- Pihan, G. A., Wallace, J., Zhou, Y. and Doxsey, S. J.** (2003). Centrosome abnormalities and chromosome instability occur together in pre-invasive carcinomas. *Cancer Research* **63**, 1398-404.
- Piperno, G. and Fuller, M. T.** (1985). Monoclonal antibodies specific for an acetylated form of alpha-tubulin recognize the antigen in cilia and flagella from a variety of organisms. *J Cell Biol* **101**, 2085-94.
- Prosser, S. L., Straatman, K. R. and Fry, A. M.** (2009). Molecular dissection of the centrosome overduplication pathway in S-phase-arrested cells. *Mol Cell Biol* **29**, 1760-73.
- Quintyne, N. J., Reing, J. E., Hoffelder, D. R., Gollin, S. M. and Saunders, W. S.** (2005). Spindle multipolarity is prevented by centrosomal clustering. *Science* **307**, 127-9.
- Rattner, J. B. and Phillips, S. G.** (1973). Independence of centriole formation and DNA synthesis. *J Cell Biol* **57**, 359-72.
- Raynaud-Messina, B., Mazzolini, L., Moisand, A., Cirinesi, A. M. and Wright, M.** (2004). Elongation of centriolar microtubule triplets contributes to the formation of the mitotic spindle in gamma-tubulin-depleted cells. *Journal of Cell Science* **117**, 5497-507.
- Rieder, C. L. and Cassels, G.** (1999). Correlative light and electron microscopy of mitotic cells in monolayer cultures. *Methods Cell Biol* **61**, 297-315.
- Robbins, E., Jentsch, G. and Micali, A.** (1968). The centriole cycle in synchronized HeLa cells. *J Cell Biol* **36**, 329-39.
- Rodrigues-Martins, A., Bettencourt-Dias, M., Riparbelli, M., Ferreira, C., Ferreira, I., Callaini, G. and Glover, D. M.** (2007a). DSAS-6 organizes a tube-like centriole precursor, and its absence suggests modularity in centriole assembly. *Curr Biol* **17**, 1465-72.
- Rodrigues-Martins, A., Riparbelli, M., Callaini, G., Glover, D. M. and Bettencourt-Dias, M.** (2007b). Revisiting the role of the mother centriole in centriole biogenesis. *Science* **316**, 1046-50.
- Ruegg, C., Yilmaz, A., Bieler, G., Bamat, J., Chaubert, P. and Lejeune, F. J.** (1998). Evidence for the involvement of endothelial cell integrin alphaVbeta3 in the disruption of the tumor vasculature induced by TNF and IFN-gamma. *Nat Med* **4**, 408-14.
- Schmidt, T. I., Kleylein-Sohn, J., Westendorf, J., Le Clech, M., Lavoie, S. B., Stierhof, Y. D. and Nigg, E. A.** (2009). Control of centriole length by CPAP and CP110. *Curr Biol* **19**, 1005-11.
- Schnackenberg, B. J., Khodjakov, A., Rieder, C. L. and Palazzo, R. E.** (1998). The disassembly and reassembly of functional centrosomes in vitro. *Proc Natl Acad Sci USA* **95**, 9295-300.
- Slep, K. C. and Vale, R. D.** (2007). Structural basis of microtubule plus end tracking by XMAP215, CLIP-170, and EB1. *Molecular Cell* **27**, 976-91.
- Sorokin, S.** (1962). Centrioles and the formation of rudimentary cilia by fibroblasts and smooth muscle cells. *J Cell Biol* **15**, 363-77.
- Sorokin, S. P.** (1968). Reconstructions of centriole formation and ciliogenesis in mammalian lungs. *Journal of Cell Science* **3**, 207-30.
- Spang, A., Courtney, I., Fackler, U., Matzner, M. and Schiebel, E.** (1993). The calcium-binding protein cell division cycle 31 of *Saccharomyces cerevisiae* is a component of the half bridge of the spindle pole body. *J Cell Biol* **123**, 405-16.
- Spektor, A., Tsang, W. Y., Khoo, D. and Dynlacht, B. D.** (2007). Cep97 and CP110 suppress a cilia assembly program. *Cell* **130**, 678-90.
- Stockinger, L. and Cireli, E.** (1965). Eine bisher unbekannte Art der Zentriolenvermehrung. *Zeitschrift für Zellforschung*, 733-740.

- Strnad, P. and Gönczy, P.** (2008). Mechanisms of procentriole formation. *Trends Cell Biol* **18**, 389-96.
- Strnad, P., Leidel, S., Vinogradova, T., Euteneuer, U., Khodjakov, A. and Gönczy, P.** (2007). Regulated HsSAS-6 levels ensure formation of a single procentriole per centriole during the centrosome duplication cycle. *Developmental Cell* **13**, 203-13.
- Szollosi, D., Calarco, P. and Donahue, R. P.** (1972). Absence of centrioles in the first and second meiotic spindles of mouse oocytes. *Journal of Cell Science* **11**, 521-41.
- Tang, C. J., Fu, R. H., Wu, K. S., Hsu, W. B. and Tang, T. K.** (2009). CPAP is a cell-cycle regulated protein that controls centriole length. *Nat Cell Biol* **11**, 825-31.
- Tilney, L. G., Bryan, J., Bush, D. J., Fujiwara, K., Mooseker, M. S., Murphy, D. B. and Snyder, D. H.** (1973). Microtubules: evidence for 13 protofilaments. *J Cell Biol* **59**, 267-75.
- Tsang, W. Y., Bossard, C., Khanna, H., Peränen, J., Swaroop, A., Malhotra, V. and Dynlacht, B. D.** (2008). CP110 suppresses primary cilia formation through its interaction with CEP290, a protein deficient in human ciliary disease. *Developmental Cell* **15**, 187-97.
- Tsou, M. F. and Stearns, T.** (2006a). Controlling centrosome number: licenses and blocks. *Curr Opin Cell Biol* **18**, 74-8.
- Tsou, M. F. and Stearns, T.** (2006b). Mechanism limiting centrosome duplication to once per cell cycle. *Nature* **442**, 947-51.
- Uetake, Y., Loncarek, J., Nordberg, J. J., English, C. N., La Terra, S., Khodjakov, A. and Sluder, G.** (2007). Cell cycle progression and de novo centriole assembly after centrosomal removal in untransformed human cells. *J Cell Biol* **176**, 173-82.
- Vladar, E. K. and Stearns, T.** (2007). Molecular characterization of centriole assembly in ciliated epithelial cells. *J Cell Biol* **178**, 31-42.
- Vorobjev, I. A. and YuS, C.** (1982). Centrioles in the cell cycle. I. Epithelial cells. *J Cell Biol* **93**, 938-49.
- Wiese, C. and Zheng, Y.** (2006). Microtubule nucleation: gamma-tubulin and beyond. *Journal of Cell Science* **119**, 4143-53.
- Wilson, E. B.** (1900). The Cell in Development and Inheritance. *Columbia University Biological Series IV 2nd edition*, page 309.
- Woese, C. R., Kandler, O. and Wheelis, M. L.** (1990). Towards a natural system of organisms: proposal for the domains Archaea, Bacteria, and Eucarya. *Proc Natl Acad Sci USA* **87**, 4576-9.
- Wolf, N., Hirsh, D. and McIntosh, J. R.** (1978). Spermatogenesis in males of the free-living nematode, *Caenorhabditis elegans*. *J Ultrastruct Res* **63**, 155-69.
- Wolff, A., de Néchaud, B., Chillet, D., Mazarguil, H., Desbruyères, E., Audebert, S., Eddé, B., Gros, F. and Denoulet, P.** (1992). Distribution of glutamylated alpha and beta-tubulin in mouse tissues using a specific monoclonal antibody, GT335. *European Journal of Cell Biology* **59**, 425-32.
- Wong, C. and Stearns, T.** (2003). Centrosome number is controlled by a centrosome-intrinsic block to reduplication. *Nat Cell Biol* **5**, 539-44.
- Wong, S. Y. and Reiter, J. F.** (2008). The primary cilium at the crossroads of mammalian hedgehog signaling. *Curr Top Dev Biol* **85**, 225-60.
- Woods, C. G., Bond, J. and Enard, W.** (2005). Autosomal recessive primary microcephaly (MCPH): a review of clinical, molecular, and evolutionary findings. *Am J Hum Genet* **76**, 717-28.
- Young, A., Dichtenberg, J. B., Purohit, A., Tuft, R. and Doxsey, S. J.** (2000). Cytoplasmic dynein-mediated assembly of pericentrin and gamma tubulin onto centrosomes. *Mol Biol Cell* **11**, 2047-56.

Zhu, F., Lawo, S., Bird, A., Pinchev, D., Ralph, A., Richter, C., Müller-Reichert, T., Kittler, R., Hyman, A. A. and Pelletier, L. (2008). The mammalian SPD-2 ortholog Cep192 regulates centrosome biogenesis. *Curr Biol* **18**, 136-41.

6 Acknowledgements

I would like to take this opportunity to thank all those who have contributed directly or indirectly to the completion of this thesis work. I want to thank notably the members of the Gönczy lab for the nice working atmosphere and Pierre for his guidance, enthusiasm and good advices throughout the past 4 years. Finally, my personal thanks are dedicated to Sandra for her loving support, as well as my parents who always looked forward to this day.

7 Curriculum Vitae

PERSONAL DETAILS

Date of birth: September 16, 1979

Place of birth: 9900 Lienz, Austria

Nationality: Austrian; residence permit B (Switzerland)

EDUCATION

PHD THESIS — 2005-2009

Swiss Institute of Experimental Cancer Research (ISREC), Lausanne, supervisor: Prof. Pierre Gönczy

Title: Functional Characterization of the SAS-4-Related Protein CPAP in Centrosome Biology of Human Cells

MASTER THESIS — 2004-2005

Institute of Molecular Pathology (IMP), Vienna, supervisor: Prof. Jan-Michael Peters

Title: Regulation of the Anaphase-Promoting Complex by the Spindle Checkpoint

UNIVERSITY STUDIES — 1999-2005

University of Vienna, Austria

Main Subject: Molecular Biology, Cell Biology and Biochemistry

Graduation: Magister rerum naturalium (comparable to Master's degree)

TRAININGS AND PROJECT PRESENTATIONS

THE EMBO MEETING - 2009

August 29 - September 1, Amsterdam, Netherlands (Poster Presentation)

FIRST EMBO CONFERENCE ON CENTROSOMES - 2008

September 12-16, Heidelberg, Germany (Poster Presentation)

EPFL LIFE SCIENCES SYMPOSIUM - 2008

August 21-23, Lausanne, Switzerland (Poster Presentation)

47TH ANNUAL ASCB MEETING - 2007

December 1-5, Washington DC, USA (Poster Presentation)

EMBO WORKSHOP - 2005

September 23-27, Heidelberg, Germany

PUBLICATION

Kohlmaier, G., Lončarek, J., Meng, X., McEwen, B. F., Mogensen, M. M., Spektor, A., Dynlacht, B. D., Khodjakov, A. and Gönczy, P. (2009). Overly long centrioles and defective cell division upon excess of the SAS-4-related protein CPAP. *Curr Biol* **19**, 1012-8.